2017-08-03

RC Traffic Barrier with GFRP Reinforcement

Paolo Rocchetti
University of Miami, paolo.rocchetti@studio.unibo.it

UNIVERSITY OF MIAMI

RC TRAFFIC RAILING DESIGNS WITH GFRP REINFORCEMENT

By

Paolo Rocchetti

A THESIS

Submitted to the Faculty
of the University of Miami
in partial fulfillment of the requirements for
the degree of Master of Science

Coral Gables, Florida

August 2017

UNIVERSITY OF MIAMI

A thesis submitted in partial fulfillment of
the requirements for the degree of
Master of Science

RC TRAFFIC RAILING DESIGNS WITH GFRP REINFORCEMENT

Paolo Rocchetti

Approved:

_____ Antonio Nanni, Ph.D. Professor of Civil, Architectural and Environmental Engineering	_____ Guillermo Claure, Ph.D. Postdoctoral of Civil, Architectural and Environmental Engineering
_____ Wimal Suaris, Ph.D. Associate Professor of Civil, Architectural and Environmental Engineering	_____ Francisco J. De Caso y Basalo, Associate Scientist of Civil, Architectural and Environmental Engineering
_____ Landolf Rhode-Barbarigos, Ph.D. Assistant Professor of Civil, Architectural and Environmental Engineering	_____ Guillermo Prado, Ph.D. Dean of the Graduate School
_____ Marco Savoia, Ph.D. Professor of Civil Engineering University of Bologna	

ROCCHETTI, PAOLO (M.S., Civil Engineering)
(August 2017)

RC Traffic Railing Designs with GFRP Reinforcement

Abstract of a thesis at the University of Miami.
Thesis supervised by Professor Antonio Nanni.
No. of pages in text. (125)

The aim of this thesis is to develop the necessary design knowledge and tools to implement an innovative Glass Fiber Reinforced Polymer (GFRP) rebar shape in traffic railings. The innovation lies in the use of GFRP continuous closed stirrups that have become recently available. The design method is based on AASHTO-LRFD Bridge Design Specification and the latest specifications issued by the Florida Department of Transportation (FDOT) for Reinforced Concrete Traffic Barriers. After the review of existing design procedures focusing on traffic barriers and understanding the mechanical characteristics of GFRP reinforcement, a modified design approach is proposed for reducing reinforcement ratios and complexity in construction. The effort included two different type of traffic railings, namely: 36"–Single Slope (36–SS) and FDOT 32" F–Shape (F32). The 36–SS is to be used as a later time test specimen. The F32 is showcased in the Halls River Bridge Replacement Project. Finally, a Mathcad application tool developed for public use as part of the FDOT design examples library illustrates the application of this configuration for traffic barriers. Continuous close GFRP stirrups champion the versatility of the FRP composite technology by accommodating to most requirements. The use of GFRP stirrups in traffic railings complements the application of non-corrosive reinforcement in transportation structures to address the demand for sustainable construction practices

Contents

Chapter 1: Introduction

1.1 Research Implication

The corrosion of the structures is one of the main issues that reduces the Service Life and strongly affects maintenance costs of infrastructures. Many studies have been done in order to define the cost of corrosion. CC Technologies and Federal Highway Administration (FHWA) did a benchmark study about the cost of corrosion, and they estimated that the total corrosion around the 3.1% of the gross domestic of the United States, which corresponds to $276 billion per year [1]. Due to aging, lack of maintenance and exposure to aggressive environment, civil infrastructure facilities in U.S. and abroad deteriorate. The total number of highway bridges in the U.S. is 614,378, according to American Society of Civil Engineer (ASCE) in 2017. 9.1 % is considered structurally deficient in 2016 and almost four out of ten of which are 50 years or older. On average there were 188 million trips across a structurally deficient bridge each day [2]. The recent estimation of the costs substitution in the U.S. of these bridges is around $123 billion. Most of the bridges are made of steel or reinforcement concrete and most of them are subjected to significant levels of corrosion. The cost of corrosion for those bridges is estimated to be $8.29 billion every year, considering maintenance as well as the replacement of structurally deficient bridges, which equals 16.4% of the total infrastructures cost[3].

The American Society of Civil Engineers (ASCE) is committed to protecting the health, safety, and welfare of the public and, as such, is equally committed to improving the nation's public infrastructure. America's civil engineers provide a comprehensive

assessment of the nation's major infrastructure categories every four years through the ASCE's Report Card for the U.S. infrastructure [2]. In 2017, infrastructures received a D+, and bridges earned a C+ (Figure 1).

The challenge for federal, state, and local governments is to increase bridge investments by $8 billion every year in order to reach the identified $76 billion which are needed for deficient bridges across the U.S.

The Florida Department of Transportation (FDOT) is the executive agency that coordinates the planning and development of the transportation system in the state of Florida. FDOT submits a plan of 5 years of works to maximize the department's production and service capabilities through increased productivity, reduced cost, innovative use of resources and strengthened organizational effectiveness and efficiency.

The work program consists of 6,987 projects starts from the year 2014/2015 through 2018/2019 and includes the construction of 762 lane miles of roadway, replacement of 76 bridges and reparation of 190 bridges.

Better corrosion management can be achieved using preventive strategies at every project and includes the change of policies, the increased awareness of large corrosion costs and potential savings, regulations, standards, development, management practices, advance of design practices and technology through research, and implementation.

All the infrastructures have to be designed with respect to the natural environment and withstand both natural and man-made hazards.

Finally, the research should study and develop new and more efficient methods and materials in order to ensure the infrastructures can be maintained longer. One of the most

important aspects is corrosion, which requires new technologies like Glass Fiber Reinforced Polymer (GFRP). This technology can reduce significantly the indirect cost of rehabilitation, maintenance and replacement of systems.

Figure 1 - ASCE Report Card for Bridge

1.2 Glass Fiber Reinforced Polymer: Components, Use and Production

A Composite material is made from two or more constituent materials with notably different physical or chemical properties. When combined, the single components produce a material with different characteristics to the originals. In the final material structures, the components remain separate and distinct Nanni, De Luca [4].

GFRP is a composite material that is made from glass fibers which provides strength and stiffness. The resin matrix, when properly embedded, transfers loads between fibers and also protects them from chemical attacks. The combination of the two materials leads to a final product with superior properties and better performance than the individual components alone. Because of the protective resin, GFRP rebars are almost not corrosive

which lead to a significant market adoption and different applications of the material in the construction industry and in infrastructures. Corrosion of reinforcing steel rebar is one of the main problems in concrete structures and a major durability concern. Over time, concrete inevitably cracks because of shrinkage or other mechanisms that expose the steel rebar to external agents that induce corrosion of the steel (chlorides, sulfates, carbon dioxide, etc.).

GFRP rebars have been analyzed as valid alternative solutions, and different GFRP products were tested in laboratory and structural application for various concrete components. Over time, such materials have been proven to be an adequate alternative to traditional steel reinforcements. Nowadays, many different manufacturers around the world produce GFRP rebar that can be used in structural applications. Each company has their own production methods and uses different resins and/or fiber types and the final product strongly depends on that [5].

The three main functions of the resin matrix are to protect the fibers from mechanical and environmental attacks, to maintain the alignment of fibers, and to guarantee proper load transfer between individual fibers. There are two classes of resins: thermoset and thermoplastic resins. Thermoset polymeric resins are the most commonly used ones to produce GFRP rebar [4]. Initially, in their virgin state, thermoset polymeric resins are usually liquid (Figure 2) at room temperature, but sometimes they are solid with a low melting point.

To properly penetrate the fibers, resins are heated to temperatures of approximately 177° C [6]. Heat treatment and catalysts are used in the curing process to solidify the resin. After

curing, the material is locked into shape and cannot be converted back to the original liquid form.

Figure 2 - Thermoset polymeric resin in liquid state

On the other hand, thermoplastic resins do not cure permanently, and can always change from solid to liquid through increased temperatures. Therefore, thermoplastics are not acceptable for structural applications. The thermoset polymeric resins, polyesters, vinyl esters, and epoxies are the most used resin-matrix materials in FRP Reinforcement rebar designated for civil engineering applications [4].

Fibers are the major load-carrying component in FRP composites. On the worldwide market, there are FRP reinforcing rebar made from various types of fibers, with different volume fractions and orientations of these filaments. One of the important aspects of these fibers is the size, which will differentiate between producers [5]. The size of the fiber is a critical element to determine how fibers will handle during the processing and how they will perform. Different types of fiber are used in FRP rebar, mostly fiberglass, followed by basalt and aramid. Carbon is also used, but typically for pre-stressed applications.

As shown in Figure 3, the engineering properties of FRP rebars highly depend on the utilized fiber type.

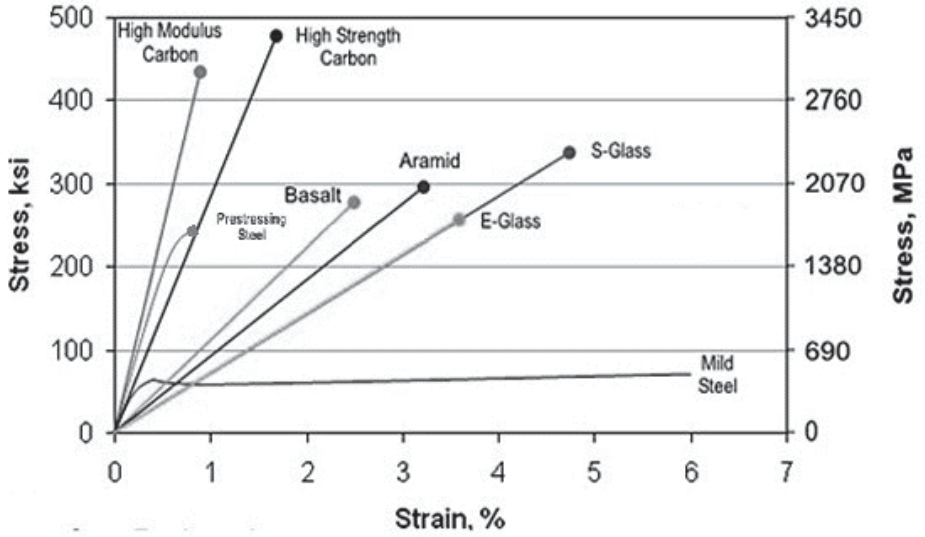

Figure 3 - Tensile stress and strain of different types of fibers [7]

According to Busel et al. [7] the tensile strain capacity of GFRP rebar is higher than the tensile strain capacity of carbon or aramid FRP rebar, while the reverse is true for the tensile strength. Fibers made from glass are among the most economic ones along with basalt, while carbon fibers are the most expensive. The cost of aramid fibers are comparable to the price of low grade carbon fibers [8].

The three main glass classes used for GFRP reinforcement are E-glass, C-glass and S-glass. E-glass, where “E” stands for “electrical application”, is the first type used to produce continuous filaments. It was first used in electrical applications due to its low conductivity and its permeability to magnetic fields. C-glass, where C stands for “chemical resistance,” is mainly used in aggressive environments and S-glass, where S stands for “stiff” is used in application where is required high strength modulus.

Although C-glass and S-glass have the highest strength properties and corrosion resistances, the E-glass is the most used for civil engineering and industrial applications because it is the easiest and cheapest to obtain [8].

Extensive variety of fibers are present on the market, which are used in GFRP reinforcement rebar as ECR-glass, A-glass, Ar-glass (alkaline resistance), D-glass, R-glass and S-2 Glass [8].

Since GFRP is a composite material the rebars are highly anisotropic (unlike steel rebar which can be considered as a isotropic material): the GFRP rebars are strong along their main axis but weak in the transversal direction [4]. Therefore, the compression and tension strength resistance are the same, and are higher than the shear strength. Moreover, in compression when the ratio between the height and width make the fiber instable and, thus, seem fragile, then the strengthening of the compressive capacity could prevent GFRP fibers from buckling.

The typical cross-sectional shape of the rebar is solid and round, but other shapes are available in the market [9](Figure 4).

The characteristics of the several cross sections present interesting and important differences, therefore to use the most suitable rebar for any project it is important to know the advantages and disadvantages of each type.

Figure 4 - GFRP rebar with different cross-sectional shapes [9]

The most used GFRP rebar manufacturing method is the Pultrusion Process. The Pultrusion process is a continuous manufacturing process used to make FRP profiles with consistent cross-sectional properties, such as rebar. It is a continuous molding process that combines fiber reinforcement and thermosetting resin. Figure 5 shows schematically the basic steps and production sequence of the pultrusion system. The process begins by inserting the fiber into the machine. To keep the fiber in tension, the reinforced fiber are threaded into the tension roller. This roller is the first component that prepares the product for its final shape by grouping them accordingly. Then the fibers pass through a resin bath for impregnation. The resin-soaked fibers are then heated in the steel forming dye to create the final shape of the material after the resin has cured. Then a pull mechanism extracts the cured product and advances it into the cutting station. The mechanical properties of GFRP are ultimately affected by the fiber volume, rate of resin polymerization, manufacturing process and the quality control process. Furthermore, the strength of the rebar depends on its diameter [9]. The production of rebar bents remains a challenge to GFRP rebar manufacturers because

rebar cannot be bent after curing when a thermoset is used [4]. The strength for normal bent rebar is reduced in current standards, with safety factors, from 40 to 50 percent compared with the tensile strength of a straight rebar with same diameter [10].

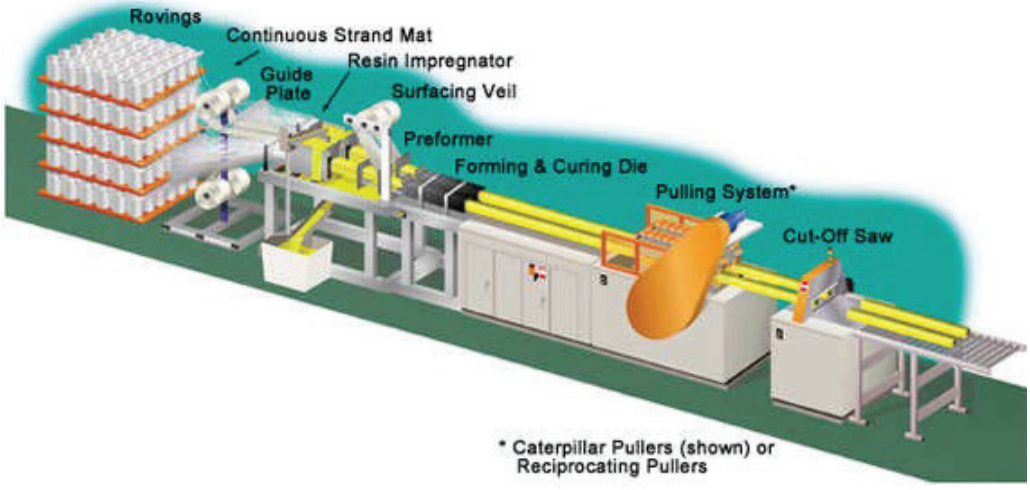

Figure 5 - Pultrusion process for the manufacture of GFRP rebar

The FRP rebar can have different diameter size, the most common and used in construction are reported in the following Table.

Table 1 - Size designation of FRP round rebar

Rebar size designation	**Nominal diameter**		**Nominal area**	
#	**in.**	**mm**	**in²**	**mm²**
2	0.25	6.4	0.05	32
3	0.37	9.5	0.11	71
4	0.5	12.7	0.2	129
5	0.62	15.9	0.31	199
6	0.75	19.1	0.44	284
7	0.87	22.2	0.6	387
8	1	25.4	0.79	510
9	1.13	28.7	1	645
10	1.27	32.3	1.27	819

AASHTO LFRD 2009 for GFRP-RC Bridge Design [11] reports the minimum required tensile strength associated to the rebar diameters that the manufacturers have to respect and is shown in Table 2.

Table 2 - Minimum Tensile Strength as reported by manufacturer, AASHTO LRFD

Rebar size designation	**Minimum Tensile Strength**	
#	**psi**	**MPa**
2	110,000	758
3	110,000	758
4	100,000	689
5	95,000	655
6	90,000	621
7	85,000	586
8	80,000	552
9	75,000	517
10	70,000	483

Since the thermo-set materials cannot be post-formed, to produce non-linear shape (as continuous closed stirrups) the shaping can only be done during the "non-totally polymerized" phase. In order to make non-linear shapes, such as continuous closed stirrups, two different manufacturing processes are used:

- A rod can be produced with "non-polymerized spots" located at the bending points; then this rod is precisely placed on a form producing the final shape; the stirrups are done when the polymerization is completed. As a result, the straight section of the stirrup will maintain typical characteristic of regularity and smoothness of the section as designed, while the bent parts will show some deformations like wrinkles on the

compressed side and irregular section on the tensed side. In this case, a reduction factor of 50% is considered for the strength in the bent regions.

- The stirrups are produced with a closed loop by positioning the uncured fiber-resin system on frames with the design curve adaptors at the bending points, which are four in the case of rectangular or square shape. A winder rotates the steel frame at a set velocity. Special bushing will reproduce the wanted curvature. From a rack the fibers are pulled into the frame and forced to submerge in a resin bath, and after that it will reach the frames. After total polymerization, the molds are taken apart to collect the finished product and recomposed for new production. With this procedure in the bent zone, where the wet fiber is easily and precisely placed on the curved bushing-mold, a fiber geometrical regularity is obtained, even better than the "non-guided" rectilinear zone. Therefore, it is correct to consider the bent part of the closed stirrups as "equivalent" diameter stirrups as the continuous zone of the rebar, as recommended by ACI 440.3R-04 PART 2.

1.3 Objectives: The Use of GRFP

The projects and the information present in this thesis is part of a larger and exiting program, where the goal is finalized to fully understand composite materials in bridge construction in order to make this technology available to professionals and bridge owners. Almost all the bridges in the U.S. and abroad are made of steel reinforced concrete, which are fully exposed to degradation related to corrosion; the maintenance and replacement of those bridges is an expensive priority. Therefore, the incrementing of the existing and the new bridge with a non-corrosive GFRP rebar as internal reinforcement for concrete bridge

components has a significant potential for extending the service life of a structure. Moreover, GFRP internal reinforced rebars are lightweight, high-strength and can substitute steel rebars in many applications. Nowadays, the initial cost of GFRP is one of the biggest disadvantages if compared to that of steel reinforcement. Since the initial cost of GFRP is considerably higher sometimes it can be seen as an unattractive alternative; but, in reality, the initial cost of a bridge is small compared to its Life Cycle Cost. The final cost of the structures may be smaller using GFRP reinforcement than steel because those reinforcements potentially can increase the serviceability life of the infrastructure and reduce the maintenance cost.

Moreover, a recent project called “Seacon” is producing an innovative sustainable concrete made with sea water, which can be reinforced only with non-corrosive rebars, as the GFRP rebars and not with normal steel reinforcement.

The advantages of those composite materials incite to build more than 190 installations with FRP in the U.S. and in more than 50, GFRP is used as a bridge deck reinforcement [3].

1.4 Traffic Barriers

A traffic barrier is used to redirect safely an errant vehicle away from a hazard, such as an oncoming car from the opposite direction, or dangerous obstacles like trees, rocks, sign supports, bridge abutments and buildings etc. [12].

Ideally, a traffic barrier should redirect and decelerate the vehicle in the road away from the hazard with a narrow angle and, at the same time, should not overturn, spin or result in significant damages to the vehicle that may cause injury or be fatal to the occupants. The

deceleration and the redirection of the vehicle should be within human tolerance and comfort levels [12].

Usually, barriers are made of steel, concrete or plastic (for temporary use only). Sometimes, steel railing are added over a concrete barrier in order to prevent the rollover of vehicles. Steel barriers can be made as guardrail, tubular sections or wire rope. It is common to use steel barriers in order to reduce the severity of a crash. Steel barriers are semi-rigid or flexible, therefore, during accidents they can deform in order to reduce the impact force to the vehicle and passengers.

In contrast, concrete traffic barriers are considered rigid since the deformation during the impact is small, no more than a few inches [12]. This displacement/deformation is called "working width". In steel barrier the working width may reach deformation up to 13 ft. (4 m), but usually it is preferred to not pass 6.5 ft. (2 m).

When high force level is required to redirect the vehicle and there is not enough working width to accommodate a deforming barrier, strong rigid barrier are used. Another reason to use rigid barrier is that repair maintenance is much lower than for deformable ones.

In the U.S., the four most common types of rigid concrete traffic barriers are the New Jersey Barrier, the F-Shape Concrete Barrier, the Single Slope Traffic Barrier and the Vertical Concrete Barrier. Usually, these are called "Safety Shape Barriers", which proved to have satisfied impact performance during impact tests [12]. None of these standard barriers are perfect and all have some imperfections, which depend on the vehicles type, angle of impact and height of the impact.

The New Jersey shape and the F-shape barrier (Figure 6) which both are descendants of the traffic barrier developed by the General Motor (called GM shape), have incorporated a steep upper slope with a shallow lower slope. If the impact has a low impact angle, the tires ascend the lower part of the slope and redirect the vehicle without the contact of sheet metal with the barrier. The upper part of the angle is made to redirect the vehicles which impact at a higher angle.

The GM shape was not developed by crash testing, and at a time when cars were larger and heavier. Now GM is considered obsolete because it demonstrated to have unacceptable performance in crash tests [13].

The most used traffic barriers in the U.S. are the New Jersey barriers. The name came from the first traffic barrier that was installed in New Jersey in 1955. Apparently no crash tests were carried out in the development of the upgraded New Jersey barrier.

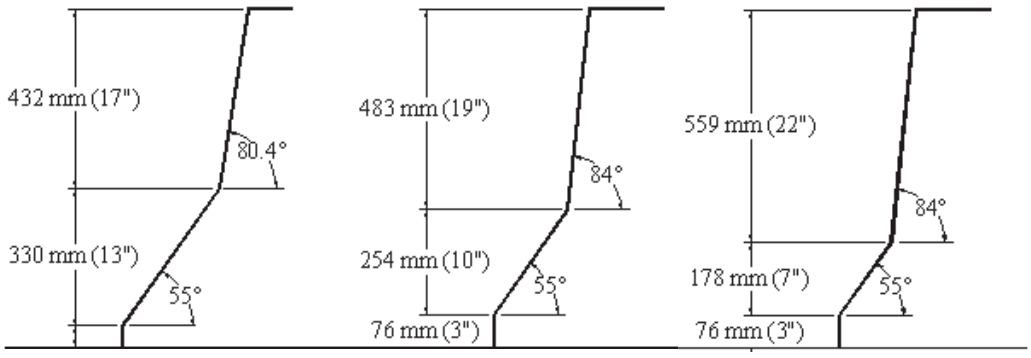

Figure 6 - Safety Shape concrete traffic barrier, (a) GM Shape, (b) New Jersey shape, (c) F-Shape [13].

The New Jersey has different height from GM shape, from 13 in. (330 mm) to 10 in. (254mm) but has a similar lower shape slope of 55°.

The vehicle impacting the slope of the barrier will present a longer time impact and, consequently, a lower peak impact force compared to a vehicle impacting a vertical barrier. This lower peak impact reduces accelerations acting on passengers as compared to a flat wall with the same height. On the other hand, tire climbing the barrier could made the vehicle to rollover. The risk of serious injury or fatality is much higher in rollover accidents than in non-rollover accidents.

The F-shape barrier were designed in order to reduce the percentage of vehicles climb and roll-over in the basic New Jersey traffic barrier (developed in 1976).

Single Slope Traffic Barriers were developed in 1989 in California as a modification of the well-known NJ barriers [19]. The aim of the Single Slope Traffic Barrier is to reduce the rollover of the vehicles during the impact, which may cause more injury and fatality. The impact force has almost a horizontal direction that will limit the climb to approximately zero (increase of the overall stability). On the other hand the peak force that will be transferred to the passenger will be higher, increasing the risk of injury [2]. For example a passenger's head slapping the side window is one injury that could occur during a lateral impact to the barrier, increasing the risk of death.

An advantage to consider in single slope barrier as compared to more complex shapes is that the performance is not as affected by changes in the roadbed's height during repaving. It is also easier to construct. Some examples are California Type 60 barrier with a single slope of 9.1° and Texas SSCB with a slope of 10.8° (Figure 7) most used for TL-5. In general for TL-4, the minimum used elevation is 32". A single slope 36" is adopted by the TxDOT and it will be used as the FDOT standard.

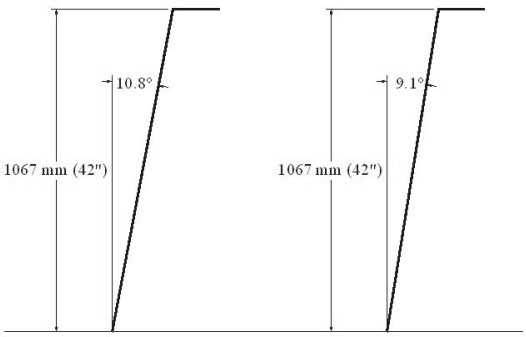

(a) (b)

Figure 7 - Single slope traffic barrier, (a) Texas SSCB, 2(b) California type 60

1.5 State of the Art: GFRP RC Railings and Barriers

The use of GFRP rebar in most of the traffic railings, until now, were involved in vertical-faced systems. In the last few years, as mentioned before, GFRP manufacturers could produce bent rebar and also closed stirrups. These new technologies allow for new design of traffic railings which are not Vertical-faced.

In North America there are several examples of field implementation that have demonstrated the validity of traffic barrier with GFRP reinforcement. Also some research projects tested the validity of this implementation. The first traffic barrier realized with GFRP reinforcement were open post-rail. In 2003 an experimental investigation on continuous GFRP RC traffic barrier was conducted by El-Salakawy et al. [14] subjected on static and pendulum impact tests.

The test results showed that traffic barriers reinforced with GFRP have similar failure behaviors as traffic barrier reinforced with steel. The ministry of transportation of Quebec (MTQ) approved the use of two traffic barriers with GFRP RC: one bridge in Val-Alain,

in 2004, on Highway 20 with a performance level of 2 and in Melbourne, in 2005, on the Highway 55 with a performance level of 3 [15, 16].

A joint project "FRP Reinforcing Rebar in Bridge Decks", involving TxDOT Texas Transport Institute, the University of Texas at Arlington, and Texas Tech University , was initiated in August 1999. The barriers used were concrete bridge railings supported by concrete posts spaced 5 ft. (1.5 m) apart. Both tests showed structural adequacy of rail. Since the collision loads imposed on the bridge railings, in full scale crash test, were easily resisted, the structural failure modes for the bridge railings with GFRP RC were not identified. The TxDOT T202 with GFRP RC, contained and redirected the truck and no measurable deflection was noted [17]. As we can see from Figure 8, the truck impacted the barrier without penetrating it, the vehicle did not overturn or spin and high damage was not recorded.

Figure 8 - Sequential Photographs for test 441382-2.

The owner of the Bridge 14802301 in Greene County (Missouri, USA), decided to use the replacement of the 70 years old slab and girder superstructure. The use of only prefabricated GFRP reinforcement for RC deck and open post railings came after two years of research and development and technology transfer project. The re-decking was done in only five days with a reduction in construction time and labor cost of more than 70% compared to the traditional process. GFRP prototypes were designed using an equivalent amount of reinforcement compared to the steel RC system. Open GFRP stirrups were used

to connect the curb to the deck and the transverse strength of the GFRP RC systems exceed the mandatory static load demand required from the code, similar to steel RC system (Figure 9).

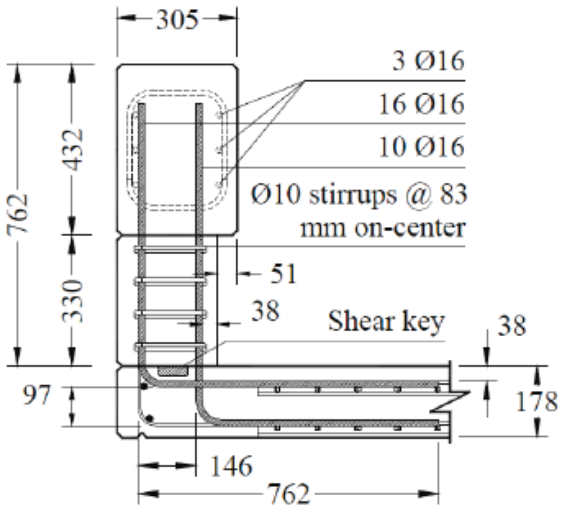

Figure 9 - Open Post railings. (units are mm) [3].

The rehabilitation of John Street CNR Overhead Bridge, (Ontario, 2012) was made using vertical-faced barriers. Two vertical straight rebar connected to the longitudinal reinforcement was the transverse reinforcement. These vertical rebars were embedded in the concrete deck before the cast of the traffic barrier. The transverse rebars used in the case of Boulevard West Bridge in Lakeshore were coupled with 90 degree bent rebar, used to increase the bond between deck and traffic barrier [18]. GFRP U bent rebar, joined in a close loop, is also used to connect the traffic barrier with the deck; an example of this is used in Eglinton Avenue Bridge, in Toronto as well as in the design of Clark's Mill Bridge with transverse reinforcement of GFRP (Figure 10).

Double head galvanized steel of 0.87 in (22 mm) with 11.8 in (300 mm) spacing connects the traffic railing to the deck and the deck reinforcement. The splicing needs to be adequate in order to transfer the load from the parapet to the bridge.

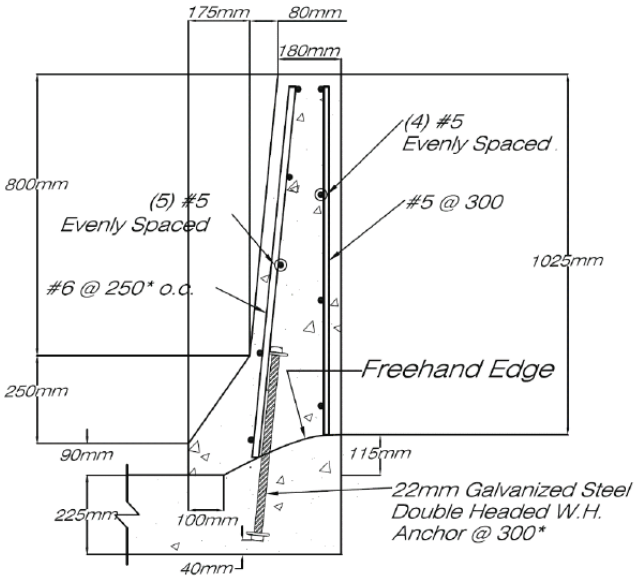

Figure 10 - Clark's Mill Bridge traffic barrier [19]

In the case of the Ross Corner bridge, double bent GFRP rebar and 90-degree of bent rebar are used (Figure 11)[20]. Those rebars are connected to the deck reinforcement. After casting the deck, another bent rebar is placed at 90-degree, connected with longitudinal and vertical rebar.

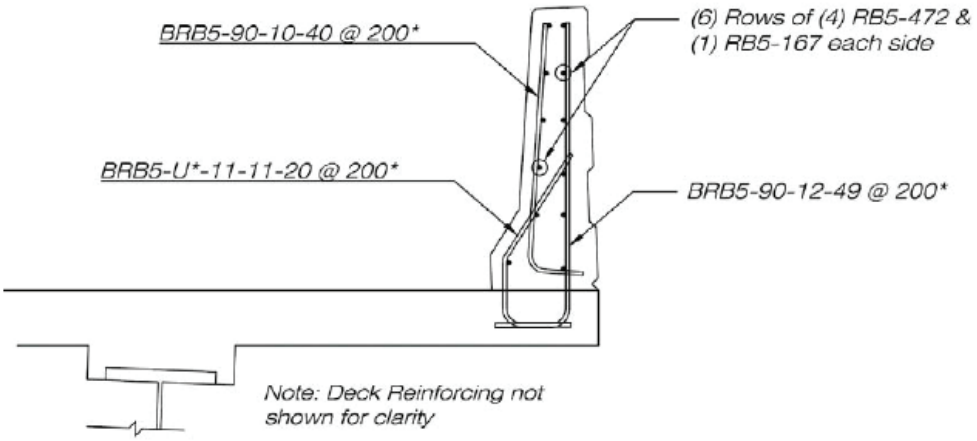

Figure 11 - Ross Corner bridge traffic railing [20]

In Baden Creek Bridge, a similar rehabilitation method was used with three different types of bent rebar in order to optimize the shape. In order to provide anchorage, the rebars are embedded inside the deck [18].

1.6 Thesis Outline

This thesis is divided in three principle parts and supported by six appendices. The first part, the Chapter 2, introduces the design method based on AASHTO-LRFD Bridge Design Specification and the latest specifications issued by the Florida Department of Transportation (FDOT) for Reinforced Concrete Traffic Barriers. In the third chapter, some final design of F-Shape 32 in. of height (F32") and Single Slope 36 in. of height (SS36") are shown, both RC traffic barriers with GFRP reinforcement. This examples includes: the design of the F32" RC Traffic Railing of the Halls River Bridge (Homosassa, FL) and the SS36" which will be used as a test specimen from Florida Department of Transportation (FDOT). The fourth chapter shows how to use the Mathcad file (reported in Appendix C) related to the design of the F32" RC traffic railings with GFRP reinforcement.

Appendix A presents the innovation aspects of Halls River Bridge and the constructability process of the bridge and the traffic railings. The calculation supporting the design of the traffic barrier F32" of the Halls River Bridge approved by FDOT is presented in Appendix B. The final drawings of the Halls River Bridge traffic railings, approved by FDOT are shown in Appendix D. In Appendix E, the calculations of SS36" made by Excel are presented and in Appendix F, the final drawings approved by FDOT which will be used as a pendulum specimen are provided.

Chapter 2: Design of Traffic Railings, GFRP RC Type Parapet

2.1 Assumptions

In traffic barriers crash testing aims to determine the structural and geometrical crashworthiness and, both, have to depend on the Service Level chosen.

There are several type of traffic railings depending on the variation in traffic volume, vehicle mix, speed, roadway alignment, condition and activities of the structure, which involve different performance requirements.

Modern traffic barrier have to be structurally and geometrically crashworthy. The protection of the passengers and drivers of vehicle in impact with the barrier, of people and property on the roadway and of the vehicles near the impact point should be considered. Other considerations includes cost-effectiveness, future rail up-grading and variation in traffic volume [21].

In 1993, the National Cooperative Highway Research Program (NCHRP) in the Report 350 produced the standard for the performance of the safety evaluation of highway features [22]. NCHRP report 350 gives a guide on the procedure of the crash testing, on the impact conditions for barriers, crash cushions and a description of the evaluation criteria of each test.

Six different test levels are defined in the Report, from TL-1 to TL-6, with an increase on each level of severity and impact loading. First of all, the test level of the project should be defined:

- Test Level One (TL-1): generally, this level is suitable for work zones with low posted speeds and very low volume, low speed local streets.

- Test Level Two (TL-2): generally, this level is suitable for work zones and most local and collector roads with favorable site conditions as well as where a small number of heavy vehicles is expected and posted speeds are reduced.

- Test Level Three (TL-3): generally, this level is suitable for a wide range of high-speed arterial highways with very low mixtures of heavy vehicles and with favorable site conditions.

- Test Level Four (TL-4): generally, this level is suitable for the majority of applications on high speed highways, freeways, expressways, and Interstate highways with a mixture of trucks and heavy vehicles.

- Test Level Five (TL-5): generally, this level is suitable for the same applications as TL-4 and where large trucks make up a significant portion of the average daily traffic or when unfavorable site conditions justify a higher level of rail resistance.

- Test Level Six (TL-6): generally, this level is suitable for applications where tanker-type trucks or similar high center of gravity vehicles are anticipated, particularly along with unfavorable site conditions.

For TL-3, traffic barrier are at least 27 in. (0.69 m), for TL-4 the minimum is 32 in. (0.81 m), for TL-5 the minimum is 42 in. and for TL-6 the minimum is 90 in. (2,23 m) [21].

The performance factors as post-impact behavior of vehicles, risk for the occupants and structural adequacy are some features that are evaluated in bridge railing design.

The impacting dynamic force of the vehicle under specific crash test conditions are converted in AASHTO in equivalent static loads to be used for structural design [22], as

transverse force F_t, longitudinal force F_l, and Vertical force F_v (Table 3). The transversal impact length Lt and longitudinal impact length Ll are also evaluated. Since serviceability requirements are not a major concern, these loads are referred to ultimate limit state conditions. The transverse load is typically the one concerned in the design load for traffic railings.

Table 3. Design Forces and Dimensions for Traffic Barriers and Railings

Design Forces and Designations	**Railing Test Levels**											
	TL-1		**TL-2**		**TL-3**		**TL-4**		**TL-5**		**TL-6**	
	kips	**kN**	**kips**	**kN**	**kips**	**kN**	**kips**	**kN**	**kips**	**kN**	**kips**	**kN**
Ft Transverse	14	60	27	120	54	240	54	240	124	552	175	778
Fl Longitudinal	5	20	9	40	18	80	18	80	41	182	58	258
Fv Vertical	5	20	5	20	18	80	18	80	80	356	80	356
Dimensions:	**in.**	**mm**	**in.**	**mm**	**in.**	**mm**	**in.**	**mm**	**in.**	**mm**	**in.**	**mm**
Lt and Ll	48	1219	48	1219	48	1219	42	1067	96	2438	96	2438
Lv	216	5486	216	5486	216	5486	216	5486	480	12192	480	12192
He	18	457	20	508	24	610	32	813	42	1067	56	1422
Min. H Height	27	686	27	686	27	686	32	813	42	1067	42	1067

In 1978, the Texas Transportation Institute studied and developed a method to evaluate the structural resistance of reinforced concrete traffic barrier [23]. This method is known as yield line theory and it is based on the conservation of energy principle and to an estimation of rupture shape to predict the ultimate strength of the barrier. First it is found a postulation of failure mode kinematic collapse mechanism that satisfies the yield criterion at the yield lines; then an upper-bound ultimate load is determined by equating the work done by the external load and the resistance forces at the yield lines. Since it is a statically indeterminate system, a redistribution of bending moments with plastic rotations have to be assumed. In this way, both longitudinal and overturning resistance could be determined and ultimate strength of the barrier can be evaluated (Figure 12).

Due to the linear elastic behavior of the GFRP rebars, moment redistribution cannot be taken in account in the analysis of indeterminate structures; therefore, the yield analysis cannot be used.

The results of a full-scale static tests on post-deck connections reinforced with GFRP rebar were presented by Matta and Nanni, in 2009. The aim of these tests were to assess the compliance with strength criteria at the deck to barrier connection, mandatory by ASSHTO Standard Specifications [10], which are used in design of bridge. Using the strength-convergence method, the strength and stiffness until failure are shown to be predictable.

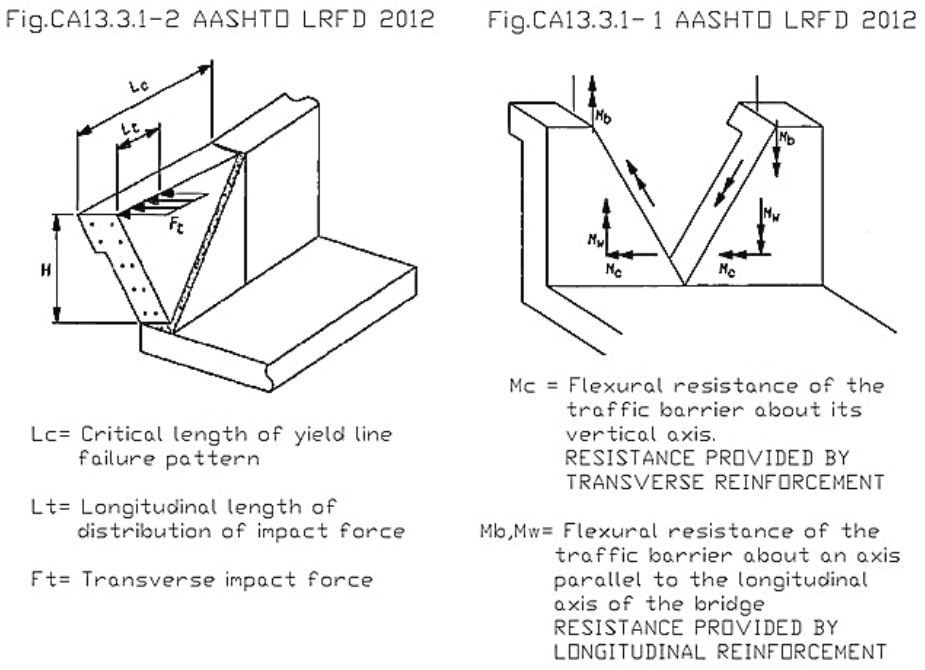

Figure 12 - Yield line analysis of concrete parapet walls for impact within wall segment.

An iterative procedure is used in order to achieve the convergence for tensile load capacity. The methodology to find the strength level of a GFRP RC railing is consistent with the requirement of AASHTO LRFD approach. Since in successful crash tests are not observed large deformations, the torsional effects on the traffic railings can be neglected. Therefore,

the behavior of the traffic barrier into a bi-dimensional system is an appropriate approximation. The design for flexural and shear of GFRP reinforced members follows AASHTO provisions. The equilibrium-convergence method provides a simple and effective method for the design of traffic barrier reinforcement. The following different failure modes may occur when dealing with GFRP railings:

- Concrete crushing;
- GFRP reinforcement rupture in flexure at the weakest connected section;
- Insufficient anchorage of the post or development length of the deck reinforcement;
- Diagonal tension cracking at the corner.

Since GFRP reinforcement members do not exhibit ductile behavior, conservative resistance factors are taken into account in order to have a higher reserve of strength in the member. While the crushing failure mode of the concrete could be evaluated with calculations, the member may not fail accordingly. If, for example, the concrete strength is higher than specified, the failure could happen due to GFRP rupture. For this reason and to establish a transition between the two value of safety factor, ϕ, a transition, a section controlled by concrete crushing is defined as a section in which $\rho_f \geq 1.4 \cdot \rho_{fb}$, and a section controlled by GFRP rupture is defined as one in which $\rho_f < \rho_{fb}$. In between is considered transition between the two values of safety factors (AASHTO LRFD, 2009 - C 2.7.4.2).

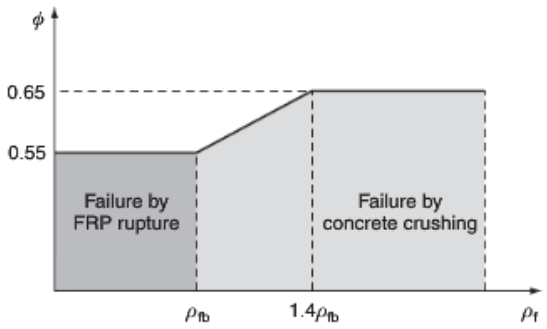

Figure 13 - Resistance factor for flexure [21]

The diagonal cracking of the corner must be avoided to prevent permanent damage in the bridge deck. It is also important that after failure the connection does not separate. When the connection between barrier and deck reaches its strength or when the beam reaches its nominal value, the ultimate transverse load is obtained. Furthermore, the connections need accurate detailing and inspection:

- Effectiveness of the barrier/deck construction joint;
- Effectiveness of the anchorage of the bent rebar within the deck;
- Developable tensile stress in straight or bent rebar in the deck;

2.2 General Design Steps

This study provides guidance for the design of a cast-in-place GFRP RC traffic barrier. The design procedure is the same for the traffic barriers F32” and SS36” and it was done using Excel.

A six-step procedure was implemented for the design of the traffic barrier:

- Input Data and Geometry
- Development Length and Connections
- Design Loads

- Flexural Verification: Limits for Reinforcement and Flexural Strength
- Shear Verification: Concrete Shear Strength and Shear Reinforcement Strength
- Results

2.3 Input Data and Geometry

The geometry and the material characteristics of the GFRP RC traffic barriers have to be defined first. The GFRP mechanical properties can be defined according to the minimum requirement of ASSHTO LFRD 2009, or from manufacturers. The concrete modulus of elasticity, the strain and the strength can comply with either FDOT requirements or with manufacturers.

The geometry of the sections F32" and Single Slope 36" is different and two sections are reported, as adopted by FDOT, in Figure 14 and Figure 15 respectively.

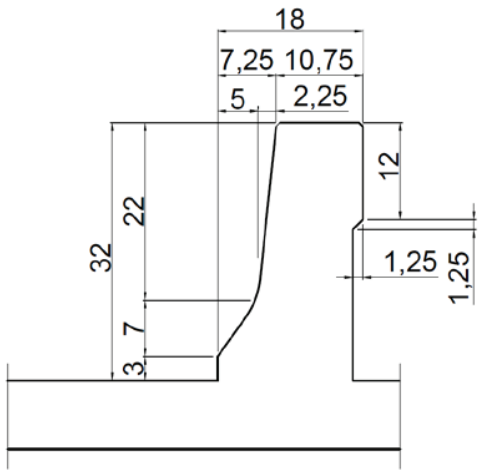

Figure 14 Typical section of F32"

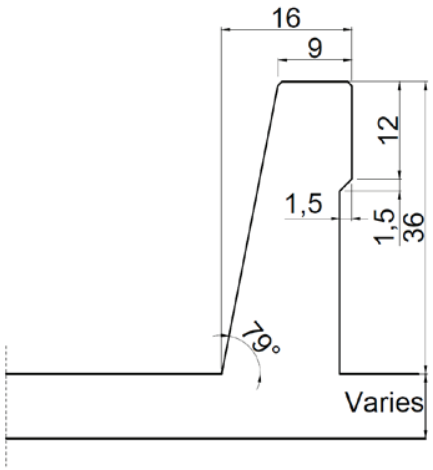

Figure 15 Typical section of SS36”

In order to reduce the gravity of the accidents approaching the bridge, the section at the approaches is usually thinner and may present a different geometry from the typical section through the railing. This change in geometry should be considered because it may alter the dimensions of the internal reinforcement.

The clear cover required strongly affects the internal reinforcement configuration of a traffic railing and the resistance of the section. Since GFRP have much higher corrosion resistance compared to steel reinforcement, it could be possible set the clear cover down to 1.5 in. (38 mm). The clear cover depends, also, on the construction method used (cast in place with a stationary removable form, slip form or precast). For example, according to FDOT, in a slip form construction the minimum concrete cover, as constructed, must not be less than 1.75 in. (44 mm).

2.4 Development Length

The internal rebars must have a minimum length to give continuity between the traffic barrier and the deck, and enough bond resistance. The minimum tension development length which should be used, according to ASSHTO LFRD Bridge Design Guide

specifications for GFRP concrete bridge deck and railings (equation 2.12.2.1-1), is determined as follows: the length L_d should not be less than the results from the equation (1) or $20 \cdot d_b$.

$$l_d = \frac{31.6 \cdot \alpha \cdot \frac{f}{\sqrt{fc'}} - 340}{13.6 \cdot \frac{C}{d_b}} \cdot d_b \qquad (1)$$

α = rebar location modification factor. It is set to 1 except for rebar with more than 12 in. (305 mm) of concrete cast below for which a value of 1.5 shall be adopted.

f_f= effective strength in reinforcement computed according to Eq. 2.9.3.1-1

C= lesser of the cover to the center of the rebar or one-half of the center-to-center spacing of the rebar being developed, in.

d_b = GFRP rebar diameter, in.

ACI-318 also allows a reduction in the computed development length based upon an excess of flexural reinforcement being provided. This reduction is computed as the ratio of the area required to the area provided. In

Figure 18 an example of minimum development length for a bent rebar is shown. The section x-x is the maximum stress section from which the minimum development length should be evaluated and must be greater than L_d.

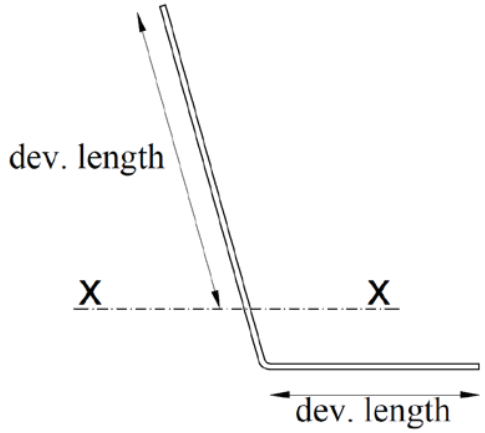

Figure 18 - Development length of a bent rebar

2.5 Design Methods with Two Independent Structural Models

AASHTO requires railings and barriers to be designed both for bending and shear forces acting to their longitudinal and vertical axis. In order to analyze how the impact load is distributed over the traffic railing, two different assumptions of "structural models" are considered. The first assumption is determined considering the traffic barrier as a beam, with a length equal to the impact Lt, pinned at the two extremities. The impact load is considered uniformly distributed over the impact length Lt at the effective height of the vehicle rollover force, He [AASHTO LRFD A13.7.2] (Figure 16). The ultimate bending moment in the center of the beam span and the maximum shear resistance at the two extremities are evaluated.

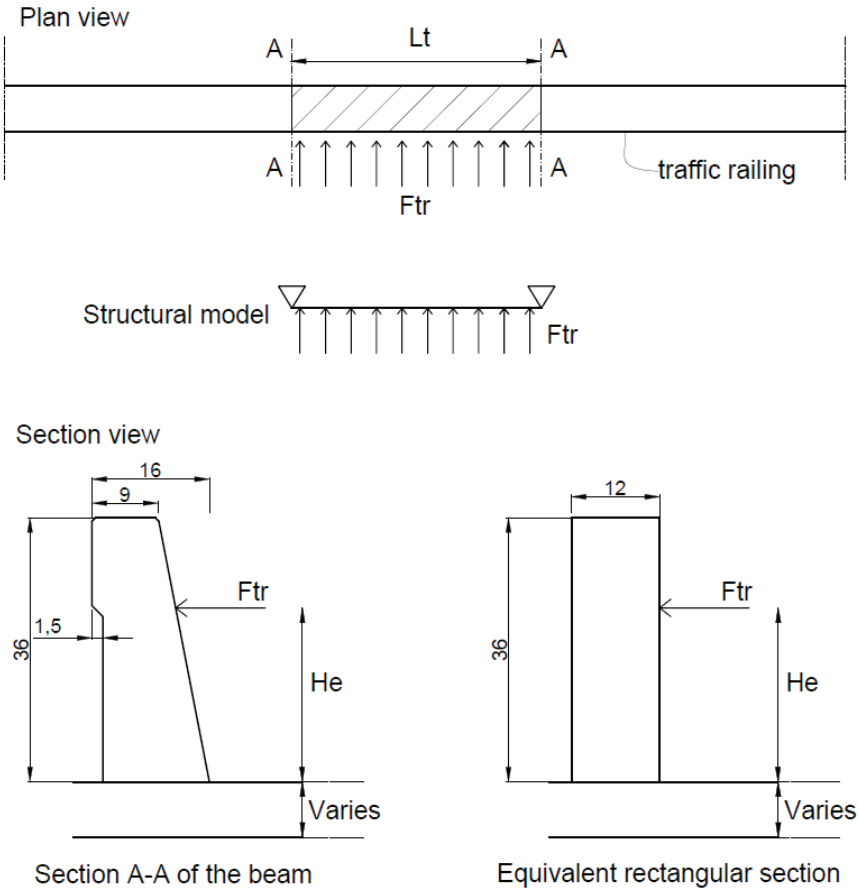

Figure 16 – First structural model

Then, the second structural model considers the traffic barrier as a cantilever slab with a unitary strip length. It is legitimate to consider a fixed restrain between deck and the traffic barrier because the corner region is very stiff and the tests show that the relative rotation between post and deck section is negligible, and mostly is developed after cracking. The transverse impact load, F_{tr} is evaluated over a unitary width. The critical horizontal section of the cantilever slab is defined as the one connected to the deck. An Equivalent continuous rectangular beam shape is used to simplify flexural and shear resistance (Figure 17).

In this way the impact force is analyzed in two failure modes independently, therefore, in each model the reactions are evaluated against the total impact forces F_{tr}. In chapter 3.2 it

is shown an example of the design of the F32” traffic barrier that are the results of this conservative design.

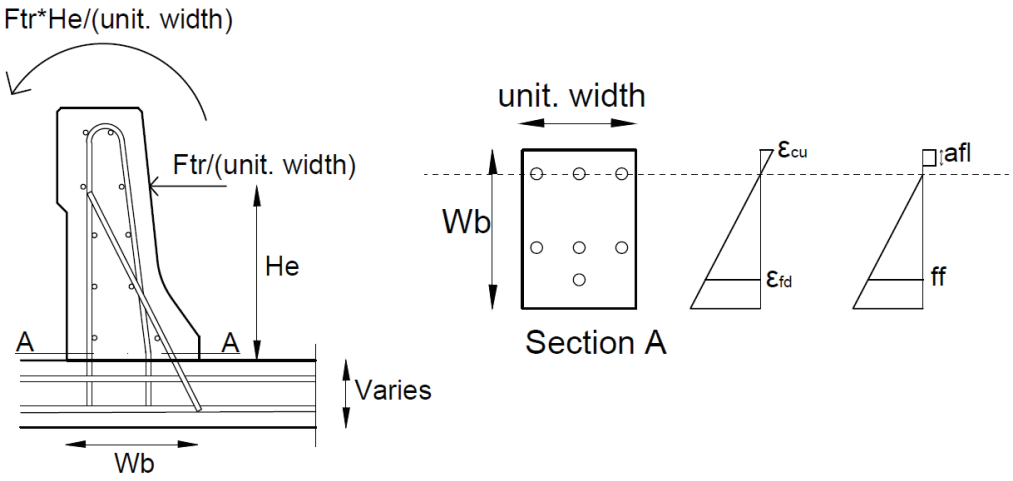

Figure 17- Second structural model

2.6 Design Methods with Two Combined Structural Models

In this thesis, another design method has been studied. The two different structural models presented in chapter 2.5 Design methods with two independent structural models are combined in this method in order to determine a more realistic design.

The traffic barrier will have reactions simultaneously: in vertical direction as a cantilever slab while in horizontal direction as a simply supported slab. In order to determine how the reactions will be redistributed during the impact, the barrier is decomposed in a strip of beams in the two principal directions (horizontal and vertical) through the impact length. The two-way slab will have the following dimensions: a length equal to the length of impact Lt and a height equal to the height of traffic barrier. Since the traffic barrier section presents, usually, an irregular geometry (in particular for F32”), an equivalent rectangular shape section is taken into account instead, therefore the thickness is an average of the traffic railing width. The slab is divided in an equal number of beams in horizontal and in

vertical directions. An equal division is required in order to conserve the same width ratio between the slab and the beams in the horizontal and vertical directions. In this way a better inertia approximation can be evaluated.

Rankine and Grashof's Method has been chosen in order to analyze the redistribution of the loads in the two principal directions. This method which has been popular in codes of practice recommendations assumes a load distribution in two orthogonal directions which are uniform over the entire slab [24]. The loads are carried only by flexure and the twisting moments are ignored. The uniform loads P_x and P_y carried in the respective horizontal (x) and vertical (y) directions are such that:

$$P_x + P_y = P$$

Where P is the total uniform applied load. The actual distributions P_x and P_y are determined by the compatibility of deflections of the center strips [24]:

$$\frac{5 \cdot \mathrm{px} \cdot L_x^4}{384 \cdot E_x \cdot I_x} = \frac{5 \cdot \mathrm{py} \cdot L_y^4}{384 \cdot E_y \cdot I_y} \qquad (2)$$

Assuming that the flexural rigidity of the strips are equal and the strip has the same size it can be determined the amount of P_x only with a geometrical relation of the two lengths:

$$P_x = \frac{L_y^4}{L_x^4 + L_y^4} \cdot P \qquad (3)$$

In a more generic case, where the modulus of elasticity or the inertia of the beam strip may vary, the following formula can be used:

$$P_x = \frac{L_y^4 \cdot Cy}{L_x^4 \cdot \mathrm{Cx} + L_y^4 \cdot Cy} \cdot P \qquad (4)$$

Where Cy and Cx depends on the inertia and the modulus of elasticity of the beams in x and y directions.

The method used follows the simple principle of continuity where, the area in intersection of the two beams in x and y directions will have the same deformation [24] . In the specific case of Rankine and Grashof's Method, the beams were both simply supported therefore the deflection at the mid-span presents the same behavior. Also, the load is equally distributed all over the slab surface.

In the case of the traffic railing, the top-side of the slab is not supported and the bottom-side is fixed, therefore, the vertical beam will behave as a cantilever beam. In addition, the traffic barrier is not subjected to an equally load distribution over its surface.

The central vertical beam and the horizontal beam, where the load is apply (at the height of the impact He), are the two beams considered. These two beams are underlined in red in the Figure 18.

The goal of this redistribution is to define the load reactions at the restrains. In order to do that, the same displacement in the intersection area between the two beams is considered. Defining then the inertia of the beams and the stiffness of the two elements, the percentage of load carried by each beam can be defined (Px and Py are punctual loads, qx and qy are relative loads over unitary length) and therefore the reactions at each sections.

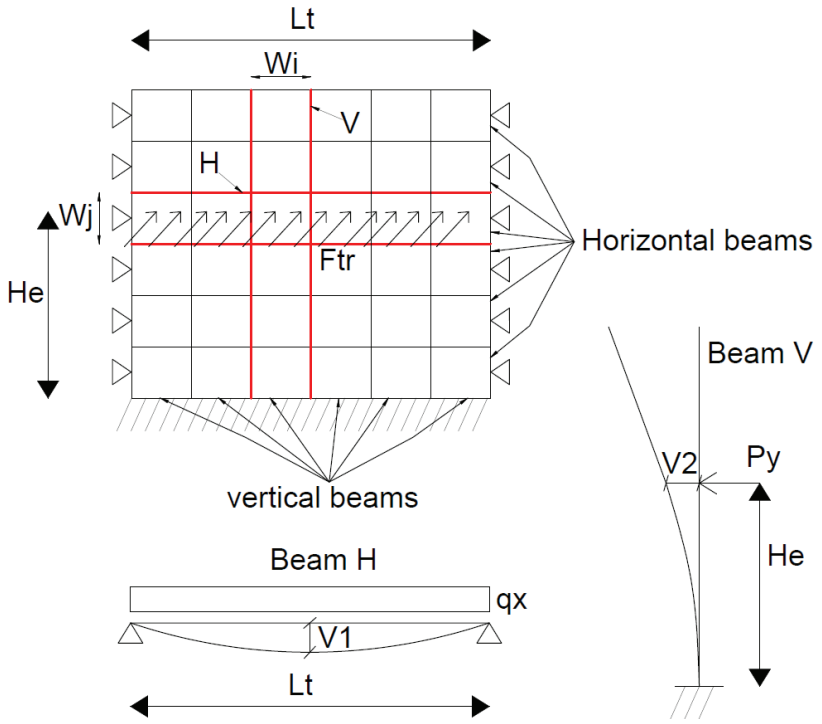

Figure 18 - division of the slab, combination of the two structural model

The displacement of the horizontal beam, for this configuration, is defined as:

$$V1 = \frac{5 \cdot qx \cdot L_t^4}{384 \cdot E \cdot I} = Cx \cdot \frac{qx}{E} \qquad (5)$$

The displacement of the vertical beam, for this configuration, is defined as:

$$V2 = \frac{P_y \cdot H_e^3}{3 \cdot E \cdot I} = \frac{q_y \cdot w_i \cdot H_e^3}{3 \cdot E \cdot I} = C2 \cdot \frac{qy}{E} \qquad (6)$$

Where w_i is the width of the vertical beam (Figure 18).

Therefore the ratio between qx and qy is defined as:

$$Cx \cdot qx = Cy \cdot qy \qquad \text{therefore} \qquad Cx/Cy = qy/qx$$

$$Ftr/Lt = q = qx + qy$$

$$q = qx + (qy/qx) \cdot qx$$

Once the values of qx and qy are found, the total reactions at critical sections can be determined (Figure 19). The total reaction at the bottom section (the fixed section with the deck) is defined as “Rv” and it can be determined as:

$$Rv = qx \cdot Lt$$

The total reactions at the vertical sections (the two pinned sections at the extremities of the traffic railing) are defined as “Rh” and it can be determined as:

$$Rh = \frac{qy \cdot Lt}{2}$$

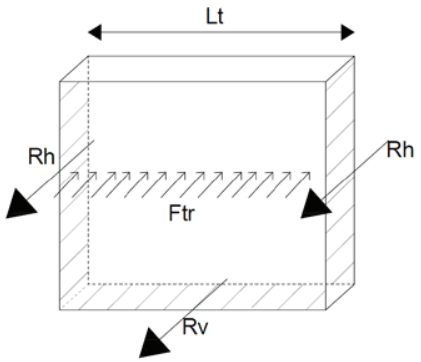

Figure 19 – Total reactions in the traffic railing subjected to the force Ftr.

In this way the reaction on each section are much smaller (with a reduction of around 50%) in respect to the design methods with two independent structural models. Therefore, less GFRP internal reinforcement is required. This is, actually a more realistic method and it results in an internal reinforcement similar to the traffic barrier reinforced with steel. This is supported also from the results of the pendulum test analyzed by El-Salakawy et al. [25] where the traffic barrier with GFRP showed a similar behavior to the one reinforced with steel.

2.7 Flexural Verification

The flexural verification will be made in both the structural models and the two different methods specified before. The different output between the two methods is the design load, therefore the ultimate bending moment.

In the first structural model the ultimate bending moment is evaluated in the midsection of the beam over the impact length Lt, which in the case of a TL-4 is set to 3.5 ft (1.07 m).

In this configuration the flexural resistance of the barrier about its vertical axis is considered. The ultimate bending moment is determined to be:

$$Mu = \frac{F}{Ltl} \cdot L^2_{tl}/8 = F \cdot L_{tl}/8 \qquad (7)$$

Where:

- F is equal to the transversal force (Ftr), in design method 1, and F is equal to qx in design method 2.
- L_{tl} is the length of the impact (TL 4)

The design of the longitudinal rebar is based on this ultimate bending moment and the Requirement Limits for Reinforcement (2.9.3.3) of AASHTO LRFD in which "the amount of tensile reinforcement shall be adequate to develop the factored flexural resistance Mr and at least satisfy the following equation":

$$A_{f,min} \geq \max\left(0.16 \cdot \sqrt{fc'}; 0.33\right) \frac{b \cdot d}{f_{fd}} \qquad (8)$$

Where:

- fc' is the specified compression strength of the concrete [ksi]

- b is the width of the cross section [in]
- d is the Distance from extreme compression fiber to centroid of tension reinforcement, for the section at the top [in]
- f_{fd} = design tensile strength of GFRP rebar considering reductions for service environment [ksi]

Once the minimum total area of longitudinal rebar necessary is determined, then the nominal resistance has to be greater than the ultimate bending moment.

If $\rho_f > \rho_{fb}$ the failure of the section is started by the crushing of the concrete, thus, the nominal resistance, based on force equilibrium and strain compatibility, may be calculated as (AASHTO LFRD 2.9.3.2.2):

$$M_n = A_f \cdot f_f \cdot (d - \frac{a}{2}) \qquad (9)$$

Where:

$$a = \frac{A_f \cdot f_f}{0.85 * fc' * b} \qquad (10)$$

- Af = area of GFRP reinforcement [in^2]
- f_f = effective strength in GFRP reinforcement at the strength and extreme event limit state as specified [ksi]
- a = depth of the stress block, [in]

If $\rho_f < \rho_{fb}$ the failure of the member is initiated by the rupture of the GFRP rebar; since the maximum concrete strain 0.003 may not be obtained, the rectangular stress block cannot be used. Therefore a more simplified and conservative evaluation of the nominal resistance of the member may be used:

$$M_n = A_f \cdot f_{fd} \cdot (d - \frac{\beta 1 \cdot c_b}{2}) \qquad (11)$$

where:

$$Cb = (\frac{\varepsilon_{cu}}{\varepsilon_{cu} + \varepsilon_{fd}}) \cdot d \qquad (12)$$

- β1 = factor taken as 0.85 for concrete strengths not exceeding 4 ksi (27 MPa). For concrete strengths exceeding 4 ksi, β1 shall be reduced at a rate of 0.05 for each 1 ksi (6.89 MPa) of strength in excess of 4 ksi, except that β1 shall not be taken to be less than 0.65.
- ε_{cu} = ultimate strain in concrete
- ε_{fd} = design tensile strain of GFRP rebar considering reductions for service environment.

The other flexural resistance check is considered at the section between the deck and the traffic barrier, following the same procedure. The connection can be considered fixed, as previously discussed, and the resistance is evaluated per linear foot (therefore the width B = 12 in). In this case the flexural resistance of the traffic barrier is evaluated as a cantilever slab and the rebar working in flexion are the bent rebar and the vertical rebar.

2.8 Shear Verification

For TL-1, TL-2 and TL-3 the shear verification is satisfied without the need for reinforcement. In the case of TL-4 shear reinforcement is required. As for the flexural verification, the shear verification is evaluated in the two different structural models. For the simple supported beam, the factored shear strength provided by the concrete is (AASHTO LFRD 2.10.3.2.1-1):

$$Vc = 0.16 \cdot \sqrt{fc'} \cdot b_w \cdot c \quad (13)$$

Where:

- bw = width of the web [in]
- c = k · d = distance from extreme compression fiber to neutral axis [in]
- k = ratio of depth of neutral axis to reinforcement depth (AASHTO LFRD 2009 Eq. 2.7.3-4)
- d= distance from extreme compression fiber to centroid of tension reinforcement [in]

In the first design method the Ultimate Shear Stress, Vu, is half of Ftr, while in the second design method the Vu is equal to the reaction Rh. In both cases the strength Vc provided by the concrete is not enough and additional shear reinforcement are required; however, sensitively less reinforcement are required following the second method.

The nominal shear resistance of the shear reinforcement, Vf, perpendicular to the axis of the member shall be evaluated as (AASHTO LFRD 2.10.3.2.2-1):

$$Vf = \frac{A_{fv} f_{fv} d}{s} \quad (14)$$

In which:

- $f_{fv} = 0.004 \cdot Ef < f_{fb}$
- Afv = area of shear reinforcement within spacing [in^2];
- f_{fv} = design tensile strength for shear; [ksi]
- S = spacing of shear reinforcement [in]
- Ef = modulus of elasticity of GFRP reinforcement [ksi]
- f_{fb} = strength of the bent portion of GFRP rebar [ksi]

In order to design the shear reinforcement, the spacing and the rebar size, which will affect the Afv, are taken into account.

The other shear check has to be done in the section between the deck and the traffic barrier. For this check the resistance of one linear foot of cross section is taken into account. The ultimate Shear Stress is evaluated over unitary length. The first design method is set to Ftr/Lt, while the second design method is set to qy.

Chapter 3: Examples of Traffic Railings, GFRP RC Type Parapet

3.1 F-Shape 32" Traffic Barrier with Continuous Closed GFRP Stirrups

In this chapter three examples of F-Shape 32" Traffic Barrier with Continuous GFRP Stirrups are shown. All of these three solutions are design followed the first design method and the TL-4.

Since GFRP have much higher corrosion resistance compared to steel reinforcement, it could be possible set the clear cover to 1.5 in. (38 mm). The first of the three examples has a minimum clear cover of 1.5 in. (38 mm). In the this example are used of continuous closed stirrups vertical #6 with an internal radius of 2.25 in. as shown in Figure 20. The spacing of the vertical reinforcement has to be consistent with the deck reinforcement spacing (in the case of Halls River Bridge spacing of deck rebar is set to 4.5 in., 114 mm and it is taken as a reference). In these design, the closed stirrups (labelled 6S) and the bent rebars (labelled 6A) have a spacing of 9 in. (228mm).

In this traffic barrier design, a #4 closed stirrup is designed as secondary shear reinforcement (labelled 4c). A total of 9 longitudinal #6 rebars are used (labelled 6L).

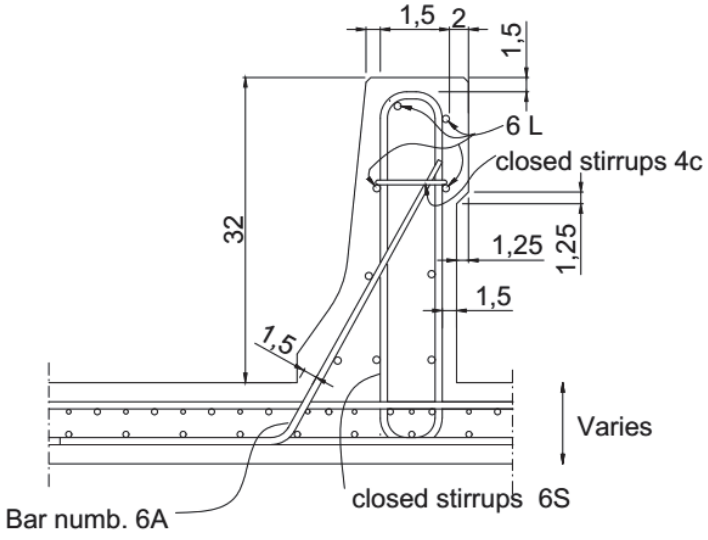

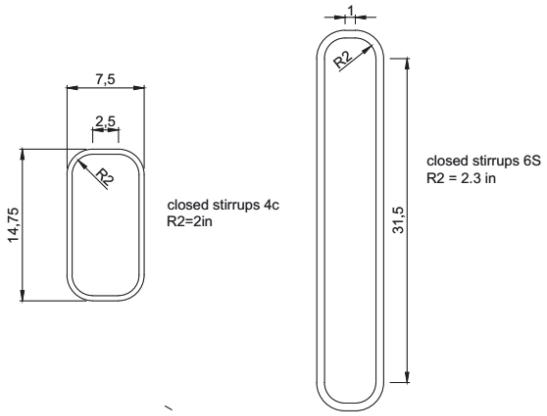

Figure 20 - Typical section with vertical close stirrups, minimum Cc=1.5 in. All measurements in inches (1in = 25.4 mm)

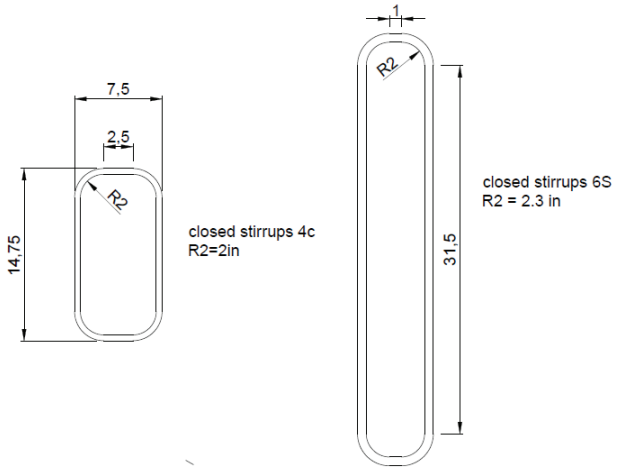

Figure 21 - Primary and Secondary closed stirrups, all measurements in inches (1in = 25.4 mm)

The second traffic barrier has a minimum clear cover of 2 in. (50.8 mm). Closed stirrups #4 are used, with the same geometry of the previous closed stirrups. In order to respect the clear cover, the stirrups have to be inclined from the vertical axis to match the slope of the concrete upper front part of the barrier as shown in the Figure 22.

In this example, since the closed stirrups are #4, the spacing is reduced down to 4.5 in. (114 mm). A total of 8 longitudinal #6 rebars are used (labelled 6L).

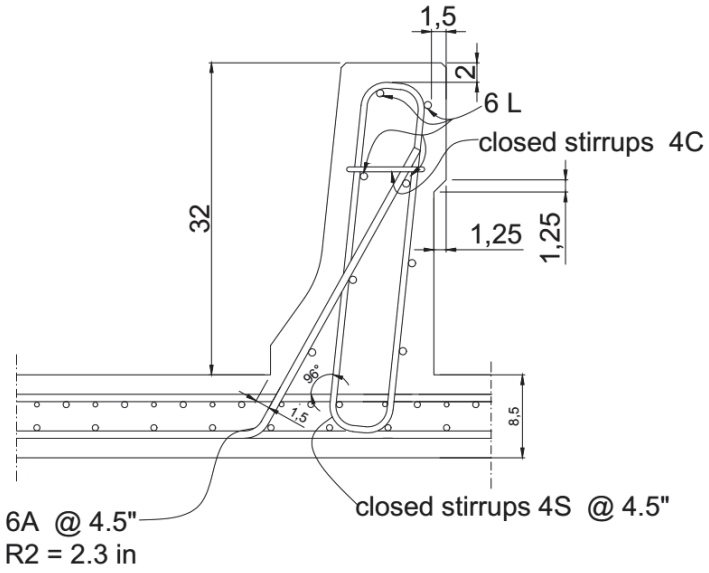

.

Figure 22 - typical section with inclined close stirrups, Cc=2 in (1in = 25.4 mm)

In the third example (Figure 23) the minimum clear cover is set to 2.5 in. (64 mm). In order to comply with that requirement, closed stirrups #5 (labelled 5R) must have an internal radius equal to the diameter Figure 23Figure 24). Both the closed stirrups 5R and bent rebars #5 (labelled 5A) have a spacing of 4.5 in. (114 mm). In this case are not used shear secondary reinforcement and the spacing of both close stirrups and bent rebar is set to 4.5 in (114 mm). A total of 9 longitudinal #6 rebars are used (labelled 6L).

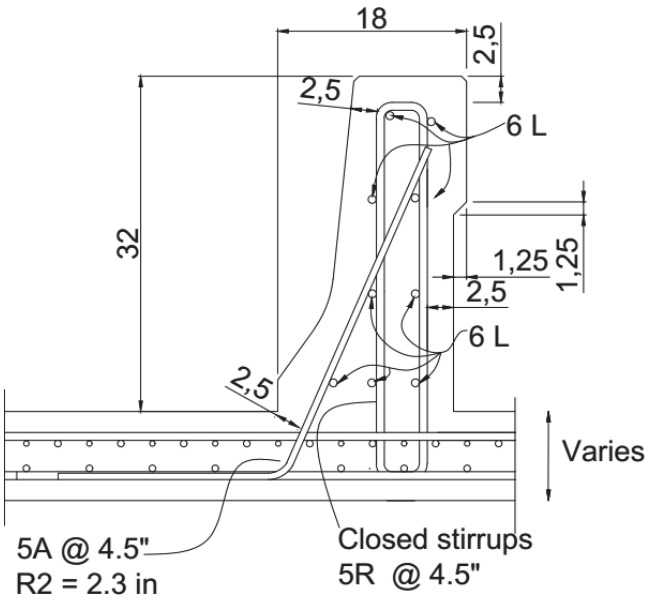

Figure 23 – Traffic barrier with Closed Stirrups with internal radius equal to diameter, Cc=2.5 in

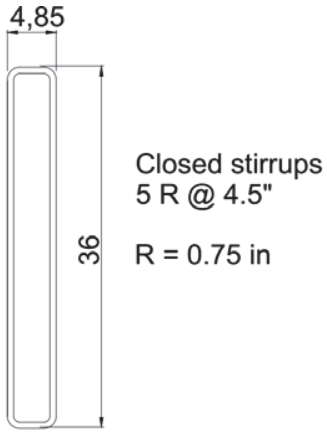

Figure 24 - Closed stirrups 5R with internal radius equal to diameter

3.2 F-Shape 32” of Halls River Bridge

The type of traffic barrier chosen for the Halls River Bridge was F-shape 32”, which was also a common solution in Florida, until now. In order to reduce the gravity of the accidents approaching the bridge, the section at the approaches is thinner and presents a single slope that gradually increases until it reaches the standard dimensions of F32”. In Figure 25, the plan view of the approaches shows how the traffic railings pass from the thinner section B-B to the regular, section A-A (Figure 26).

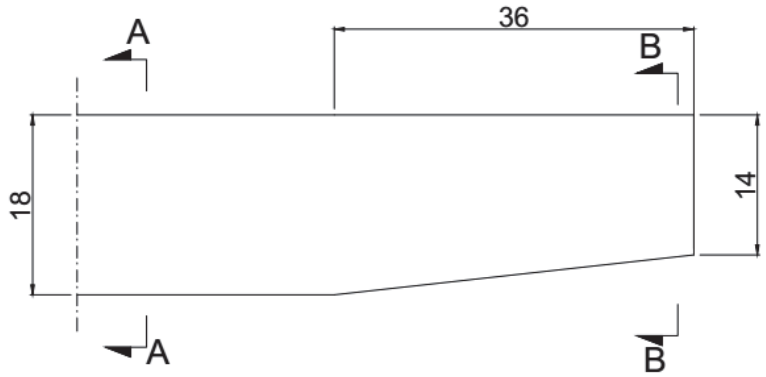

Figure 25 - Plan view traffic railing approach

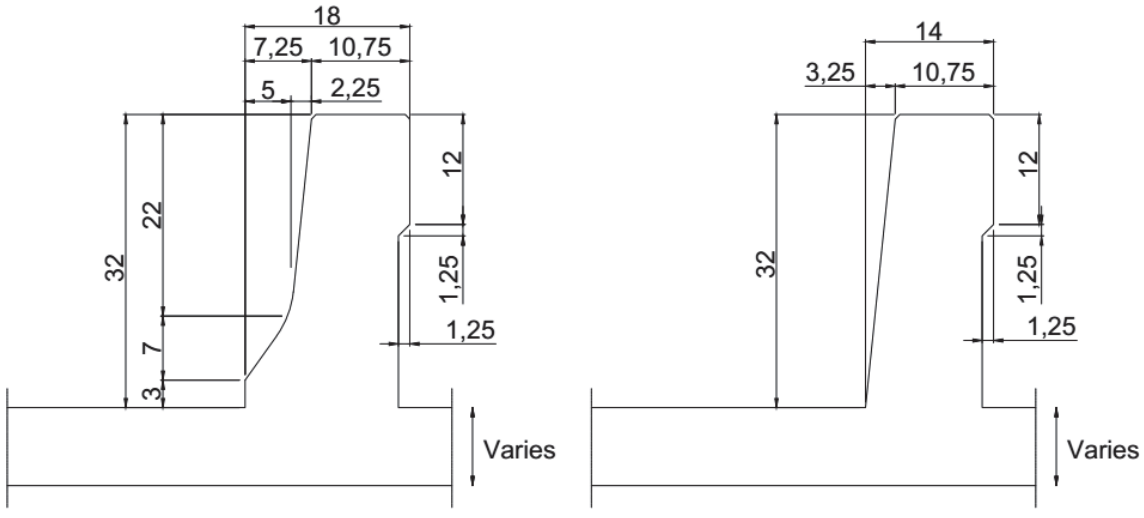

(a) (b)

Figure 26 - Geometry of typical section A-A (a) and typical section B-B (b)

In order to comply with the construction steps of the bridge the “South Side Traffic Railing” will be cast together with the deck, while the “North Side traffic Railing” will be inserted into the deck.

A slip form will be used as casting method and the minimum clear cover is set to 2.5 in. (64 mm) for both the railings. In order to guarantee continuity between the deck and the traffic railing and to fix the rebars during the casting, the transverse rebars of the traffic barrier must be tied with the deck reinforcements. The deck reinforcements have a spacing of 4.5 in. (114 mm), then the reinforcement of the traffic barrier should have a spacing of 4.5 in. or a multiple of it. The configuration of the longitudinal rebars is composed of two layers of five #5 rebars, disposed in the front and in the back of the railing. The transverse reinforcement of the South Side Halls River Bridge Traffic Barriers are non-continuous closed stirrups #5 (name used: 5V and 5P) with a spacing of 4.5 in. (114 mm). Bent rebars #5 (name used: 5A) are disposed with a spacing of 9 in. (228 mm) in order to increment the bending resistance in the most critical section (at the bottom in connection with the deck) and to improve the connection between the traffic barrier and the deck.

The transverse reinforcement of the North Side Halls River Bridge Traffic Barriers are drilled in the existing deck (name used 5P and 5D)(Figure 27). The shape of the rebars will be different as shown in Figure 27.

In Section B-B, for both the railings, transverse rebars (5D, 5V and 5A) will slightly change in dimensions in order to insure the clear cover in all the sections.

Figure 28 and Figure 29 are showing respectively the South Side of typical section A-A and section B-B of Halls River Bridge Traffic Railings. In Figure 30 and in Figure 31 the typical sections A-A and B-B of the North Side are shown. Full drawings are shown in Appendix D

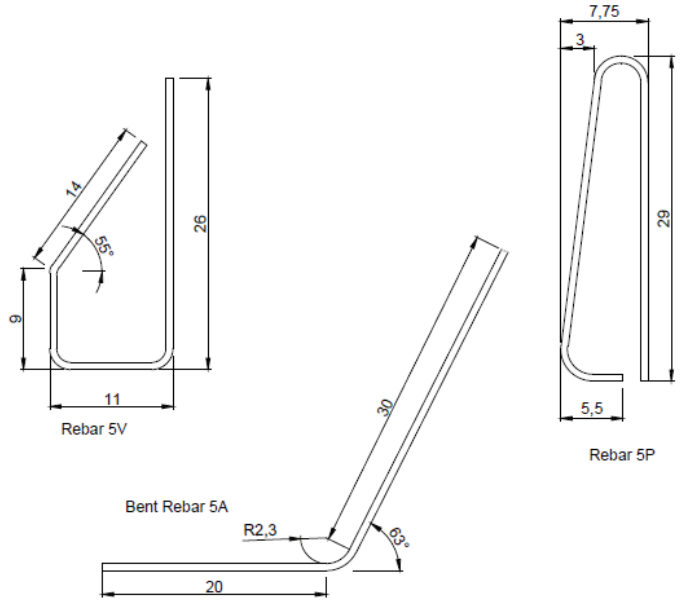

Figure 29 - Rebar used in Halls River Bridge, typical section A-A South Side

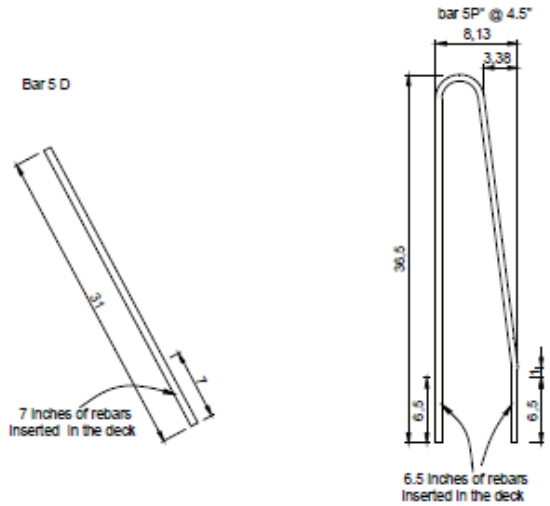

Figure 27 - Rebar used in Halls River Bridge, typical section A-A North Side

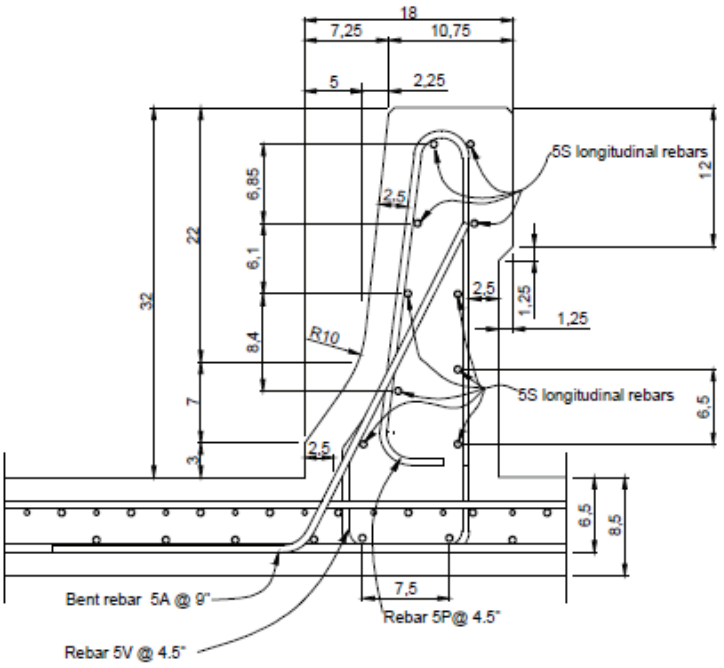

Figure 28 - typical section A-A South Side

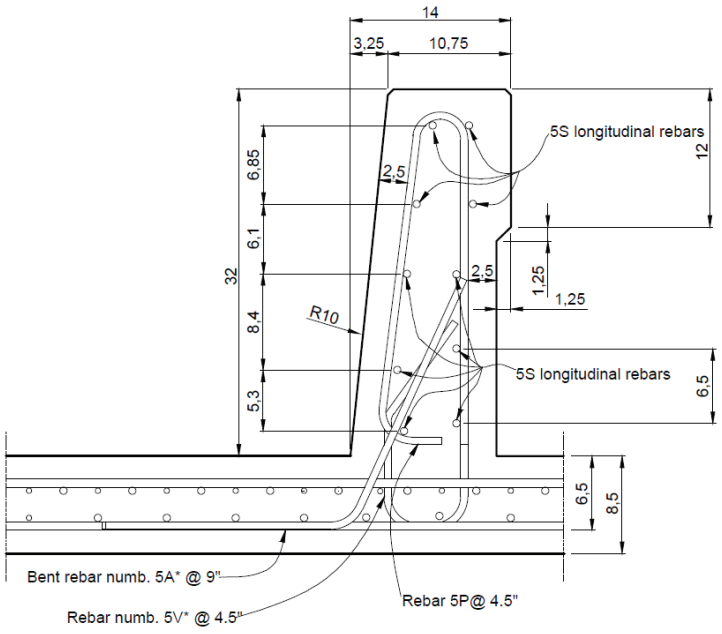

Figure 29 - Typical section B –B south side

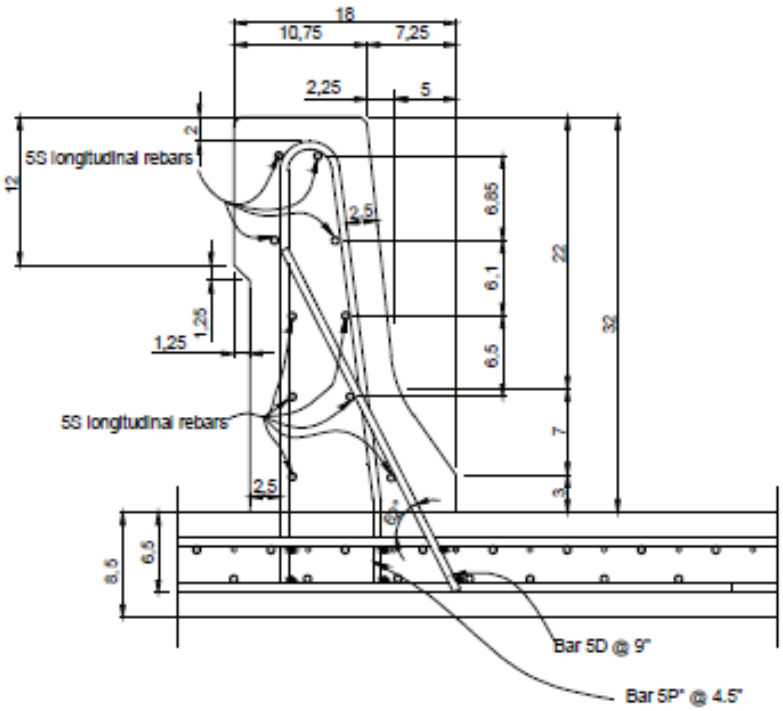

Figure 30 - Typical section A-A North Side

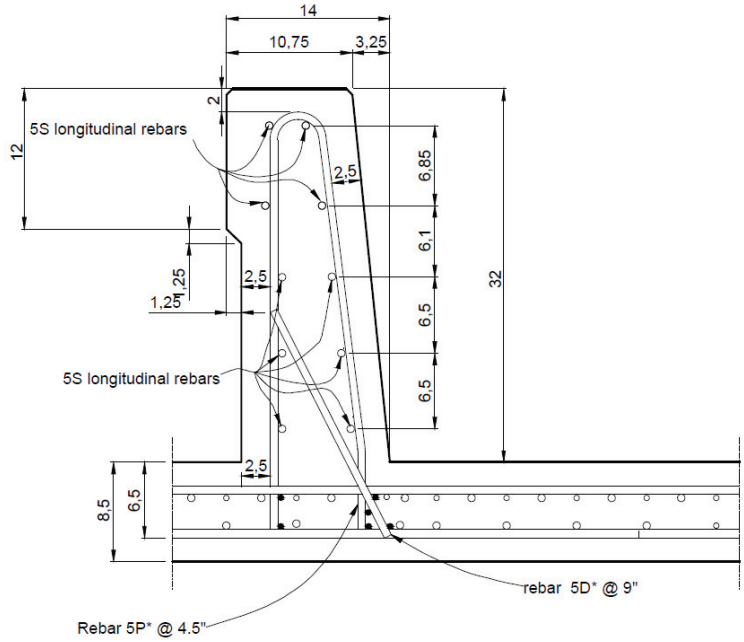

Figure 31 - Typical section B - B

3.3 Single Slope 36”

The Single Slope 36” (SS36”) is the type of traffic barrier chosen from the FDOT as the new basic default traffic railing in Florida. In this chapter two different internal reinforcement layouts are studied: SS36” with Rectangular Closed GFRP Stirrups and SS36” with Trapezoidal Closed GFRP Stirrups. The SS36” with Rectangular Closed GFRP Stirrups are designed following the first design method and a TL-4. The typical section of SS36” is shown in Figure 32. The internal reinforcement of this barrier will present continuous closed rectangular stirrups number 6 (labelled 6C) and bent rebars number 6 (labelled 6F) both every 6 in. (152 mm). A total of ten longitudinal rebars number 6 (labelled 6L) with a spacing of 7.5 inches (190 mm) are presented in this design. The rebar at the front will be in tension for impact near an open joint and the same rebars are used as in the back.

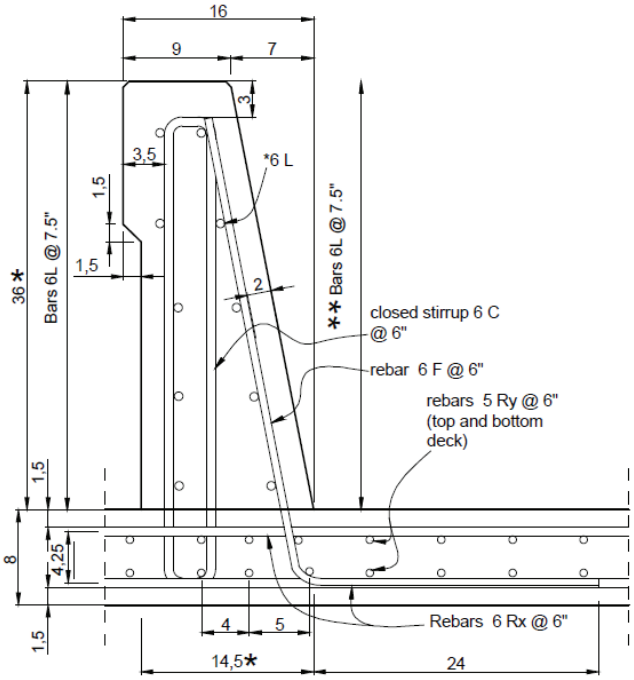

Figure 32 - Traffic barrier 36” single slope with Closed Rectangular GFRP Stirrups, all measurements in inches (1in = 25.4 mm)

As shown in Figure 33, the vertical reinforcements are aligned with the deck reinforcement (represented as dash line in Figure 33) in order to tie them together. The closed rebars (6C) are positioned on the right side of the deck rebars and bent rebars (6F) at the left side.

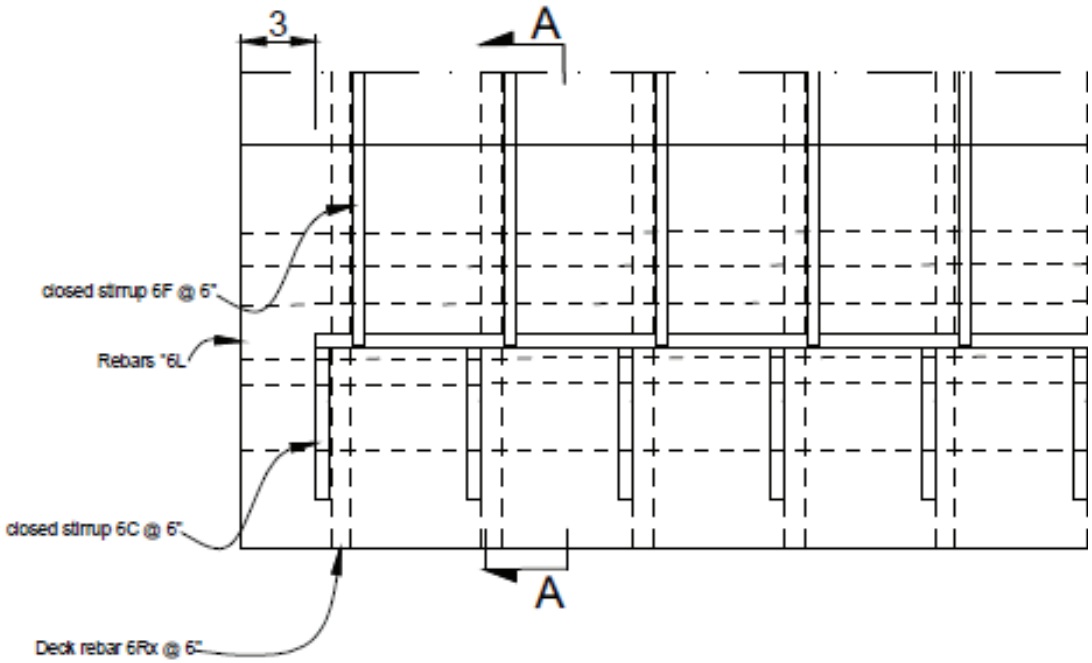

Figure 33 - plan view of the Traffic barrier 36” single slope with close rectangular GFRP stirrups, all measurements in inches (1in = 25.4 mm)

The SS36” with Trapezoidal Closed Stirrups is designed as well for the TL-4. The first difference from the SS36” with Rectangular GFRP Stirrups, is that the second design method is used (the one that combined the two structural models) which is less conservative and more realistic. It has been defined that, in this way, the maximum reactions at the critical section are considerably reduced, therefore, the ultimate bending moment and the ultimate shear acting on the traffic barrier are reduced as well. It is clear that consequently the traffic barrier needs less shear and bending reinforcement in order to support these modified design loads.

There are two type of vertical reinforcements: closed trapezoidal stirrups 5C and bent rebar 5D (Figure 34) both #5 (instead of 6 in the previous design) and both with a spacing of 8 in. (200 mm) (instead of 6 in. in the previous design). Furthermore, the closed stirrups is trapezoidal in the shape of the concrete section, which will optimize the moment resistance at the section in the bottom and give a better confinement to the concrete section. It has been decided, as shown in Figure 35, to collocate the two vertical reinforcement alternate with a relative spacing of 4 in. (102 mm) in order to spread better the reinforcement through the traffic barrier.

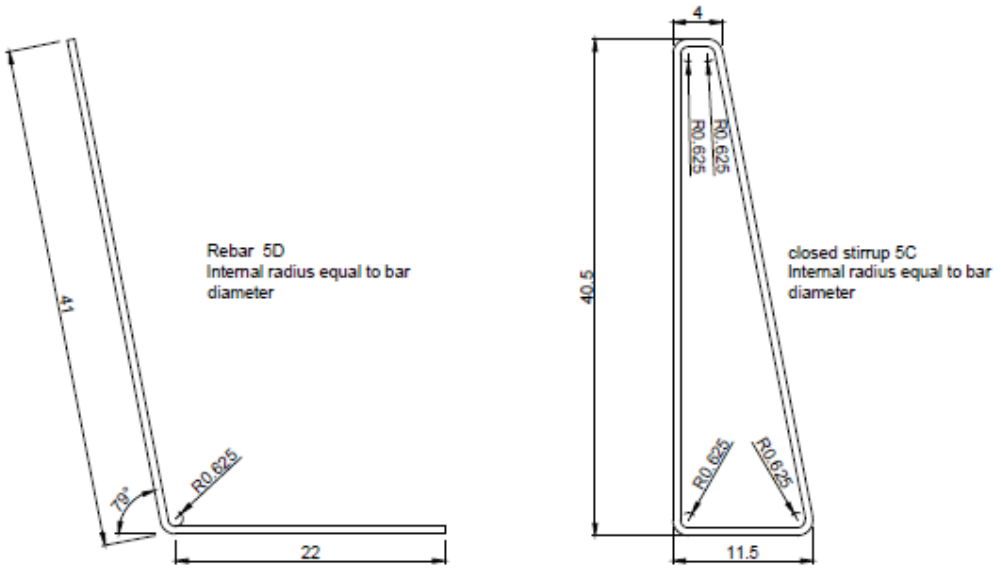

Figure 34 - vertical reinforcement 5D and 5C, all measurements in inches (1in = 25.4 mm)

This Traffic Railing SS36" will be used at a later time as a pendulum test specimen. Three equivalent traffic barriers, with those reinforcement will be built in order to perform the impact pendulum test. Every specimen will present the same internal reinforcement as shown in Figure 36 and Figure 37, through the length of 12 ft.

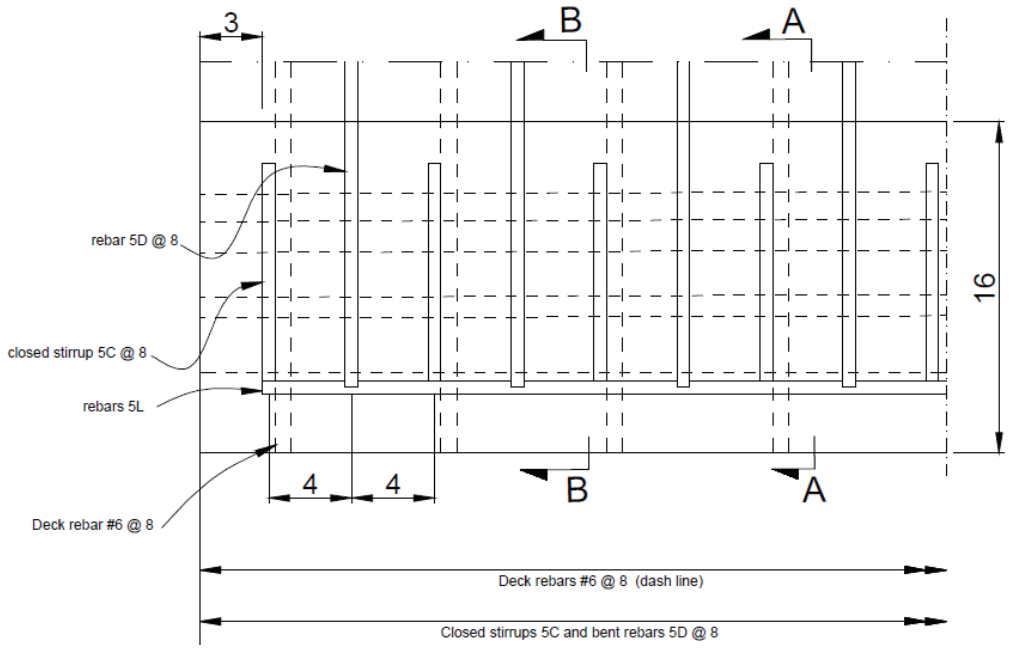

Figure 35 - Plan View pendulum specimen single slope 36” all measurements in inches

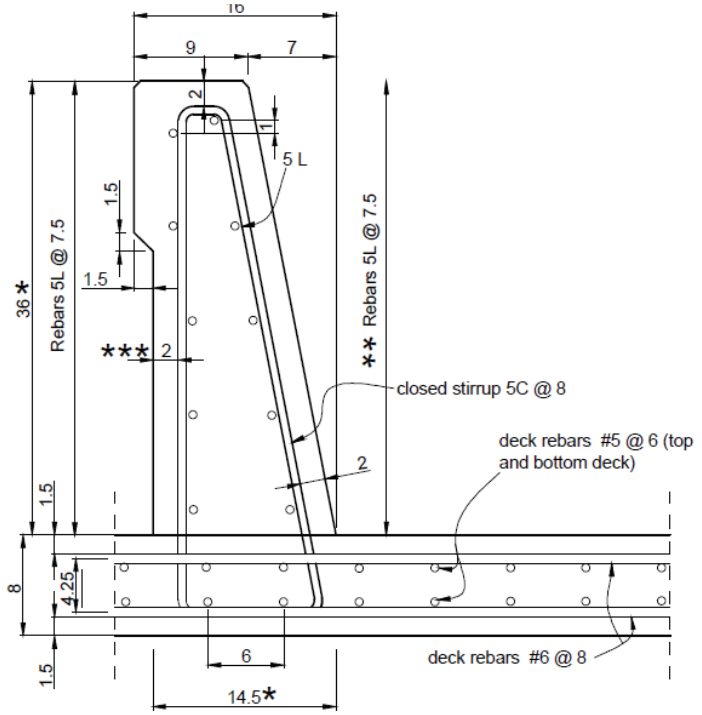

Figure 36 - Pendulum specimen single slope 36” section A-A, all measurements in inches

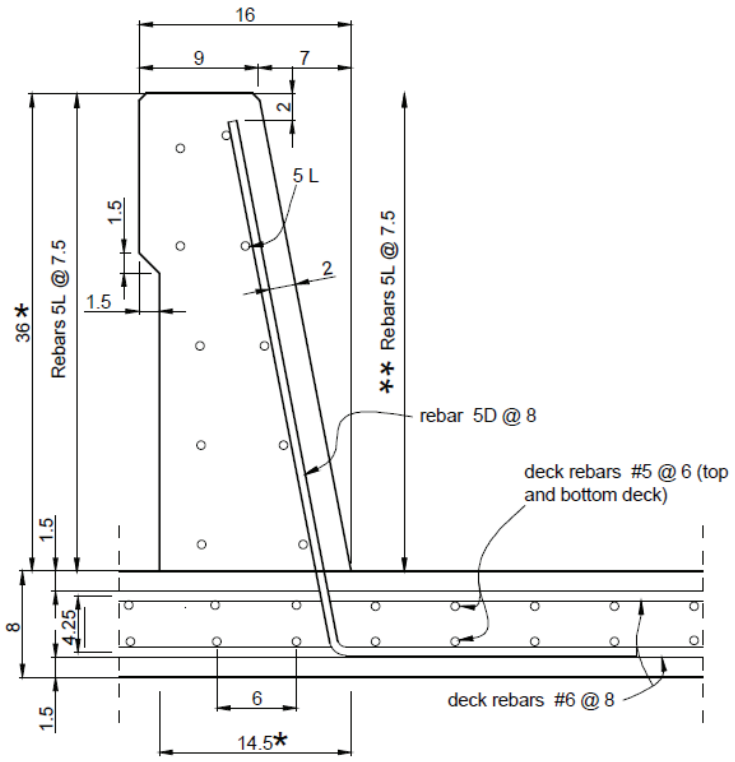

Figure 37 - Pendulum specimen single slope 36” section A-A, all measurements in inches

Chapter 4: Mathcad Code Check

4.1 Remarks

The design of the traffic barrier F32" has been also implemented with the "PTC Mathcad software". The design is divided in 5 parts. Part A defines the traffic railings geometry, the concrete mechanical characteristics and the rebars characteristics. Part B is related to the design of the necessary development length for the bent rebars. In Part C, the design loads are shown. The flexural verification, in Part C, is subdivided in three main design checks: the limits for reinforcement are determined in the first design check; in the second one, the flexural strength for the structural Model 1 is established; in the third subdivision the flexural strength for the structural Model 2 is determined.

4.2 Geometry, Concrete and GFRP Rebar Characteristics

In this part, all of the data that characterize the traffic railing are chosen. Once these data are defined, the program automatically provides, in the consecutive parts, the corresponding results from all the checks required, following the ASSHTO LFRD, ACI and FDOT standards and requirements.

The first subsection introduces, first of all, the type of traffic barrier, which is a Concrete parapet, and the geometry model, which a traffic railing F32". Then the required test level can be defined. As shown in Figure 38 a T.L. from 1 to 4 can be selected with the cursor according to AASHTO LRFD 2014 13.7.2.

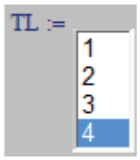

TL = 4 Test Level [AASHTO LRFD 2014, 13.7.2]

Traffic railings should be at least 42 in for TL-5 and 90 in for TL-6 [AASHTO LRFD 2014, 13.7.3.2].

Figure 38 - Test Level Selection

The clear cover of the concrete traffic barrier can be defined or modified only in this section. The height and the width correspond to the F32" traffic railing as shown from FDOT 2015 (page 59). The concrete strength, strain and concrete modulus are related to the preexisting characteristics of Halls River Bridge and can be modified only in this section as well. In order to change those data in the program requires the symbol ":=".

Subsequently, the GFRP rebars characteristics are chosen. As shown in Figure 39 the bar size of all the reinforcement rebars can be selected with the cursor.

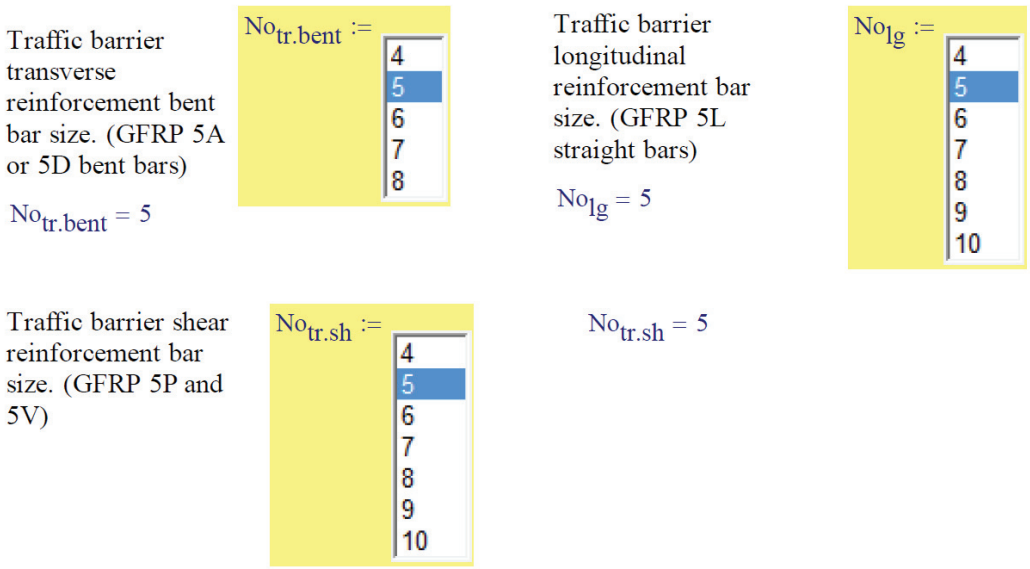

Figure 39 - Bar size selection

In the next step, the spacing of the transverse rebars are chosen, and consequently the quantity of rebars for foot is evaluated (Figure 40).

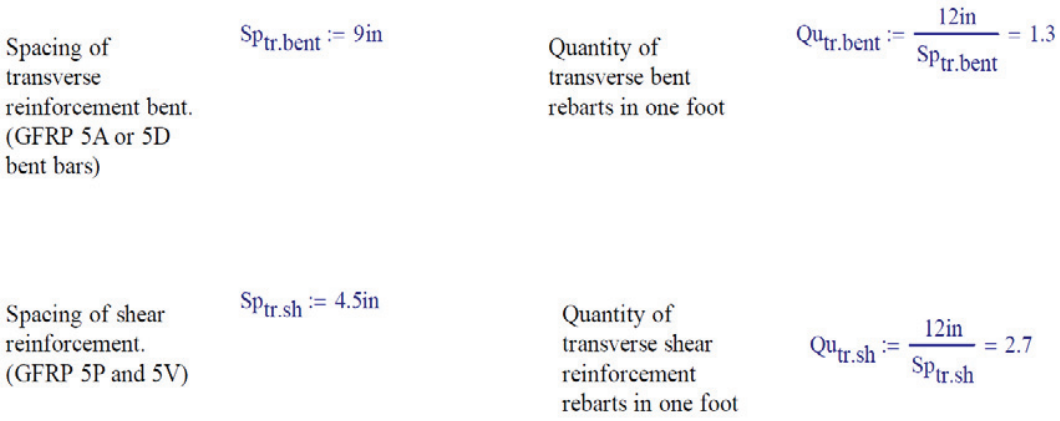

Figure 40 - Spacing of transverse rebar selection

Then, the quantity of longitudinal rebars on the front side and the back side of the F32" can be selected (Figure 41).

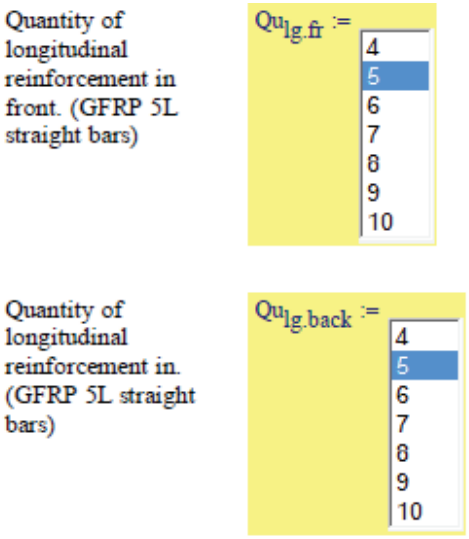

Figure 41 - Quantity of longitudinal reinforcement selection

The GFRP mechanical properties can be picked according to the minimum requirement of ASSHTO LFRD 2009, or from the manufacturing rebar characteristics if provided. Once the size of the rebars is defined, a loop automatically associates the design tensile strength of GFRP bars, considering reductions for service environment [AASHTO GFRP 2009, 2.9.3.3] (Figure 42).

$$f_{fu.lg} := \begin{cases} 100ksi & \text{if } No_{lg} = 4 \\ 95ksi & \text{if } No_{lg} = 5 \\ 90ksi & \text{if } No_{lg} = 6 \\ 85ksi & \text{if } No_{lg} = 7 \\ 80ksi & \text{if } No_{lg} = 8 \\ 75ksi & \text{if } No_{lg} = 9 \\ 70ksi & \text{if } No_{lg} = 10 \end{cases}$$

Figure 42 - Loop of design tensile strength of GFRP bars

With a similar loop, the diameter and the area of each rebars are automatically determined (Figure 43) according to table 4.5.4-1 [ASSHTO GFRP 2009].

$$diam_{No_{lg}} := \begin{cases} 0.5in & \text{if } No_{lg} = 4 \\ 0.625in & \text{if } No_{lg} = 5 \\ 0.750in & \text{if } No_{lg} = 6 \\ 0.875in & \text{if } No_{lg} = 7 \\ 1in & \text{if } No_{lg} = 8 \\ 1.128in & \text{if } No_{lg} = 9 \\ 1.270in & \text{if } No_{lg} = 10 \end{cases}$$

$$Area_{No.tr.bent} := \frac{\left(diam_{No_{tr.bent}}\right)^2 \cdot \pi}{4} = 2.1 \times 10^{-3}\, ft^2$$

Figure 43 - Loop of diameters and area determination for GFRP rebar

In this first subchapter, the distance from the extreme compression fiber to centroid of tension reinforcement is also calculated in the critical section related to the two structural models taken into consideration, according to AASHTO GFRP 2009, 2.9.3.3.

$$D := W_t - \frac{\left(diam_{No_{lg}}\right)}{2} - c_c = 7.9 \cdot in \qquad D_{bottom} := W_b - c_c - \frac{diam_{No_{tr.bent}}}{2} = 13.9\, in$$

The GFRP reinforcement ratio is evaluated for the transversal section (ρ_1) and for the bottom longitudinal one ($\rho_{2bottom}$) which are related to the two structural models.

$$\rho_1 := \frac{Qu_{lg} \cdot Area_{No.lg}}{(H \cdot D)} = 1.2 \cdot \%$$

$$\rho_{2.bottom} := Area_{No.tr.sh} \cdot \frac{\left(Qu_{tr.sh} \cdot 2 + Qu_{tr.bent}\right)}{\left(12in \cdot D_{bottom}\right)} = 1.2 \cdot \%$$

4.3 Development Length and Reinforcement Splices

In the second part, the determination of the minimum development length is calculated according to AASHTO GFRP 2009, 2.12.2.1. The data used by this subchapter followed what is defined in the previous chapter, and the final output is the development length of the transverse bent rebars.

The transverse and longitudinal GFRP reinforcement ratio producing the balanced condition are estimated according with AASHTO GFRP 2009, 2.7.4.2-2:

$$\rho_{fbtr} := 0.85 \cdot \beta_{1.super} \cdot \frac{f'_{c.super} \cdot E_f \cdot \varepsilon_{cu}}{f_{fd.tr.bent} \cdot \left(E_f \cdot \varepsilon_{cu} + f_{fd.tr.bent}\right)} = 1.2 \cdot \%$$

$$\rho_{fblg} := 0.85 \cdot \beta_{1.super} \cdot \frac{f'_{c.super} \cdot E_f \cdot \varepsilon_{cu}}{f_{fd.lg} \cdot \left(E_f \cdot \varepsilon_{cu} + f_{fd.lg}\right)} = 1.2 \cdot \%$$

These values were used in the following chapters in order to evaluate if the failure would be initiated in the concrete or in GFRP rebars.

Then, the effective strength of the transverse reinforcement is evaluated according to AASHTO GFRP 2009, 2.9.3.1-1.

$$f_{ftr} := \min\left[\sqrt{\frac{\left(E_f \cdot \varepsilon_{cu}\right)^2}{4} + \frac{0.85 \cdot \beta_{1.super} \cdot f'_{c.super}}{\rho_1} \cdot E_f \cdot \varepsilon_{cu}} - 0.5 \cdot \left(E_f \cdot \varepsilon_{cu}\right), f_{fd.tr.bent}\right] = 66.5 \cdot ksi$$

In order to define the development length for the bent rebars AASHTO GFRP 2009, 2.12.2.1 is followed:

$$l_{D.tr} := \frac{31.6 \cdot \alpha \cdot \frac{f_{ftr}}{\sqrt{f'_{c.super} \cdot ksi}} - 340}{13.6 + \frac{C_{ctr}}{diam_{No_{tr.bent}}}} \cdot diam_{No_{tr.bent}} = 19.2 \cdot in$$

4.4 Design Loads

The design loads are referred to the specification made in AASHTO LRFD 2014, A13.7.2 for the Traffic Level 4, but can be changed for each of the six different test levels. The effective height of the vehicle rollover force is evaluated as defined by AASHTO LRFD

$$H_e := G_V - 12 \cdot W_V \cdot \frac{B}{\left(2 \cdot F_{tr_{4,TL}}\right)} = 23.8 \cdot in$$

2014, A13.2-1:

where the height of the vehicle center of gravity above bridge deck (G_v), the weight of the vehicle corresponding to the required test level (W_v), the out-to-out wheel spacing on one axle (B) and transverse vehicle impact force for the selected T.L. distributed over 1ft length (F_{tr}).

The ultimate bending moment and the ultimate shear force on longitudinal (Structural Model 1) and vertical direction (Structural Model 2) are evaluated:

$$M_{u1} := \frac{\frac{F_{tr_{4,TL}}}{L_{t_{4,TL}}} \cdot \left(L_{t_{4,TL}}\right)^2}{8} = 24 \cdot kip \cdot ft \qquad V_{u2} := \frac{F_{tr_{4,TL}} \cdot ft}{L_{t_{4,TL}}} = 15.4 \cdot kip$$

$$V_{u1} := \frac{F_{tr_{4,TL}}}{ft} \cdot 1\,\frac{ft}{2} = 27 \cdot kip \qquad M_{u2} := \left(V_{u2} \cdot H_e\right) = 31 \cdot ft \cdot kip$$

where L_t is the longitudinal length of distribution of the impact force according to the T.L. selected before.

4.5 Flexural Verification

The part regarding the flexural verification is subdivided in three different checks. The first one regards the minimum amount of longitudinal reinforcement for flexural tensile reinforcement according to AASHTO GFRP 2009, 2.9.3.3:

$$A_{f\_min} := \max\left[0.16\sqrt{f'_{c.super}\cdot ksi}\,\frac{HD}{f_{fd.lg}}, \left(0.33\cdot\frac{HD}{f_{fd.lg}}\right)\frac{kip}{in^2}\right] = 1.4\cdot in^2$$

Once, in the first part, the number and the size of the longitudinal rebars have been defined, the total amount of area provided (Af_long) is automatically evaluated. Therefore, the output will show if the longitudinal rebars utilized are enough or not in order to satisfy the minimum reinforcement check as shown in Figure 44.

$$check\_flexural\_minimum\_reinforcement := \begin{cases} \text{"VERIFIED"} & \text{if } A_{f\_long} \geq A_{f\_min} \\ \text{"NOT VERIFIED"} & \text{otherwise} \end{cases}$$

$$check\_flexural\_minimum\_reinforcement = \text{"VERIFIED"}$$

Figure 44 - check of minimum reinforcement required for flexural

The next check is regarding the flexural strength of the Structural Model 1, where the structure is evaluated as a simply supported beam with a length equal to the impact length Lt. First of all, the depth of the equivalent rectangular stress block is found according to AASHTO GFRP 2009, 2.9.3.2.2-3:

$$a_{fl} := \frac{A_{f\_long}\cdot f_{fd.lg}}{0.85\cdot f'_{c.super}\cdot H} = 0.7\cdot in$$

The distance from the compression fiber to the neutral axis at balanced condition is calculated referring to AASHTO GFRP 2009, 2.9.3.2.2-4:

$$c_b := \frac{\varepsilon_{cu}}{\varepsilon_{cu} + \varepsilon_{fdNo.lg}} D = 1.8\cdot in$$

Once defined the internal longitudinal reinforcement, the critical section and the corresponding critical distance from extreme compression fiber to centroid of tension reinforcement (D) and the nominal flexural resistance M_n are evaluated. If the GFRP reinforcement ratio provided in the critical section ($\rho 1$) is greater than longitudinal GFRP reinforcement ratio producing balanced condition multiply by 1.4 (ρ_{flg}) , the failure will be

initiated by the concrete crash and the first equation will evaluate the nominal moment. On the other hand, if the GFRP reinforcement ratio is smaller or equal, the failure will be governed by the GFRP rebars and the nominal moment will be evaluated with the second equation as shown below:

$$M_n := \begin{cases} \left[A_{f\_long} \cdot f_{fd.lg} \cdot \left(D - \frac{a_{fl}}{2} \right) \right] & \text{if } \rho_1 > \rho_{flg} \\ \left[A_{f\_long} \cdot f_{fd.lg} \cdot \left(D - \frac{\beta_{1.super} \cdot c_b}{2} \right) \right] & \text{if } \rho_1 \le \rho_{flg} \end{cases}$$

Figure 45 - Nominal flexural resistance evaluation

Also the resistance factor for flexure depends on the ratio of GFRP reinforcement, and it is evaluated following AASHTO GFRP 2009, 2.9.3.2.2-1 (Figure 46).

$$\Phi_{fl} := \begin{cases} 0.55 & \text{if } \rho_1 \le \rho_{fblg} \\ \left(0.3 + 0.25 \cdot \frac{\rho_{flg}}{\rho_{fblg}} \right) & \text{if } \rho_{fblg} < \rho_1 < 1.4 \cdot \rho_{fblg} \\ 0.65 & \text{if } \rho_1 \ge 1.4 \cdot \rho_{fblg} \end{cases}$$

Figure 46 - Resistance factor for flexure

Once defined the nominal flexural resistance and the resistance factor, the factored flexural resistance (M_r) is evaluated. As shown in Figure 47, it will be shown automatically if the check for flexural resistance is verified or not verified.

$$check\_flexural\_resistance\_1 := \begin{pmatrix} \text{"VERIFIED"} & \text{if } M_r \ge M_{u1} \\ \text{"NOT VERIFIED"} & \text{otherwise} \end{pmatrix}$$

check_flexural_resistance_1 = "VERIFIED"

Figure 47 - Check for flexural resistance for structural model 1

The nominal flexural resistance for the structural Model 2, where the traffic railing is analyzed as a cantilever beam model taken to be the bottom of the railing, will be evaluated in the same way as for structural Model 1. What will change is the rebars position, the associated distance from extreme compression fiber to centroid of tension reinforcement (D_{bottom}) and the distance from extreme compression fiber to centroid of tension reinforcement for stirrups (5V). The nominal flexural resistance is:

$$M_{n.2} := \begin{cases} \left[(Q \cdot A \cdot f) \cdot \left(D_b - \frac{a_{fl.2}}{2}\right) + \left(Qu_{tr.sh} \cdot Area_{No.tr.sh} \cdot f_{fd.tr.sh}\right) \cdot \left(D_{str} - \frac{a_{fl.2}}{2}\right)\right] & \text{if } \rho_2 > \rho_{flg} \\ \left[(Q \cdot A \cdot f) \cdot \left(D_b - \frac{\beta_{1.super} \cdot c_{b.2}}{2}\right) + \left(Qu_{tr.sh} \cdot Area_{No.tr.sh} \cdot f_{f.tr}\right) \cdot \left(D_{str} - \frac{\beta_{1.super} \cdot c_{b.2}}{2}\right)\right] & \text{if } \rho_2 \le \rho_{flg} \end{cases}$$

As for structural Model 1, the check for flexural resistance will show if is verified or not (Figure 48).

$$check\_flexural\_resistance\_2 := \begin{cases} \text{"VERIFIED"} & \text{if } M_{r.2} \ge M_{u2} \\ \text{"NOT VERIFIED"} & \text{otherwise} \end{cases}$$

check_flexural_resistance_2 = "VERIFIED"

Figure 48 - Check for flexural resistance for structural model 2

4.6 Shear Verification

The shear verification is divided in four different parts. The first part evaluates the concrete shear resistance for the structural Model 1. First, the ratio of depth of neutral axis to reinforcement depth (k) will be evaluated, from there the distance from extreme compression fiber to neutral axis (C_{fl}) is evaluated, according to AASHTO GFRP 2009, 2.10.3.2. The nominal shear strength provided by the concrete is defined following AASHTO GFRP 2009, 2.10.3.2.1-1:

$$V_c := \min\left(0.16\sqrt{f'_{c.super}\cdot ksi}\cdot b_w\cdot C_{fl}, 0.32\cdot\sqrt{f'_{c.super}\cdot ksi}\cdot b_w\cdot C_{fl}\right) = 20\cdot kip$$

The resistance factor for shear as 0.75 is assessed and the factored shear strength provided by the concrete is defined following AASHTO GFRP 2009, 2.7.4.2. Then, the check will show if the shear resistance of the concrete will be enough or if shear reinforcement is required. As shown in Figure 49, the shear capacity of the concrete, in this case, is not enough and shear reinforcement rebars are required.

$$\text{check\_concrete\_shear\_resistance\_1} := \begin{cases} \text{"VERIFIED: SHEAR REINFORCEMENT NOT REQUIRED"} & \text{if } \Phi_{sh}\cdot V_c > V_u \\ \text{"NOT VERIFIED: SHEAR REINFORCEMENT REQUIRED"} & \text{otherwise} \end{cases}$$

$$\text{check\_concrete\_shear\_resistance\_1} = \text{"NOT VERIFIED: SHEAR REINFORCEMENT REQUIRED"}$$

Figure 49 - check for concrete shear resistance

The second shear check is about the shear reinforcement strength for structural Model 1. According to AASHTO GFRP 2009, 2.10.3.2.2-2, the design tensile strength for shear is evaluated, considering the minimum resistance between the bent portion and the straight one set to 0.004 • Ef:

$$f_{fv} := \min\left(0.004\cdot E_f, f_{fb}\right) = 26\cdot ksi$$

The maximum spacing of shear reinforcement is evaluated following AASHTO GFRP 2009, 2.10.3.2.2.1:

$$s_{sh\_max} := \frac{Area_{No.tr.sh}\cdot f_{fv}\cdot D_{av}}{V_{f\_required}} = 4.5\cdot in$$

In the first part the design spacing ($Sp_{tr.sh}$) of the transverse rebars has been defined and it must be bigger than the maximum spacing found before, therefore the check will be as shown in Figure 50.

$$check\_shear\_resistance\_1 := \begin{cases} \text{"VERIFIED"} & \text{if } s_{sh\_max} > Sp_{tr.sh} \\ \text{"NOT VERIFIED: MORE SHEAR REINFORCEMENT REQUIRED"} & \text{otherwise} \end{cases}$$

$check\_shear\_resistance\_1 = \text{"VERIFIED"}$

Figure 50 - shear check resistance structural model 1

For Structural Model 2, the other two shear resistance checks are the same as before. As for the flexural resistance for strength Model 2, the section considered is the one at the bottom. The concrete shear resistance check will be as shown in Figure 51.

$$check\_concrete\_shear\_resistance\_2 := \begin{cases} \text{"VERIFIED: SHEAR REINFORCEMENT NOT REQUIRED"} & \text{if } \Phi_{sh} \cdot V_{c.2} > V_u \\ \text{"NOT VERIFIED: SHEAR REINFORCEMENT REQUIRED"} & \text{otherwise} \end{cases}$$

$check\_concrete\_shear\_resistance\_2 = \text{"NOT VERIFIED: SHEAR REINFORCEMENT REQUIRED"}$

Figure 51 - concrete shear resistance

As well as before shear reinforcement is required, and the last check determines the spacing of the transverse reinforcement for this structural model.

$$check\_shear\_resistance\_2 := \begin{cases} \text{"VERIFIED"} & \text{if } s_{sh\_max\_2} > Sp_{tr.sh} \\ \text{"NOT VERIFIED: MORE SHEAR REINFORCEMENT REQUIRED"} & \text{otherwise} \end{cases}$$

$check\_shear\_resistance\_2 = \text{"VERIFIED"}$

Figure 52 - shear check resistance structural model 2

Chapter 5: Conclusion

The GFRP internal reinforcement has been demonstrated to be a valid solution for traffic railings. The design of parapet and railing reinforced with GFRP remains incomplete in codes and standards in the United States (for example in ACI and AASHTO). Considering the increased use of GFRP reinforcement in the last years, full design criteria and provision for RC GFRP traffic railings should be available soon. This study shows two different traffic barrier designs with GFRP reinforcement, F32" and SS36", and it underlines the innovation and sustainability that the FDOT and the University of Miami are always searching for in a state of the art bridge construction project.

The approached design should consider, first of all, the right connection between the traffic railing and the deck. This check strongly depends on the geometry of the connections. Once determined a suitable geometry for the connections, the flexural and shear check should be analyzed based on AASHTO-LRFD Bridge Design Specification, AASHTO-LRFD Bridge Design Guide Specification for GFRP-Reinforced Concrete Bridge Decks and Traffic Railings and specification by FDOT. This thesis has proposed two approaches for design of GFRP RC Traffic Railings: the more conservative design method, in which the two models are separated, (the first proposed approach) or the less conservative design method that combined the two different structural models (the second proposed approach). Referring to the latter, the internal reinforcement quantities are comparable to RC traffic railing reinforced with steel reinforcement. For both the traffic railings, the calculations are made by Excel and, for the F32", by Mathcad as well in order to create an easy tool to implement in future design projects.

Both the traffic barrier F32” and SS36” are considered Safety Shapes Traffic Barriers and have been designed with innovative shape internal GFRP stirrups. One of the F32” traffic barriers analyzed in this thesis has been accepted as the traffic railing of the Halls River Bridge (Homosassa, FL). One of the SS36” will be tested with an impact pendulum tests by FDOT. Innovative internal GFRP reinforcement shapes are used in both the designs and will translate into low maintenance costs and longer life of structures supported by the non-corrosive nature of FRP composites [26].

Reference List

1. Koch, G.H., M. Brongers, N.G. Thompson, Y.P. Virmani, and J.H. Payer, *Corrosion costs and preventive trategies in the United States.* 2002.

2. ASCE. *Infrastructure report card* 2017; Available from: https://www.infrastructurereportcard.org/cat-item/bridges/.

3. Rinaldi, V., A. Nanni, and M. Savoia, *Design of GFRP Reinforcement for Concrete Bridge Structural Components.* 2015.

4. Nanni, A., A. De Luca, and H. Zadesh, *Reinforced concrete with FRP bars: Mechanism and Design.* 2014.

5. Ruiz, A., G. Schaper, R. Kampman, and J. Harnisch, *Performance Evaluation of Glass Fiber Polymer (GFRP) Reinforcing Bars* 2016, FH Munster Univeristy of Applied Sciences.

6. Joshi, S.C., Y.C. Lam, and U. Win Tun, *Improved cure optimization in pultrusion with pre-heating and die-cooler temperature.* Elsevier, 2003.

7. Busel, J.P., *Fiber reinforced polymer (FRP) composite rebars.* American composites manufacturers associations, 2012.

8. Bagherpour, S., *Polyester, Chapter 7 Fibre Reinforced Polyester Composites*. InTech. 2012.

9. Claure, G., A. Nanni, W. Suaris, F.J. De Caso y Basalo, M.W. Fahmy, and J. Onyango, *Non-Traditional Shape GFRP Rebars for Concrete Reinforcement*, in *Civil, Architectural and Environmental Engineering*. 2015, University of Miami.

10. ACI, *Guide For the Desing And Construction Of Structural Concrete Reinforced With Fiber-Reinforced Polymer*. March 2015, American Concrete Institute Committee 440: Farmington Hills, MI.

11. AASHTO, *AASHTO LRFD Bridge Design Guide Specifications for GFRP Reinforced Concrete Bridge Decks and Traffic Railings Nov.* 2009.

12. Grzebieta, R.H., R. Zou, and T. Jiang, *Roadside hazard and barrier crashworthiness issues confronting vehicle and barrier manufactures and government regulators.*

13. *NCHRP Report 115: Guardrail Performance and Design, Highway Research Board, National Research Council.* National Cooperative Highway Research Program 1971.

14. El-Salakawy, E., B. Benmokrane, R. Masmoudi, Brière, F. , and E. Breaumier, *Concrete Bridge Barriers Reinforced With Glass Fiber-Reinforced Polymer Composite Bars*. 2003. **ACI Struct. J., 100(6) 815–82.**

15. Code, C.H.B.D., *Canadian Highway Bridge Design Code*, in *CAN/CSA-S6-06*

2006, CSA.

16. Benmokrane, B., E. El-Salakawy, S. El-Gamal, and S. Goulet, *Construction and Testing of Canada's First Concrete Bridge Deck Totally Reinforced With Glass FRP Bars: Val-Alain Bridge on Highway 20 East.* **J. Bridge Eng., 12(5), 632–64**.

17. Buth, C.E., W.F. Williams, R.P. Bligh, W.L. Menges, and R.R. Haug, *Performance of the txdot t202 (mod) bridge rail reinforced with fiber reinforced polymer bars*. 2003.

18. Liao, H., *Rehabilitation of the Baden Creek Bridge, Vector Corrosion Technologies*.

19. CBCL Consulting Engineers, *Clark's Mill Bridge, Prince County*. 2007: Canada.

20. *Ross Corner Bridge Canada*. 2011, Aslan FRP.

21. AASHTO, *AASHTO LRFD Bridge Design Specifications, Seventh edition, American Association of State Highway and Transportation Officials*. 2014: Washington.

22. Ross, H.E., D.L. Sicking, R.A. Zimmer, and J.D. Michie, *Recommended Procedures for the Safety Performance Evaluation of Highway Features*, N.R. 350, Editor. 1993.

23. Hirsch, T.J., *nalytical Evaluation Of Texas Bridge Rails To Contain Buses And Trucks*, in *College Station*, T.T. Institute, Editor.

24. Fernando, J.S., *A Generalized Strip Method of Reinforced Concrete Slab Design*, in *Department of civil and municipal engineering*. 1977, University College London: London.

25. El-Salakawy, E., F. Brière, R. Masmoudi, B. Tighiouart, and B. Benmokrane, *Impact test on concrete bridge barriers reinforced with gfrp composite bars.* August 2001.

26. Khatibmasjedi, S., F. De Caso y Basalo, and A. Nanni, *SEACON: Redefining Sustainable Concrete*, in *Fourth International Conference on Sustainable Construction Materials and Technologies*. Las Vegas, USA,.

Appendix A: Halls River Bridge, Innovation Aspects and Construction Process

The Halls River Bridge is an ambitious project of FDOT in which the University of Miami and Seacon are also involved. It is an important project with the objective to demonstrate the possibility of producing sustainable concrete using seawater and salt-contaminated aggregates (natural or recycled). The combination of this new idea of concrete with noncorrosive reinforcement is the base for the construction of durable and economical concrete infrastructures.

The Halls River Bridge is located in Homosassa in the north part of Tampa, (Figure 53) and it will take the place of an existing bridge.

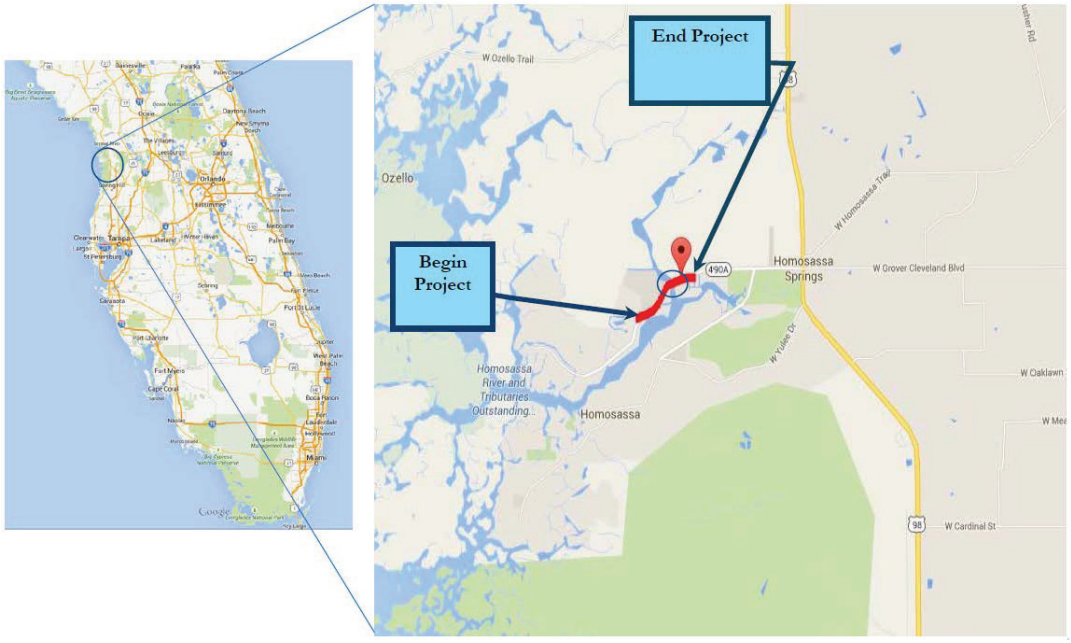

Figure 53 - Halls River Bridge position

All the reinforcements inside the bridge will be made by composite materials (CFRP and GFRP). This is an extremely innovative work since construction where steel is not used is, nowadays, rare. This is a new concept of bridge; in fact, according to Florida Department of Transportation, Halls River Bridge is the first of its kind in Florida.

The estimated cost of the project is around $6.9 million, which will be paid entirely by the Federal Highway Administration; the construction probably will take 310 days.

Figure 54 - Existing bridge over the Halls River

The configuration of the new bridge will be 185.9 ft. (57 m), with 5 spans characterized by two 12 ft. (3.6 m) lanes, two 8 ft. (2.4 m) shoulders, and the traffic will be separated from the pedestrian area on both sides of the bridge by a railing and traffic barrier.

Different materials are used for the reinforcement of the different parts of the structure. In particular, deck, parapets and bent caps are reinforced by GFRP rebar and stirrups (Figure 55).

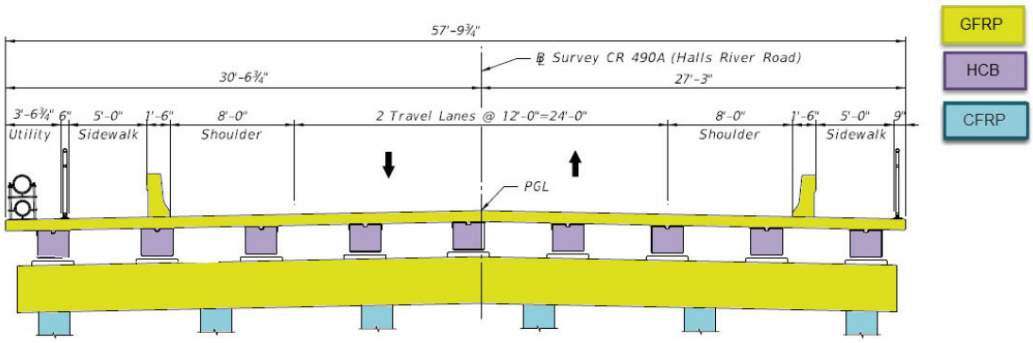

Figure 55 - FRP material in the new Halls River Bridge

The construction of the Halls River Bridge is divided in five main phases and the traffic barriers have to be installed in different time in order to address the constructability phases. The construction of the bridge has to be finished in very restricted time and one main goal is to allow the traffic of the vehicles through the Halls River Bridge during the demolition of the old bridge and the construction of the new one.

In the first phase of bridge construction, the two lane (two-way) are shifted to one lane (two-way) on existing structure, provisory New Jersey barrier (or type "K" barrier) is installed on the existing structure and then the north side of the existing bridge is demolished (left side in the Figure 56).

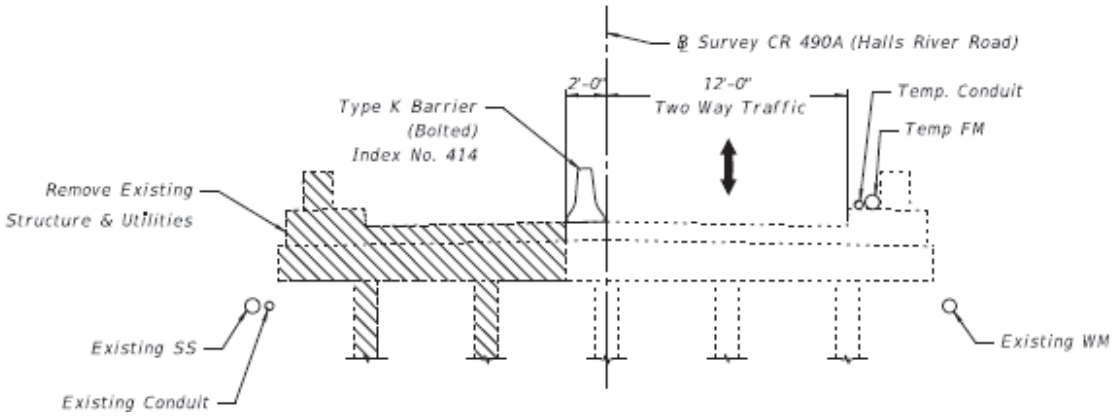

Figure 56 - First Phase of construction

In the second phase of construction, the north side of the new bridge will be built and provisory traffic barrier type “K” will be installed (Figure 57). In this phase it is not possible to build the permanent north side traffic barrier because it will be necessary, during phase three, to guarantee enough space for two way traffic in that lane.

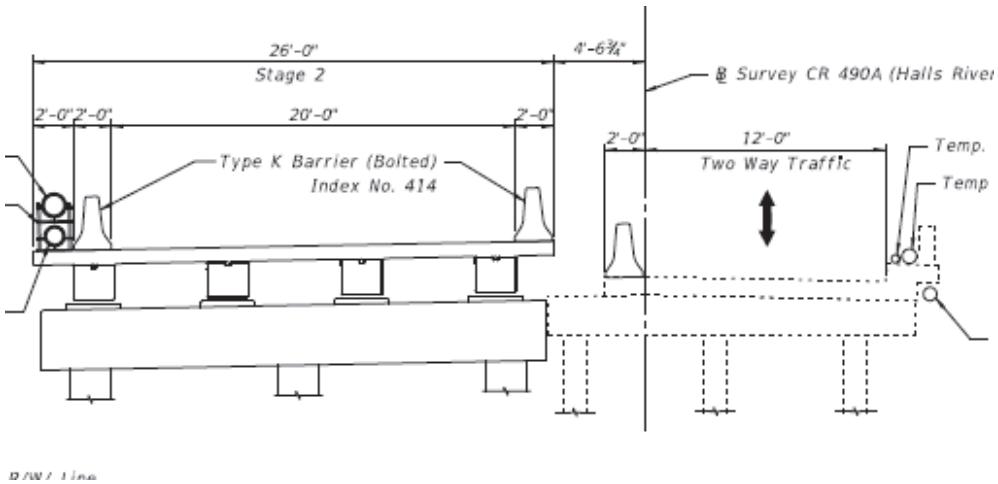

Figure 57 - Second Phase of construction

In the third phase, the two way lane will be shifted to the new side of the bridge, then the South Side of the old bridge will be demolished and the remaining portion of the bridge will be constructed. In this phase, the South Side permanent traffic railing F32” will be cast with the deck.

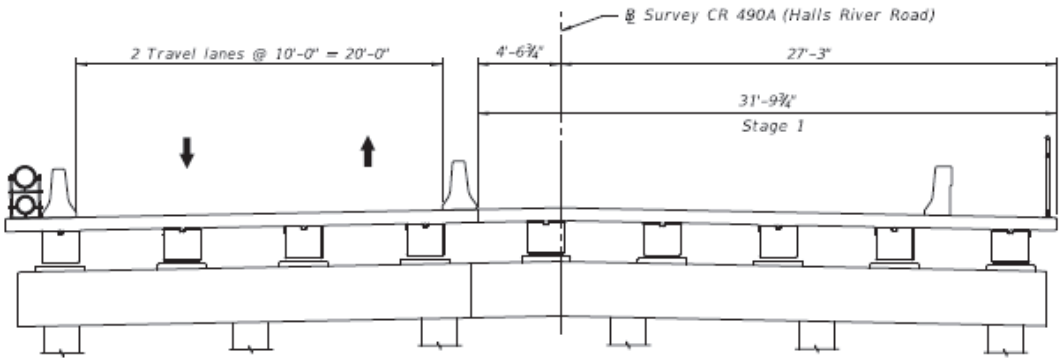

Figure 58 - Third phase of construction

In the fourth stage (Figure 59), the traffic from the North Side will be shifted to the South Side of the new structure in order to build the North Side Traffic Barrier F32".

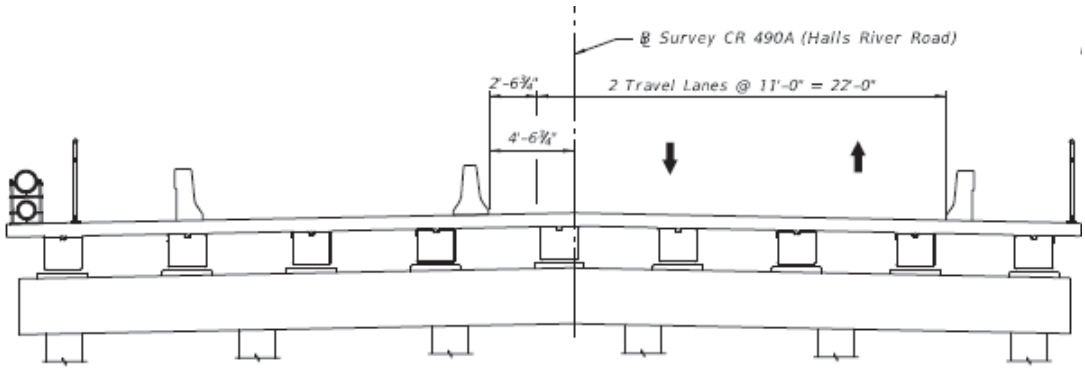

Figure 59 - Fourth phase of construction

In the last phase (Figure 60), the provisory traffic railing K type will be removed and the traffic will be shifted to the final alignment of the new structure.

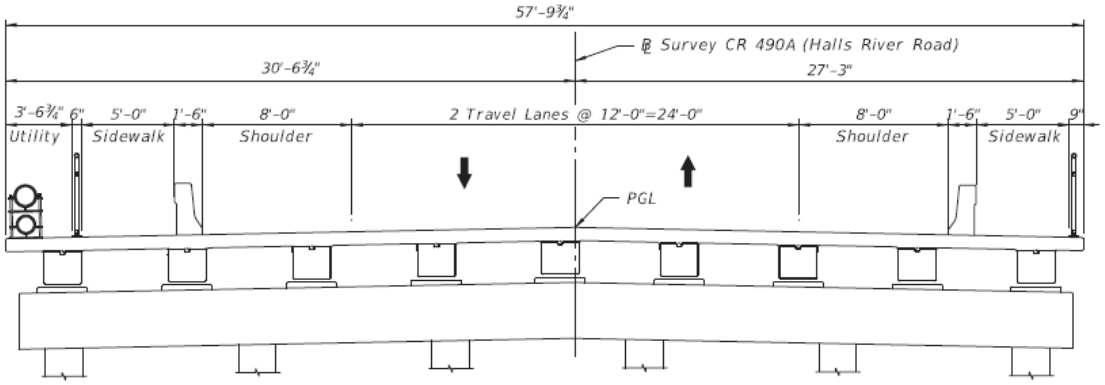

Figure 60 - Fifth phase of construction

The construction of the traffic railings of the South Side will be made in two main steps. In the first step the bent rebar 5A (5A* for the section B-B) and rebar 5V (5V* for the section B-B) will be tied with the deck rebars "493-6S2", which have a spacing of 4.5 in (114 mm). The rebar 5V will be placed every 4.5 in. (114 mm) and the bent rebar 5A every 9 in. (228 mm). Then the rebar 5A and 5V will be cast with the deck (Figure 61 - First step Section A-A and B-B South Side).

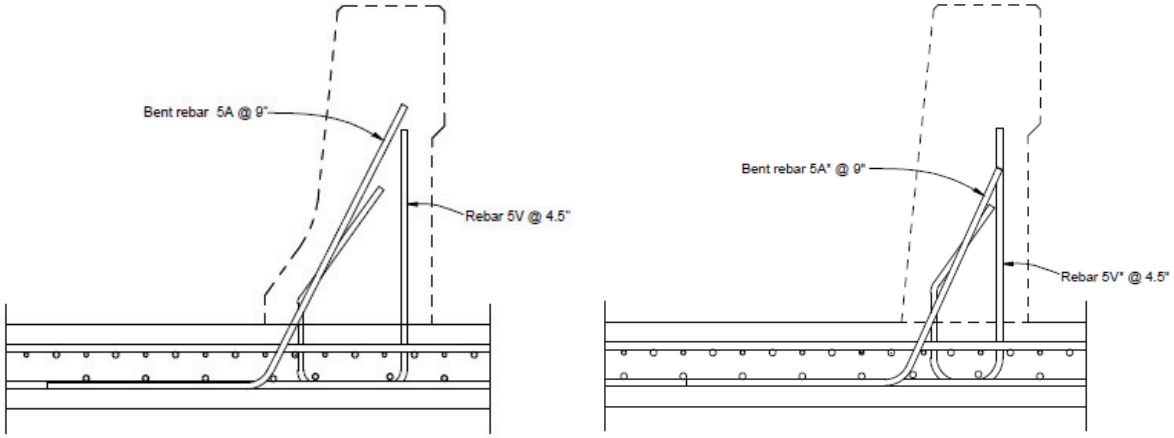

Figure 61 - First step Section A-A and B-B South Side

In the second step the rebar 5P will be tied to the rebar 5V (5V* for section B-B) and 5A (5A* for section B-B) every 4.5 in. (114 mm) and the longitudinal rebar 5S will be tied to the stirrups 5P. Then the traffic barrier will be cast (Figure 62).

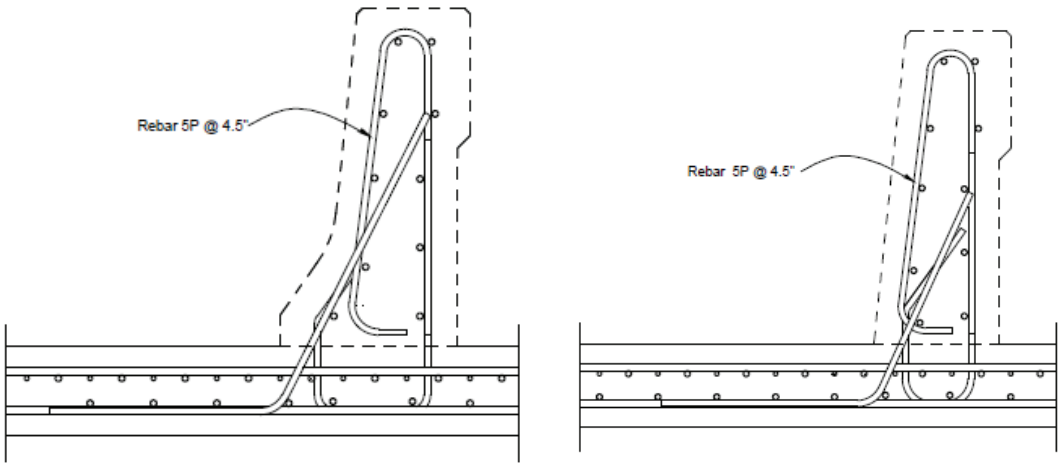

Figure 62 - Second step Section A-A and B-B South Side

The construction of the North Side Traffic Barrier will be made in two main steps as well but will be more complicated than the construction of the traffic barriers on the other side. In fact, in order to insert the traffic barrier after the casting of the deck and give structural connection between deck and traffic railings it is necessary to drill the rebars inside the existing deck.

To drill the rebars inside the deck without damaging the concrete deck and the deck rebars, those rebars have to be inserted in the correct place and allow a faster drilling. “Blockout” will be casted with the deck during the first step. In order not to damage the deck rebars during the drilling, Blockouts must have a minimum distance of ¼ in. with deck rebar. Additional supporting rebars are needed to ensure that, during construction, blockout will maintain design position (perfectly verticals and with precise horizontal spacing). They may be made of both, GFRP or PVC; even if PVC is less expensive, GFRP is recommended because it has better adherences when tied to the supporting rebars, since PVC presents a smooth surface. Blockouts 5i will be placed every 4.5 in. and 5d every 9 in. (Figure 63).

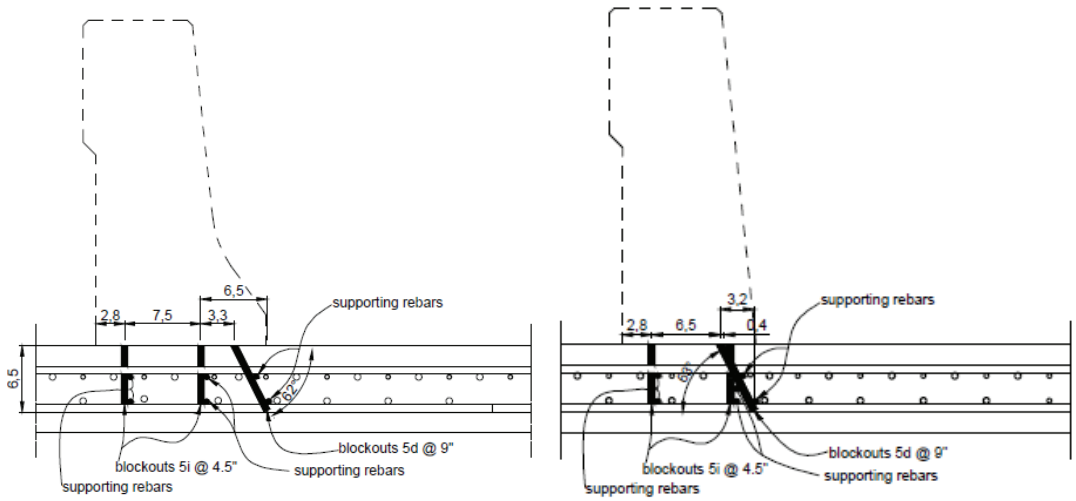

Figure 63 - First step Section A-A and B-B North Side

In the second step (Figure 64), after the casting of the deck, blockouts 5i and 5d will be removed by drilling them. Then rebar 5P* will be inserted and anchored with epoxy in the halls made by removing 5i and rebar 5D. Longitudinal rebars 5S will be tied to rebar 5P* and, ultimately, the traffic barrier will be cast.

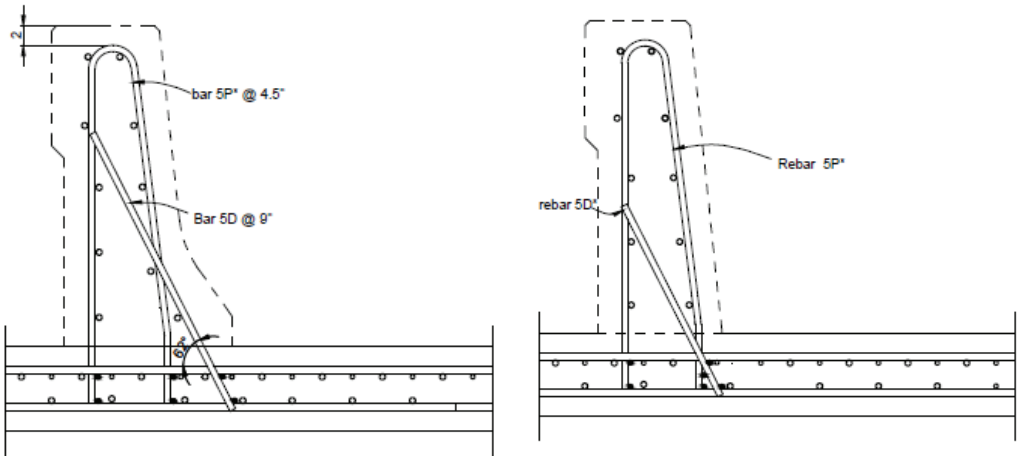

Figure 64 - Second step Section A-A and B-B North Side

Appendix B

CALCULATIONS TO SUPPORT GFRP-RC TRAFFIC RAILING DESIGN

HALLS RIVER BRIDGE REPLACEMENT PROJECT

FEBRUARY 23rd 2017

UNIVERSITY OF MIAMI

College of Civil Architectural & Environmental Engineering

Paolo Rocchetti
Guillermo Claure
Antonio Nanni

TRAFFIC RAILING DESIGN

Input data in green cells		
Geometry and concrete		
height of parapet	32	in
width of parapet - top	10.75	in
width of parapet - bottom	16.75	in
effective distance stirrups - bottom	10.3	in
Clear cover	2.5	in
f_c'	5.5	ksi
ε_{cu}	0.003	
ϕ lime rock	0.9	
Ec	3841	ksi

AASHTO LRFD 2009 for GFRP-RC Bridge Design Table 4.5.4-1
Designation of GFRP Round bars

Table 4.5.4-1—Designation of GFRP Round bars

Bar Size Designation	Nominal Diameter, in.	Nominal Area, in.^{2}
2	0.250	0.05
3	0.375	0.11
4	0.500	0.20
5	0.625	0.31
6	0.750	0.44
7	0.875	0.60
8	1.000	0.79
9	1.128	1.00
10	1.270	1.27

AASHTO LRFD 2009 for GFRP-RC Bridge Design Table 4.6.1-1
Minimum Tensile Strength for GFRP Bars

Bar Size Designation	Minimum Tensile Strength as Reported by Manufacturer, psi
2	110,000
3	110,000
4	100,000
5	95,000
6	90,000
7	85,000
8	80,000
9	75,000
10	70,000

Input data in green cells

GFRP Reinforcement

Name/numb	diameter (in)	Area section (in2)	f_{fu} (ksi)	f_{fd} (ksi)	ε_{fu}	ε_{fd}
5A bent (or 5D)	0.625	0.31	95	66.5	0.0146	0.010
5P; 5V	0.625	0.31	95	66.5	0.0146	0.010
5S longitudinal back	0.625	0.31	95	66.5	0.0146	0.010
5L longitudinal front	0.625	0.31	95	66.5	0.0146	0.010

Ef	6500.0	ksi
Ce	0.7	Environ. Reduction
ffv	26.00	ksi

Rebars working in flexion: Mechanism 1 (Simply supported with load distributed in a span of 3.5 ft.)

type	number	total number	diameter (in)	Area section (in2)	D (in)	height of section (in)
5S longitudinal b	5	10	0.625	0.307	7.938	10.750

Rebars working in flexion: Mechanism 2 (Cantilever section with load at impact location)

type	number	Spacing (in)	diameter (in)	Area section (in2)	D (in)	height of section (in)
5P; 5V	2.67	4.50	0.63	0.31	10.30	16.75
5A bent (or 5D)	1.33	9.00	0.63	0.31	13.94	16.50

Rebars working for shear: Mechanism 1

type	number of legs	number rebars	spacing (in)	diameter (in)	Area section (in2)	D (in)	height of section (in)
5P; 5V	1	2.67	4.50	0.63	0.31	9.07	11.00

Rebars working for shear: Mechanism 2

type	number of legs	number rebars	spacing (in)	diameter (in)	Area section (in2)	D (in)	height of section (in)
5P; 5V	2	2.67	4.50	0.63	0.31	10.30	16.75
5A bent (or 5D)	1	1.33	9.00	0.63	0.31	13.94	16.50

Results & Verifications

Check	Verified if Ratio<1

Development Length			Lreq/L
Lreq	19.20	in	
L provided	20.00	in	
VERIFIED			0.96

Flexural Verification			
Limits for reinforcement			
VERIFIED			
Af/Afmin	1.07		
Flexural Strength Mechanism 1			Mreq/Mr
VERIFIED			0.46
Flexural Strength Mechanism 2			Mreq/Mr
VERIFIED			0.94

Shear Verification	
Shear resistance only concrete	
NOT VERIFIED (Shear Reinforcement Required)	
Shear resistance with shear reinforcement	
Mechanism 1	Vfreq/Vf
VERIFIED	0.999
Mechanism 2	Vfreq/Vf
NOT VERIFIED (ADD Bent Bar)	1.03
Mechanism 2 including Bent bar	Vfreq/Vf
VERIFIED	0.83

Design Load and Failure Mechanisms

Design Loads (TL - 4)		
AASHTO LRFD 2014 A13.7.2 (crash test)		
Mechanism 1		
Gv	27	in
Wv	4.5	kips
B	6.5	ft.
Ftr	54	kips
He	23.75	in
Ltl	3.5	ft.

Mechanism 1 (Simply supported with load distributed in a span of 3.5 ft.)		
Mu	15.75	kip*ft.
Vu	27	kips

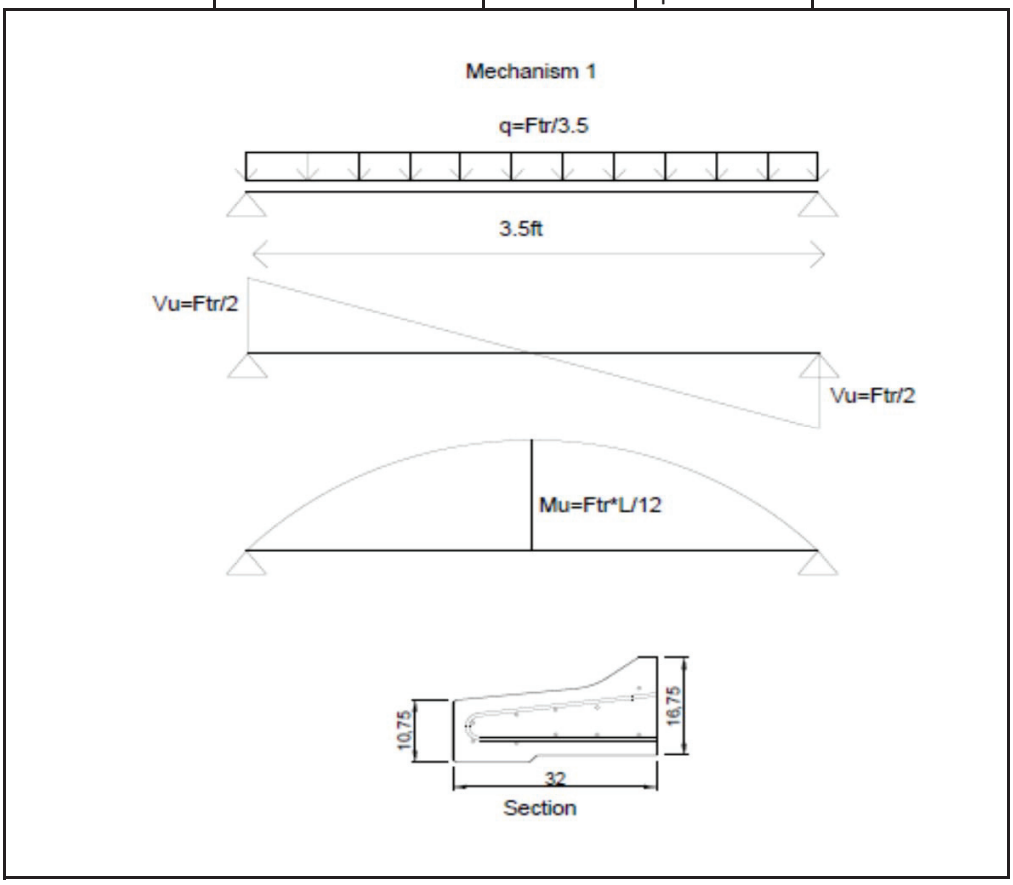

Mechanism 2 (Cantilever section		
Vu	15.4	kips/ft.
Mu	30.5	Kips*ft./ft.

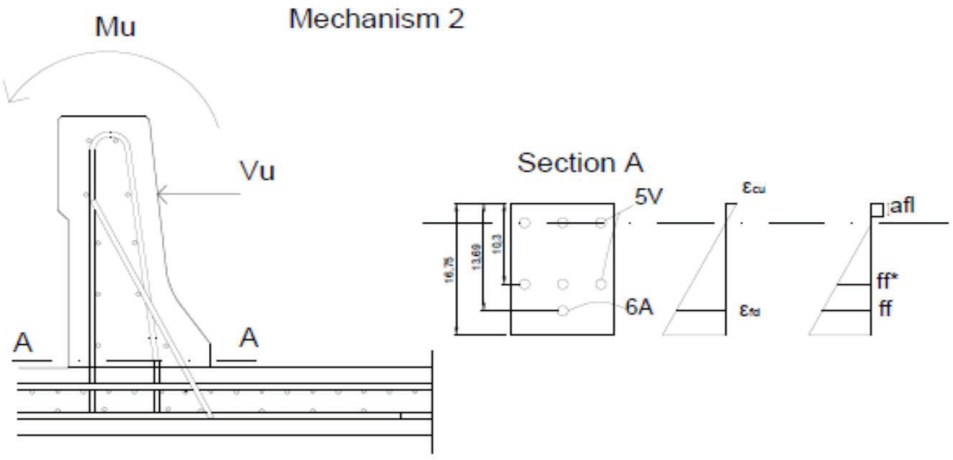

Development Length and Strength Reduction Factors

Geometry and concrete proprierty		
height parapet	32	in
Cc	2.5	in
$f_{c'super}$	5.5	ksi
ε_{cu}	0.003	
Ec	3841	ksi

Gfrp Reinforcement				
Name/numb	diameter (in)	Area section	f_{fu} (ksi)	f_{fd} (ksi)
5A bent (or 5D)	0.625	0.307	95	66.5
5P; 5V	0.625	0.307	95	66.5
5S longitudinal back	0.625	0.307	95	66.5
5L longitudinal front	0.625	0.31	95	95
ffv	26.00	ksi		

AASHTO LRFD 2009 for GFRP-RC Bridge Design, 2009

$$\phi = \begin{cases} 0.55 & \text{for } \rho_f \le \rho_{fb} \\ 0.3 + 0.25\dfrac{\rho_f}{\rho_{fb}} & \text{for } \rho_{fb} < \rho_f < 1.4\rho_{fb} \\ 0.65 & \text{for } \rho_f \ge 1.4\rho_{fb} \end{cases} \qquad (2.7.4.2\text{-}1)$$

Safety factors		
Mechanism 1	ϕfl	0.55
Mechanism 2	ϕfl	0.55
Shear factor	ϕsh	0.75

AASHTO LRFD 2009 for GFRP-RC Bridge Design, 2009

$$\ell_d = \frac{31.6\,\alpha\dfrac{f_f}{\sqrt{f'_c}} - 340}{13.6 + \dfrac{C}{d_b}} d_b \qquad (2.12.2.1\text{-}1)$$

Development Length		
AASHTO GFRP 2009 2.12.2.1		
β1	0.775	
$f_{c'super}$	5.5	ksi
Ef	6500.0	ksi
ε_{cu}	0.003	
f_{fd}	66.50	ksi
Ce	0.7	envi. Red
f_{fu}	95.0	ksi
ρ_{fb}	1.24	%
coefficient	1.4	
$1.4*\rho_{f\,b}$	1.73	%
α	1	
ff	66.5	ksi
C	2.8125	in
Ntot bars	10	
$\rho_{f\ \text{mechanism 1}}$	1.21	%
$\rho_{f\ \text{mechanism 2}}$	1.22	%
L	19.20	in

Flexural verification		
Limits for reinforcement		
D	7.94	in
B	32	In
f_{fd}	66.5	ksi
Af, min	1.4	in2
Af, provided	1.54	in2
VERIFIED		
Afmin/Af	1.07	

Flexural Strenght: Mechanism 1		
D (in)	7.94	in
ff	66.5	ksi
If failure is governed by rupture of concrete		
afl	0.68	in
Mn	65	kips*ft
ϕfl	0.55	
Mr	35.5	kips*ft
Mu	15.75	kip*ft
If failure is governed by rupture of gfrp		
ε_{fd}	0.010	
ε_{cu}	0.003	
cb	1.80	
β1	0.775	
f_{fd}	66.50	ksi
Mn	61.59	kips*ft
ϕfl	0.55	
Mr	33.9	kips*ft
Mu	15.75	kip*ft
Mr in current case		
Mr	33.9	Kip*ft
Mu/Mr	0.46	
VERIFIED		

Flexural Verification

AASHTO LRFD 2009 for GFRP-RC Bridge Design, 2009

$$\rho_{fb} = 0.85\beta_1 \frac{f_c'}{f_{fd}} \frac{E_f \varepsilon_{cu}}{E_f \varepsilon_{cu} + f_{fd}} \qquad (2.7.4.2\text{-}2)$$

$$f_f = \sqrt{\frac{\left(E_f \varepsilon_{cu}\right)^2}{4} + \frac{0.85\beta_1 f_c'}{\rho_f} E_f \varepsilon_{cu}} - 0.5 E_f \varepsilon_{cu} \le f_{fd} \qquad (2.9.3.1\text{-}1)$$

$$A_{f,\min} \ge \max\left(0.16\sqrt{f_c'}; 0.33\right) \frac{bd}{f_{fd}} \qquad (2.9.3.3\text{-}1)$$

$$M_n = A_f f_f \left(d - \frac{a}{2}\right) \qquad (2.9.3.2.2\text{-}1)$$

$$a = \frac{A_f f_f}{0.85 f_c' b} \qquad (2.9.3.2.2\text{-}2)$$

$$M_n = A_f f_{fd} \left(d - \frac{\beta_1 c_b}{2}\right) \qquad (2.9.3.2.2\text{-}3)$$

$$c_b = \left(\frac{\varepsilon_{cu}}{\varepsilon_{cu} + \varepsilon_{fd}}\right) d \qquad (2.9.3.2.2\text{-}4)$$

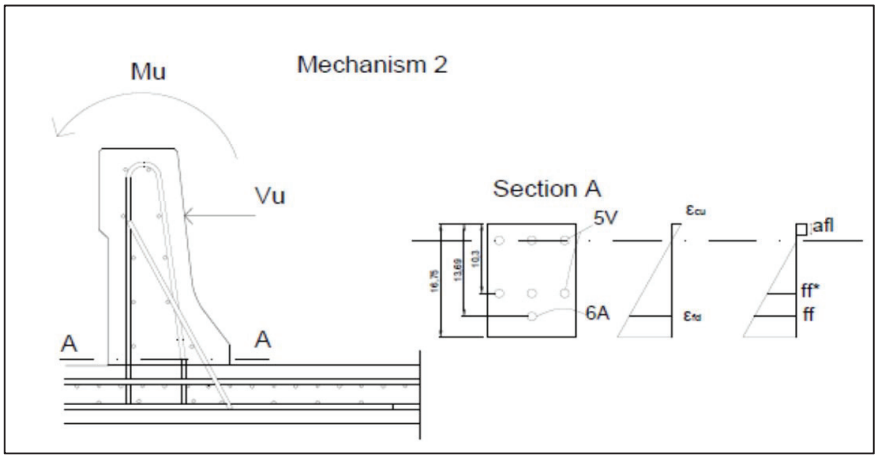

Flexural Strenght: Mechanism 2			
	Vu	15.428571	Kips/ft
	He	1.98	ft
	B	12	in
	Area	2.05	in2
	D	13.94	in
	ρ_f	1.22	
If failure is governed by rupture of concrete			
	ff	66.5	ksi
	ϕfl	0.55	
Contribution of 5A bent rebars	numb of bars	1.333	
	Af, provided	0.41	in2
	D	13.94	in
	afl	1.46	in
	Mn	29.96	
	Mr	16.48	
Contribution of stirrups 5V	ff*	49.1	ksi
	D	10.30	in
	numb of bars	2.667	
	Af, provided	0.82	in2
	Mn	32.09	Kips*ft/ft
	Mr	17.65	Kips*ft/ft
	Mr total	34.13	Kips*ft/ft
	Mu/Mr	0.89	
If failure is governed by rupture of gfrp			
	ϕfl	0.55	
Contribution of 5A bent rebars	D	13.94	in
	ρ_f	1.33	
	Af	0.409	in2
	cb	3.16	in
	β	0.775	
	f_{fd}	66.50	ksi
	Mn	28.8	Kips*ft/ft
	Mr	15.86	Kips*ft/ft
Contribution of close 5V	ff*	49.1	ksi
	D	10.30	in
	Af, provided	0.82	in2
	Mn	30.43	Kips*ft/ft
	Mr	16.74	Kips*ft/ft
	Mr total	32.60	Kips*ft/ft
	Mu / Mr tot	0.94	
	Mr in current case		
	Mr	32.6	Kip*ft
	Mu/Mr	0.94	
	VERIFIED		

Shear Verification

AASHTO LRFD 2009 for GFRP-RC Bridge Design, 2009

$$k = \sqrt{2\rho_f n_f + (\rho_f n_f)^2} - \rho_f n_f \qquad (2.7.3\text{-}4)$$

$$A_{f,v} \geq 0.05 \frac{b_w s}{f_{fv}} \qquad (2.10.2.2.1\text{-}1)$$

$$V_c = 0.16\sqrt{f'_c} b_w c \qquad (2.10.3.2.1\text{-}1)$$

$$V_f = \frac{A_{fv} f_{fv} d}{s} \qquad (2.10.3.2.2\text{-}1)$$

$$f_{fv} = 0.004 E_f \leq f_{fb} \qquad (2.10.3.2.2\text{-}2)$$

Shear verification Mechanism 1		
B	32	in
ρf	0.0121	
ϕlimerock	0.9	
Ec	3841.5	ksi
Ef	6500.0	ksi
nf	1.69	
k	0.1828	
D	9.07	in
C	1.66	in
Vc	19.92	kips
ϕsh	0.75	
ϕsh*Vc	14.94	
Vu	27	
NOT VERIFIED (Shear Reinforcement Required)		

5P; 5V		
Vf requ.	16.08	kips
Afv	0.28	in2
Shear resistance 5P and 5V		
B	32	in
Area section	0.307	in2
n. of legs	1	
Af	0.307	in2
ffv	26.00	ksi
d	9.07	in
Spacing	4.5	in
Vf	16.10	kips

Vf tot	16.10	kips
VERIFIED		
Vfreq/Vf	0.9991	

Shear verification Mechanism 2		
B	12	in
ρf	0.0121	
Vu	15.4	kips/ft
ϕlimerock	0.9	
Ec	3841.5	ksi
Ef	6500.0	ksi
nf	1.69	
k	0.1828	
D	13.94	in
C	2.55	in
Vc	7.74	kips
ϕsh	0.75	
ϕsh*Vc	5.8	kips
Vf requ.	3.67	kips/ft
S	4.5	in
N° 5V per foot	2.67	n per foot
n. of legs	2	
rebar per foot	5.3	
Area	0.307	in2
area tot	1.64	in2
ffv	26.00	ksi
Vf	3.55	kips/ft
NOT VERIFIED (ADD Bent Bar)		
Vfreq/vf	1.03	
Shear resistance by bent bar		
S	9	in
bent bar	1.3	n per foot
Area	0.307	in2
area tot	0.41	in2
ffv	26.00	ksi
Vf	0.89	kips/ft
Vf tot	4.43	
VERIFIED		
Vfreq/vf	0.83	

Appendix C

Mathcad Design Calculations for Traffic Railing

F-Shape 32”

May 7th 2017

UNIVERSITY OF MIAMI
College of Civil Architectural & Environmental Engineering

Paolo Rocchetti

A. Type, Geometry and Concrete

Type of traffic barrier : Concrete parapet [AASHTO LRFD 2014, A13.1.1]

Geometrical model: Section Thru F-Shape Railing 32 in in height [FDOT 2015, pag.59]

TL :=
1
2
3
4

TL = 4 Test Level [AASHTO LRFD 2014, 13.7.2]

Traffic railings should be at least 42 in for TL-5 and 90 in for TL-6 [AASHTO LRFD 2014, 13.7.3.2].

Concrete clear cover $c_c := 2.5in$

Height of traffic railing $H := 32in$

Width of traffic railing (top) $W_t := 10.75in$

Width of traffic railing (bottom) $W_b := 16.75in$

Width of traffic railing average $W_{av} := 12in$

Specified compressive strength of concrete $f'_{c.super} := 5.5ksi$

Ultimate strain in concrete $\varepsilon_{cu} := 0.003$

Correction factor for Florida limerock coarse aggregate $\Phi_{limerock} := 0.9$

Concrete modulus of elasticity [FDOT LRFD design example#2] $E_c := \Phi_{limerock} \cdot 1820 \quad f'_{c.super} \cdot ksi = \sqrt[3]{8 \times 10^{3} \cdot ksi}$

Table 4.5.4-1—Designation of GFRP Round bars

Bar Size Designation	Nominal Diameter, in.	Nominal Area, in.^{2}
2	0.250	0.05
3	0.375	0.11
4	0.500	0.20
5	0.625	0.31
6	0.750	0.44
7	0.875	0.60
8	1.000	0.79
9	1.128	1.00
10	1.270	1.27

Bar Size Designation	Minimum Tensile Strength as Reported by Manufacturer, psi
2	110,000
3	110,000
4	100,000
5	95,000
6	90,000
7	85,000
8	80,000
9	75,000
10	70,000

Traffic barrier transverse reinforcement bent bar size. (GFRP 5A or 5D bent bars)

$No_{tr.bent} := 5$

$No_{tr.bent} = 5$

Traffic barrier longitudinal reinforcement bar size. (GFRP 5L straight bars)

$No_{lg} := 5$

$No_{lg} = 5$

Traffic barrier shear reinforcement bar size. (GFRP 5P and 5V)

$No_{tr.sh} := 5$

$No_{tr.sh} = 5$

Recall:

$No_{tr.bent} = 5$ Traffic barrier transverse reinforcement bent bar size. (GFRP 5A or 5D bent bars)

$No_{lg} = 5$ Traffic barrier longitudinal reinforcement bar size. (GFRP 5L straight bars)

$No_{tr.sh} = 5$ Traffic barrier shear reinforcement bar size. (GFRP 5P and 5V)

Spacing of transverse reinforcement bent. (GFRP 5A or 5D bent bars)

$Sp_{tr.bent} := 9in$

Quantity of transverse bent rebarts in one foot

$Qu_{tr.bent} := \frac{12in}{Sp_{tr.bent}} = 1.3$

Spacing of shear reinforcement. (GFRP 5P and 5V)

$Sp_{tr.sh} := 4.5in$

Quantity of transverse shear reinforcement rebarts in one foot

$Qu_{tr.sh} := \frac{12in}{Sp_{tr.sh}} = 2.7$

Quantity of longitudinal reinforcement in front. (GFRP 5L straight bars)

$Qu_{lg.fr} :=$ 4 5 6 7 8 9 10

Quantity of longitudinal reinforcement in. (GFRP 5L straight bars)

$Qu_{lg.back} :=$ 4 5 6 7 8 9 10

$Qu_{lg} := Qu_{lg.fr} + Qu_{lg.back} = 10$

Environmental reduction factor [ASSHTO 2009 2.6.1.2]

$C_e := 0.7$

GFRP rebars modulus of elasticity

$E_f := 6500ksi$

Tensile strength for product certification as reported by manufacturers for transverse bent rebars:

$$f_{fu.tr.bent} := \begin{cases} 100ksi & \text{if } No_{tr.bent} = 4 \\ 95ksi & \text{if } No_{tr.bent} = 5 \\ 90ksi & \text{if } No_{tr.bent} = 6 \\ 85ksi & \text{if } No_{tr.bent} = 7 \\ 80ksi & \text{if } No_{tr.bent} = 8 \end{cases}$$

Design tensile strength of GFRP bars considering reductions for service environment for transverse bent rebars [AASHTO GFRP 2009, 2.9.3.3]

$f_{fd.tr.bent} := f_{fu.tr.bent} \cdot C_e = 66.5 \cdot ksi$

$$f_{fu.lg} := \begin{cases} 100ksi & \text{if } No_{lg} = 4 \\ 95ksi & \text{if } No_{lg} = 5 \\ 90ksi & \text{if } No_{lg} = 6 \\ 85ksi & \text{if } No_{lg} = 7 \\ 80ksi & \text{if } No_{lg} = 8 \\ 75ksi & \text{if } No_{lg} = 9 \\ 70ksi & \text{if } No_{lg} = 10 \end{cases}$$

Design tensile strength of GFRP bars considering reductions for service environment for longitudinal rebars [AASHTO GFRP 2009, 2.9.3.3]

$f_{fd.lg} =: f_{fu.lg} \cdot C_e = 66.5 \cdot ksi$

$$f_{tr.sh} := \begin{cases} 100ksi & \text{if } No_{lg} = 4 \\ 95ksi & \text{if } No_{lg} = 5 \\ 90ksi & \text{if } No_{lg} = 6 \\ 85ksi & \text{if } No_{lg} = 7 \\ 80ksi & \text{if } No_{lg} = 8 \\ 75ksi & \text{if } No_{lg} = 9 \\ 70ksi & \text{if } No_{lg} = 10 \end{cases}$$

Design tensile strength of GFRP bars considering reductions for service environment for transverse shear reinforcement [AASHTO GFRP 2009, 2.9.3.3]

$f_{fd.tr.sh} := f_{tr.sh} \cdot C_e = 66.5 \cdot ksi$

Diameters and area of corrisponding GFRP rebars (TABLE 4.5.4-1):

$$\text{diam}_{\text{No}_{lg}} := \begin{cases} 0.5\,\text{in} & \text{if } \text{No}_{lg} = 4 \\ 0.625\,\text{in} & \text{if } \text{No}_{lg} = 5 \\ 0.750\,\text{in} & \text{if } \text{No}_{lg} = 6 \\ 0.875\,\text{in} & \text{if } \text{No}_{lg} = 7 \\ 1\,\text{in} & \text{if } \text{No}_{lg} = 8 \\ 1.128\,\text{in} & \text{if } \text{No}_{lg} = 9 \\ 1.270\,\text{in} & \text{if } \text{No}_{lg} = 10 \end{cases}$$

$$\text{Area}_{\text{No.tr.bent}} := \frac{\left(\text{diam}_{\text{No}_{tr.bent}}\right)^2 \cdot \pi}{4} = 2.1 \times 10^{-3}\,\text{ft}^2$$

$$\text{diam}_{\text{No}_{tr.bent}} := \begin{cases} 0.5\,\text{in} & \text{if } \text{No}_{tr.bent} = 4 \\ 0.625\,\text{in} & \text{if } \text{No}_{tr.bent} = 5 \\ 0.750\,\text{in} & \text{if } \text{No}_{tr.bent} = 6 \\ 0.875\,\text{in} & \text{if } \text{No}_{tr.bent} = 7 \\ 1\,\text{in} & \text{if } \text{No}_{tr.bent} = 8 \\ 1.128\,\text{in} & \text{if } \text{No}_{tr.bent} = 9 \\ 1.270\,\text{in} & \text{if } \text{No}_{tr.bent} = 10 \end{cases}$$

$$\text{Area}_{\text{No.lg}} := \frac{\left(\text{diam}_{\text{No}_{lg}}\right)^2 \cdot \pi}{4} = 2.1 \times 10^{-3}\,\text{ft}^2$$

$$\text{diam}_{\text{No}_{tr.sh}} := \begin{cases} 0.5\,\text{in} & \text{if } \text{No}_{tr.sh} = 4 \\ 0.625\,\text{in} & \text{if } \text{No}_{tr.sh} = 5 \\ 0.750\,\text{in} & \text{if } \text{No}_{tr.sh} = 6 \\ 0.875\,\text{in} & \text{if } \text{No}_{tr.sh} = 7 \\ 1\,\text{in} & \text{if } \text{No}_{tr.sh} = 8 \\ 1.128\,\text{in} & \text{if } \text{No}_{tr.sh} = 9 \\ 1.270\,\text{in} & \text{if } \text{No}_{tr.sh} = 10 \end{cases}$$

$$\text{Area}_{\text{No.tr.sh}} := \frac{\left(\text{diam}_{\text{No}_{tr.sh}}\right)^2 \cdot \pi}{4} = 2.1 \times 10^{-3}\,\text{ft}^2$$

Distance from extreme compression fiber to centroid of tension reinforcement at the critical section

$$D := W_t - \frac{\left(diam_{No_{lg}}\right)}{2} - c_c = 7.9 \cdot in$$

Distance from extreme compression fiber to centroid of tension reinforcement at the critical section for a Cantiliver beam mechanism taken to be the bottom of the railing [AASHTO GFRP 2009, 2.9.3.3]

$$D_{bottom} := W_b - c_c - \frac{diam_{No_{tr.bent}}}{2} = 13.9\,in$$

GFRP reinforcement ratio [ASSHTO 2.7.4.2]

$$\rho_1 := \frac{Qu_{lg} \cdot Area_{No.lg}}{(H \cdot D)} = 1.2 \cdot \%$$

GFRP reinforcement ratio [ASSHTO 2.7.4.2]

$$\rho_{2.bottom} := Area_{No.tr.sh} \cdot \frac{\left(Qu_{tr.sh} \cdot 2 + Qu_{tr.bent}\right)}{\left(12in \cdot D_{bottom}\right)} = 1.2 \cdot \%$$

Stress-block coefficient [ACI 318-14]

$$\beta_{1.super} := \begin{cases} 0.85 & \text{if } f'_{c.super} = 4000psi \\ 1.05 - 0.05 \cdot \frac{f'_{c.super}}{1000psi} & \text{if } 4000psi < f'_{c.super} < 8000psi \\ 0.65 & \text{otherwise} \end{cases} = 0.8$$

B. Development Length and Reinforcement Splices

Transversal bent GFRP reinforcement ratio producing balanced condition [AASHTO GFRP 2009, 2.7.4.2-2]:

$$\rho_{fbtr} := 0.85 \cdot \beta_{1.super} \cdot \frac{f'_{c.super} \cdot E_f \cdot \varepsilon_{cu}}{f_{fd.tr.bent} \cdot \left(E_f \cdot \varepsilon_{cu} + f_{fd.tr.bent}\right)} = 1.2 \cdot \%$$

Longitudinal GFRP reinforcement ratio producing balanced condition [AASHTO GFRP 2009, 2.7.4.2-2]:

$$\rho_{fblg} := 0.85 \cdot \beta_{1.super} \cdot \frac{f'_{c.super} \cdot E_f \cdot \varepsilon_{cu}}{f_{fd.lg} \cdot \left(E_f \cdot \varepsilon_{cu} + f_{fd.lg}\right)} = 1.2 \cdot \%$$

Transverse GFRP reinf. ratio at start of concrete crash [AASHTO GFRP 2009, 2.7.4.2] $\rho_{ftr} := 1.4 \cdot \rho_{fbtr} = 0.017$

Long. GFRP reinf. ratio at start of concrete crash [AASHTO GFRP 2009, 2.7.4.2] $\rho_{flg} := 1.4 \cdot \rho_{fblg} = 0.017$

Rebar location modification factor [AASHTO GFRP 2009, 2.12.2.2.1] $\alpha := 1$

Effective tensile strength of transverse reinforcement [AASHTO GFRP 2009, 2.9.3.1-1]:

$$f_{ftr} := \min\left[\sqrt{\frac{\left(E_f \cdot \varepsilon_{cu}\right)^2}{4} + \frac{0.85 \cdot \beta_{1.super} \cdot f'_{c.super}}{\rho_1} \cdot E_f \cdot \varepsilon_{cu}} - 0.5 \cdot \left(E_f \cdot \varepsilon_{cu}\right), f_{fd.tr.bent}\right] = 66.5 \cdot ksi$$

$$C_{ctr} := c_c + 0.5\, diam_{No_{tr.bent}} = 2.8 \cdot in \qquad \text{[AASHTO GFRP 2009, 2.12.2.1]}$$

Transverse top reinforcement development length [AASHTO GFRP 2009, 2.12.2.1-1]:

$$l_{D.tr} := \frac{31.6 \cdot \alpha \cdot \frac{f_{ftr}}{\sqrt{f'_{c.super} \cdot ksi}} - 340}{13.6 + \frac{C_{ctr}}{diam_{No_{tr.bent}}}} \cdot diam_{No_{tr.bent}} = 19.2 \cdot in$$

C. Design Loads

Height of the vehicle center of gravity above bridge deck [AASHTO LRFD 2014, A13.7.2]

$$G_v := 27in$$

Weight of the vehicle corresponding to the required test level [AASHTO LRFD 2014, A13.7.2]

$$W_v := 4.5kip$$

Out-to-out wheel spacing on one axle [AASHTO LRFD 2014, A13.7.2]

$$B := 6.5in$$

Transverse vehicle impact forces from TL-1 to TL-6 distributed over 1ft length at height H(e) above the bridge deck [AASHTO LRFD 2014, A13.7.2]

$$F_{tr} := (13.5kip \quad 27kip \quad 54kip \quad 54kip \quad 124kip \quad 175kip)$$

Transverse vehicle impact force for the selected TL distributed over 1ft length at height H(e) above the bridge deck [AASHTO LRFD 2014, A13.7.2]

$$\left(F_{tr}\right)_{4,TL} := 54kip$$

Effective height of the vehicle rollover force [AASHTO LRFD 2014, A13.2-1]

$$H_e := G_v - 12 \cdot W_v \cdot \frac{B}{\left(2 \cdot F_{tr_{4,TL}}\right)} = 23.8 \cdot in$$

Longitudinal length of distribution of impact force from TL-1 to TL-6 along the railing located at height H(e) above the deck [AASHTO LRFD 2014, A13.2]

$$L_t := (4ft \quad 4ft \quad 4ft \quad 3.5ft \quad 8ft \quad 8ft)$$

Longitudinal length of distribution of impact force for the selected TL along the railing located at height H(e) above the deck [AASHTO LRFD 2014, A13.2]

$$L_{t_{4,TL}} := 3.5ft$$

Ultimate Bending moment on longitudinal direction acting on the length of distribution of the impact force (structural model 1)

$$M_{u1} := \frac{\frac{F_{tr_{4,TL}}}{L_{t_{4,TL}}} \cdot \left(L_{t_{4,TL}}\right)^2}{8} = 24 \cdot kip \cdot ft$$

Ultimate Shear force on longitudinal direction acting on the length of distribution of the impact force (strucutral model 1)

$$V_{u1} := \frac{F_{tr_{4,TL}}}{ft} \cdot 1\,\frac{ft}{2} = 27 \cdot kip$$

Ultimate Shear force on vertical direction acting on the length of distribution of the impact force (structural model 2)

$$V_{u2} := \frac{F_{tr_{4,TL}} \cdot ft}{L_{t_{4,TL}}} = 15.4 \cdot kip$$

Ultimate Bending moment on vertical direction acting on the length of distribution of the impact force (structural model 2)

$$M_{u2} := \left(V_{u2} \cdot H_e\right) = 31 \cdot ft \cdot kip$$

D. Flexural Verification

D1. Limits for Reinforcement

Distance from extreme compression fiber to centroid of tension reinforcement at the critical section

$$D := W_t - \frac{\left(diam_{No_{lg}}\right)}{2} - c_c = 7.9 \cdot in$$

Width of cross section [AASHTO GFRP 2009, 2.9.3.3]

$$H := 32in$$

Design tensile strength of GFRP bars considering reductions for service environment [AASHTO GFRP 2009, 2.9.3.3]

$$f_{fd.lg} = 66.5\,ksi$$

Minimum requirement for flexural tensile reinforcement [AASHTO GFRP 2009, 2.9.3.3]:

$$A_{f\_min} := \max\left[0.16\sqrt{f'_{c.super} \cdot ksi}\,\frac{HD}{f_{fd.lg}}, \left(0.33 \cdot \frac{HD}{f_{fd.lg}}\right)\frac{kip}{in^2}\right] = 1.4 \cdot in^2$$

Area of reinforcement provided

$$A_{f\_long} := Qu_{lg.back} \cdot Area_{No.lg} = 1.5 \cdot in^2$$

Minimum requirement for flexural tensile reinforcement [AASHTO GFRP 2009, 2.9.3.3]

$$A_{f\_min} = 1.4 \cdot in^2$$

$$check\_flexural\_minimum\_reinforcement := \begin{cases} \text{"VERIFIED"} & \text{if } A_{f\_long} \geq A_{f\_min} \\ \text{"NOT VERIFIED"} & \text{otherwise} \end{cases}$$

check_flexural_minimum_reinforcement = "VERIFIED"

D2. Flexural Strength Structural model 1

Distance from extreme compression fiber to centroid of tension reinforcement [AASHTO GFRP 2009, 2.9.3.3]

$D = 7.9 \cdot in$

Effective strength in GFRP reinforcement [AASHTO GFRP 2009, 2.9.3.1-1]

$f_{fd.lg} = 66.5 \cdot ksi$

Tensile strength of longitudinal reinforcement for product certification as reported by GFRP manufacturers [AASHTO GFRP 2009, 2.6.1.2]

$f_{fu.lg} = 95 \cdot ksi$

Area of reinforcement provided

$A_{f\_long} := Qu_{lg.back} \cdot Area_{No.lg} = 1.5\,in^2$

Depth of equivalent rectangular stress block [AASHTO GFRP 2009, 2.9.3.2.2-3]:

$$a_{fl} := \frac{A_{f\_long} \cdot f_{fd.lg}}{0.85 \cdot f'_{c.super} \cdot H} = 0.7 \cdot in$$

Concrete ultimate strain [AASHTO GFRP 2009, 2.9.2.1]

$\varepsilon_{cu} = 0.003$

Design strain of longitudinal reinforcement considering reduction for service environment [AASHTO GFRP 2009, 2.6.1.2]

$\varepsilon_{fdNo.lg} =: 0.0102$

GFRP reinforcement ratio [AASHTO GFRP 2009, 2.7.4.2]

$\rho_{flg} = 0.017$

Distance from extreme compression fiber to neutral axis at balanced condition [AASHTO GFRP 2009, 2.9.3.2.2-4]

$$c_b := \frac{\varepsilon_{cu}}{\varepsilon_{cu} + \varepsilon_{fdNo.lg}} D = 1.8 \cdot in$$

$$M_n := \begin{cases} \left[A_{f\_long} \cdot f_{fd.lg} \cdot \left(D - \frac{a_{fl}}{2} \right) \right] & \text{if } \rho_1 > \rho_{flg} \\ \left[A_{f\_long} \cdot f_{fd.lg} \cdot \left(D - \frac{\beta_{1.super} \cdot c_b}{2} \right) \right] & \text{if } \rho_1 \le \rho_{flg} \end{cases}$$

Nominal flexural resistance [AASHTO GFRP 2009, 2.9.3.2.2-1,2.9.3.2.2-3]

$M_n = 61.5 \cdot kip \cdot ft$

$$\Phi_{fl} := \begin{cases} 0.55 & \text{if } \rho_1 \le \rho_{fblg} \\ \left(0.3 + 0.25 \cdot \frac{\rho_{flg}}{\rho_{fblg}} \right) & \text{if } \rho_{fblg} < \rho_1 < 1.4 \cdot \rho_{fblg} \\ 0.65 & \text{if } \rho_1 \ge 1.4 \cdot \rho_{fblg} \end{cases}$$

Resistance factor for flexure [AASHTO GFRP 2009,2.7.4.2-1]

$\Phi_{fl} = 0.6$

Factored flexural resistance [AASHTO GFRP 2009, 2.9.3.2.1-1]

$M_r := \Phi_{fl} \cdot M_n = 34 \cdot kip \cdot ft$

Ultimate bending moment due to impact force on longitudinal direction $M_{u1} = 24 \cdot kip \cdot ft$

$$check\_flexural\_resistance\_1 := \begin{pmatrix} \text{"VERIFIED"} & \text{if } M_r \geq M_{u1} \\ \text{"NOT VERIFIED"} & \text{otherwise} \end{pmatrix}$$

check_flexural_resistance_1 = "VERIFIED"

D3. Flexural Strength Structural Model 2

Distance from extreme compression fiber to centroid of tension reinforcement at the critical section for a Cantiliver beam mechanism taken to be the bottom of the railing $D_{bottom} = 13.9\,in$

Distance from extreme compression fiber to centroid of tension reinforcement at the critical section for stirrups (5V)
[AASHTO GFRP 2009, 2.9.3.3] $D_{str} := 10.3in$

The effective strength in the reinforcement 5V close when failure is initiated by crushing of the concrete. $f_{f.tr} := f_{fd.tr.sh} \cdot \frac{D_{str}}{D_{bottom}} = 49.1\,ksi$

Depth of equivalent rectangular stress block [AASHTO GFRP 2009, 2.9.3.2.2-3]:

$$a_{fl.2} := \frac{Qu_{tr.sh} \cdot Area_{No.tr.sh} \cdot f_{fd.lg} + Qu_{tr.bent} \cdot Area_{No.tr.bent} \cdot f_{fd.lg}}{0.85 \cdot f'_{c.super} \cdot 12in} = 1.5 \cdot in$$

Concrete ultimate strain [AASHTO GFRP 2009, 2.9.2.1] $\varepsilon_{cu} = 0.003$

Design strain of transverse reinforcement considering reduction for service environment [AASHTO GFRP 2009, 2.6.1.2] $\varepsilon_{fd.tr} := 0.0102$

Distance from extreme compression fiber to neutral axis at balanced condition
[AASHTO GFRP 2009, 2.9.3.2.2-4]

$$c_{b.2} := \frac{\varepsilon_{cu}}{\varepsilon_{cu} + \varepsilon_{fdNo.lg}} D_{bottom} = 3.2 \cdot in$$

$Q := Qu_{tr.bent}$ $f := f_{fd.tr.bent}$ $\rho_2 := \rho_{2.bottom}$

$A := Area_{No.tr.bent}$ $D_b := D_{bottom}$

$$M_{n.2} := \begin{cases} \left[(Q \cdot A \cdot f) \cdot \left(D_b - \frac{a_{fl.2}}{2}\right) + \left(Qu_{tr.sh} \cdot Area_{No.tr.sh} \cdot f_{fd.tr.sh}\right) \cdot \left(D_{str} - \frac{a_{fl.2}}{2}\right)\right] & \text{if } \rho_2 > \rho_{flg} \\ \left[(Q \cdot A \cdot f) \cdot \left(D_b - \frac{\beta_{1.super} \cdot c_{b.2}}{2}\right) + \left(Qu_{tr.sh} \cdot Area_{No.tr.sh} \cdot f_{f.tr}\right) \cdot \left(D_{str} - \frac{\beta_{1.super} \cdot c_{b.2}}{2}\right)\right] & \text{if } \rho_2 \le \rho_{flg} \end{cases}$$

Nominal flexural resistance [AASHTO GFRP 2009, 2.9.3.2.2-1,2.9.3.2.2-3] $M_{n.2} = 59.2 \cdot kip \cdot ft$

$$\Phi_{fl} := \begin{cases} 0.55 & \text{if } \rho_1 \le \rho_{fblg} \\ \left(0.3 + 0.25 \cdot \frac{\rho_{flg}}{\rho_{fblg}}\right) & \text{if } \rho_{fblg} < \rho_1 < 1.4 \cdot \rho_{fblg} \\ 0.65 & \text{if } \rho_1 \ge 1.4 \cdot \rho_{fblg} \end{cases}$$

Resistance factor for flexure [AASHTO GFRP 2009,2.7.4.2-1] $\Phi_{fl} = 0.6$

Factored flexural resistance [AASHTO GFRP 2009, 2.9.3.2.1-1] $M_{r.2} := \Phi_{fl} \cdot M_{n.2} = 33 \cdot k$

Ultimate bending moment due to impact force on longitudinal direction $M_{u2} = 31\,kip \cdot ft$

$$check\_flexural\_resistance\_2 := \begin{pmatrix} \text{"VERIFIED"} & \text{if } M_{r.2} \ge M_{u2} \\ \text{"NOT VERIFIED"} & \text{otherwise} \end{pmatrix}$$

check_flexural_resistance_2 = "VERIFIED"

E. Shear Verification

E1. Concrete shear strength structural model 1

Width of the web [AASHTO GFRP 2009, 2.10.2.2.2] $b_w := H = 32 \cdot in$

GFRP reinforcement ratio factored flexural resistance [AASHTO GFRP 2009, 2.7.4.2] $\rho_{flg} = 1.7 \cdot \%$

Concrete modulus of elasticity [FDOT LRFD design example#2] $E_c := \Phi_{limerock} \cdot 1820 \sqrt{f'_{c.super} \cdot ksi} = 3.8 \times 10^3 \cdot ksi$

Modulus of elasticity of longitudinal GFRP reinforcement $E_f = 6.5 \times 10^3 \cdot ksi$

Modular ratio $n_f := \frac{E_f}{E_c} = 1.7$

Ratio of depth of neutral axis to reinforcement depth [AASHTO GFRP 2009, 2.7.3-4] $\kappa =: \sqrt{\left(2 \cdot \rho_1 \cdot n_f + \rho_1 \cdot n_f\right)^2} - \rho_1 \cdot n_f = 0.2$

Average distance from extreme compression fiber to centroid of tension reinforcement [AASHTO GFRP 2009, 2.9.3.3]

$D_{av} := 9.1in$

Distance from extreme compression fiber to neutral axis [AASHTO GFRP 2009, 2.10.3.2]

$C_{fl} := k \cdot D_{av} = 1.7 \cdot in$

Nominal shear strength provided by the concrete [AASHTO GFRP 2009, 2.10.3.2.1-1]:

$V_c := \min\left(0.16\sqrt{f'_{c.super} \cdot ksi} \cdot b_w \cdot C_{fl}, 0.32 \cdot \sqrt{f'_{c.super} \cdot ksi} \cdot b_w \cdot C_{fl}\right) = 20 \cdot kip$

Resistance factor for shear [AASHTO GFRP 2009, 2.7.4.2]

$\Phi_{sh} := 0.75$

Factored shear strength provided by the concrete [AASHTO GFRP 2009, 2.10.2.1-1]

$\Phi_{sh} \cdot V_c = 15 \cdot kip$

Ultimate shear force due to impact force on longitudinal direction

$V_{u1} = 27 \cdot kip$

$check\_concrete\_shear\_resistance\_1 := \begin{cases} \text{"VERIFIED: SHEAR REINFORCEMENT NOT REQUIRED"} & \text{if } \Phi_{sh} \cdot V_c \geq V_u \\ \text{"NOT VERIFIED: SHEAR REINFORCEMENT REQUIRED"} & \text{otherwise} \end{cases}$

check_concrete_shear_resistance_1 = "NOT VERIFIED: SHEAR REINFORCEMENT REQUIRED"

E2. Shear reinforcement strength structural model 1

Required nominal shear resistance provided by the GFRP shear reinforcement [AASHTO GFRP 2009, 2.10.2.1-1, 2.10.3.1-1]

$V_{f\_required} := \frac{V_{u1}}{\Phi_{sh}} - V_c = 16 \cdot kip$

Diameter of shear GFRP reinforcement

$diam_{No_{tr.sh}} = 0.6 \cdot in$

Area of shear GFRP reinforcement

$Area_{No.tr.sh} = 0.3 \cdot in^2$

Internal radius of the shear bent GFRP bar

$r_{b.sh} := 2.1in$

Average distance from extreme compression fiber to centroid of tension reinforcement [AASHTO GFRP 2009, 2.9.3.3]

$D_{av} = 9.1 \cdot in$

Strength of the bent portion of a GFRP bar [AASHTO GFRP 2009, 2.10.3.2.2-3]

$$f_{fb} := \min\left[\left(0.05\cdot\frac{r_{b.sh}}{diam_{No_{tr.sh}}} + 0.3\right)\cdot f_{fd.tr.sh}, f_{fd.tr.sh}\right] = 31.1\cdot ksi$$

Modulus of elasticity of shear GFRP reinforcement $E_f = 6.5\times 10^3\cdot ksi$

Design tensile strength for shear [AASHTO GFRP 2009, 2.10.3.2.2-2] $f_{fv} := \min\left(0.004\cdot E_f, f_{fb}\right) = 26\cdot ksi$

Maximum spacing of shear reinforcement [AASHTO GFRP 2009, 2.10.3.2.2.1] $s_{sh\_max} := \frac{Area_{No.tr.sh}\cdot f_{fv}\cdot D_{av}}{V_{f\_required}} = 4.5\cdot in$

Design spacing of shear reinforcement [AASHTO GFRP 2009, 2.10.3.2.2.1] $Sp_{tr.sh} = 4.5\cdot in$

check_shear_resistance_1 := "VERIFIED" if $s_{sh\_max} > Sp_{tr.sh}$; "NOT VERIFIED: MORE SHEAR REINFORCEMENT REQUIRED" otherwise

check_shear_resistance_1 = "VERIFIED"

Required nominal shear resistance provided by the GFRP shear reinforcement [AASHTO GFRP 2009, 2.10.2.1-1, 2.10.3.1-1] $V_{f\_required} = 16\cdot kip$

E3. Concrete shear strength structural model 2

Width of the web [AASHTO GFRP 2009, 2.10.2.2.2] $b_{w.2} := W_{av} = 12\,in$

GFRP reinforcement ratio factored flexural resistance [AASHTO GFRP 2009, 2.7.4.2] $\rho_{flg} = 1.7\cdot\%$

Concrete modulus of elasticity [FDOT LRFD design example#2] $E_{ca} := \Phi_{limerock}\cdot 1820\sqrt{f'_{c.super}\cdot ksi} = 3.8\times 10^3\cdot ksi$

Modulus of elasticity of longitudinal GFRP reinforcement $E_f = 6.5\times 10^3\cdot ksi$

Modular ratio $n_f = 1.7$

Ratio of depth of neutral axis to reinforcement depth [AASHTO GFRP 2009, 2.7.3-4] $k_2 := \sqrt{2\cdot\rho_{2.bottom}\cdot n_f + \left(\rho_{2.bottom}\cdot n_f\right)^2} - \rho_{2.bottom}\cdot n_f = 0.2$

Average distance from extreme compression fiber to centroid of tension reinforcement $D_{aw} := 9.1in$

[AASHTO GFRP 2009, 2.9.3.3]

Distance from extreme compression fiber to neutral axis [AASHTO GFRP 2009, 2.10.3.2] $C_{fl.2} := k \cdot D_{bottom} = 2.5 \cdot in$

Nominal shear strength provided by the concrete [AASHTO GFRP 2009, 2.10.3.2.1-1]:

$V_{c.2} := \min\left(0.16\sqrt{f'_{c.super} \cdot ksi} \cdot b_{w.2} \cdot C_{fl.2}, 0.32 \cdot \sqrt{f'_{c.super} \cdot ksi} \cdot b_{w.2} \cdot C_{fl.2}\right) = 11.5 \cdot kip$

Resistance factor for shear [AASHTO GFRP 2009, 2.7.4.2] $\Phi_{sh} := 0.75$

Factored shear strength provided by the concrete [AASHTO GFRP 2009, 2.10.2.1-1] $\Phi_{sh} \cdot V_{c.2} = 8.6 \cdot kip$

Ultimate shear force due to impact force on longitudinal direction $V_{u2} = 15.4 \cdot kip$

check_concrete_shear_resistance_2 := "VERIFIED: SHEAR REINFORCEMENT NOT REQUIRED" if $\Phi_{sh} \cdot V_{c.2} \geq V_u$
"NOT VERIFIED: SHEAR REINFORCEMENT REQUIRED" otherwise

check_concrete_shear_resistance_2 = "NOT VERIFIED: SHEAR REINFORCEMENT REQUIRED"

E4. Shear reinforcement strength structural model 2

Required nominal shear resistance provided by the GFRP shear reinforcement [AASHTO GFRP 2009, 2.10.2.1-1, 2.10.3.1-1] $V_{f\_required.2} := \frac{V_{u2}}{\Phi_{sh}} - V_c = 0.6 \cdot kip$

Diameter of shear GFRP reinforcement $diam_{No_{tr.sh}} = 0.6 \cdot in$

Area of shear GFRP reinforcement $Area_{No.tr.sh} = 0.3 \cdot in^2$

Internal radius of the shear bent GFRP bar $r_{b.sh} := 2.1in$

Average distance from extreme compression fiber to centroid of tension reinforcement [AASHTO GFRP 2009, 2.9.3.3] $D_{av} = 9.1 \cdot in$

Strength of the bent portion of a GFRP bar [AASHTO GFRP 2009, 2.10.3.2.2-3]

$f_{fb} = 31.1\,ksi$

Modulus of elasticity of shear GFRP reinforcement $E_f = 6.5 \times 10^3 \cdot ksi$

Design tensile strength for shear
[AASHTO GFRP 2009, 2.10.3.2.2-2] $f_{fv} = 26\,ksi$

Maximum spacing of shear reinforcement
[AASHTO GFRP 2009, 2.10.3.2.2.1] $s_{sh\_max\_2} := \frac{Area_{No.tr.sh} \cdot f_{fv} \cdot in}{V_{f\_required.2}} = 13.3 \cdot in$

Design spacing of shear reinforcement [AASHTO GFRP 2009, 2.10.3.2.2.1] $Sp_{tr.sh} = 4.5 \cdot in$

$$check\_shear\_resistance\_2 =: \begin{cases} \text{"VERIFIED"} & \text{if } s_{sh\_max\_2} > Sp_{tr.sh} \\ \text{"NOT VERIFIED: MORE SHEAR REINFORCEMENT REQUIRED"} & \text{otherwise} \end{cases}$$

check_shear_resistance_2 = "VERIFIED"

Appendix D

FINAL DRAWINGS OF F-32” GFRP-RC TRAFFIC RAILING DESIGN

HALLS RIVER BRIDGE REPLACEMENT PROJECT

FEBRUARY 24th 2017

UNIVERSITY OF MIAMI
College of Civil Architectural & Environmental Engineering

Paolo Rocchetti
Guillermo Claure
Antonio Nanni

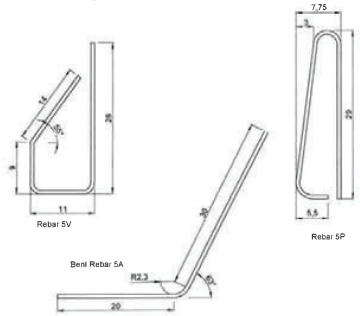

GFRP Rebars

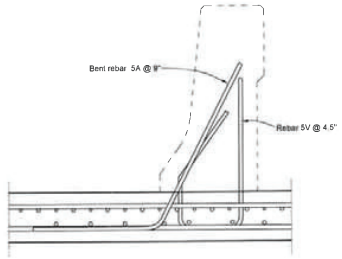

Construction: STEP 1

Note:

- tie rebars 5V @ 4 1/2" o. c. to the deck rebars 493-6S2.
- tie rebars 5A @ 9" o.c. to the deck rebars 493-6S2
- rebars 5V and 5A to be cast with deck

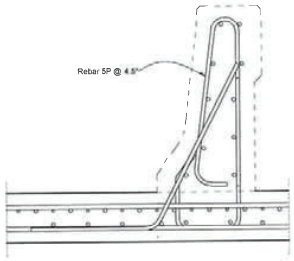

Construction: STEP 2

note:

- tie rebars 5P @ 4 1/2" o.c. to railing reinforcement 5A and 5V.
- tie the longitudinal rebars 5S to railing stirrups as per section A-A.

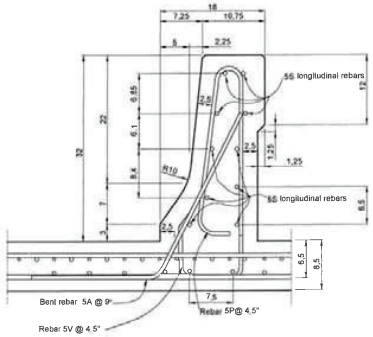

SECTION A-A
TYPICAL SECTION THRU TRAFFIC RAILING

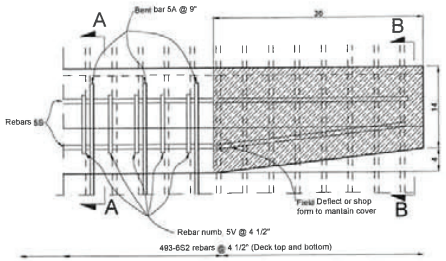

Plan - Railing End Transition
(Showing Closed stirrups 5A, 5V, and Deck rebars 493-6S2)

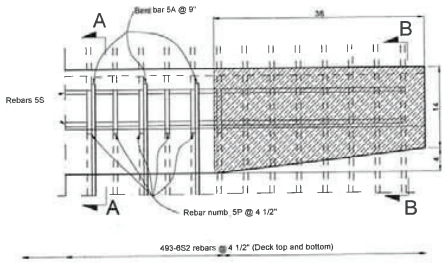

Plan - Railing End Transition
(Showing Closed stirrups 5A, 5P, and Deck rebars 493-6S2)

02/28/17

02/24/17	UNIVERSITY OF MIAMI	TRAFFIC RAILING South Side (5S option)	Sheet NO.
		(32" F SHAPE-GFRP REINFORCED) Section A-A	UM 11- 1

GFRP bent rebars

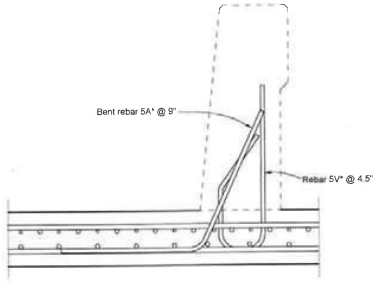

Construction: step 1

Note:

- tie rebars 5V* @ 4 1/2" o. c. to the deck rebars 493-6S2.
- tie rebars 5A* @ 9" o.c. to the deck rebars 493-6S2
- rebars 5V* and 5A* to be cast with deck

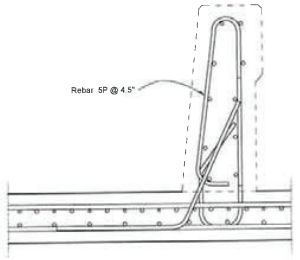

Construction: step 2

note:

- tie rebars 5P @ 4 1/2" o.c. to railing reinforcement 5A* and 5V*.
- tie the longitudinal rebars 5S at stirrups.

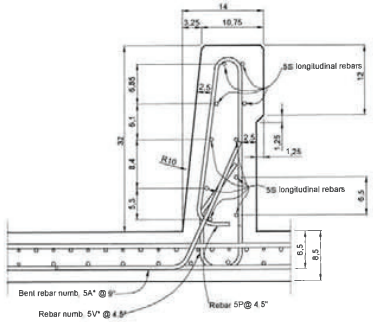

SECTION B-B
TYPICAL SECTION THRU TRAFFIC RAILING

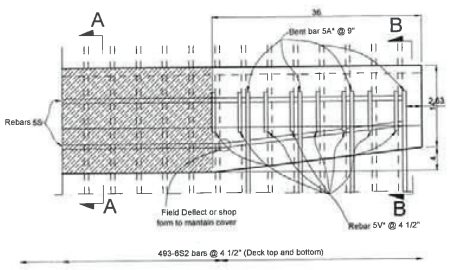

Plan - Railing End Transition
(Showing Closed stirrups 5A*, 5V*, and Deck rebars 493-6S2)

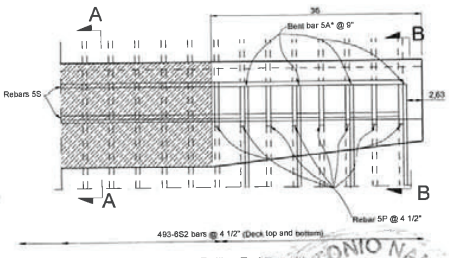

Plan - Railing End Transition
(Showing Closed stirrups 5A*, 5P, and Deck rebars 493-6S2)

ANTONIO NANNI
02/28/17

02/24/17	UNIVERSITY OF MIAMI	TRAFFIC RAILING South Side (5S option)	Sheet NO.
		(32" F SHAPE-GFRP REINFORCED) Section B-B	UM 1 - 2

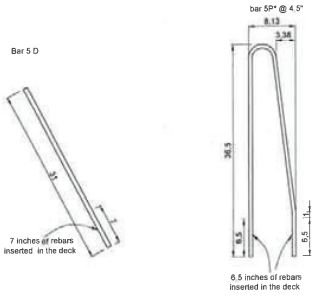

GFRP Rebars

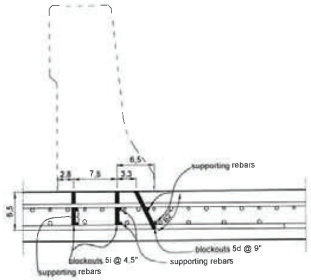

Construction: step 1

note:
- blockouts 5i and 5d could be GFRP or PVC pipes tied to specifically provided supporting rebars
- blockouts must be 1/4" clear of deck reinforcement
- blockouts 5i and 5d to be removed/drilled for step 2
- preferably use gfrp for better adherences when tied to deck reinforcement since pvc present a not faverable smooth surface

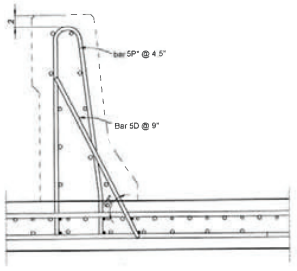

Construction: step 2

note:
- remove/drill blockouts 5i and 5d,
- insert epoxi/anchored rebars 5P* and 5D
- tie longitudinal rebars 5S to railings stirrups as per section A-A

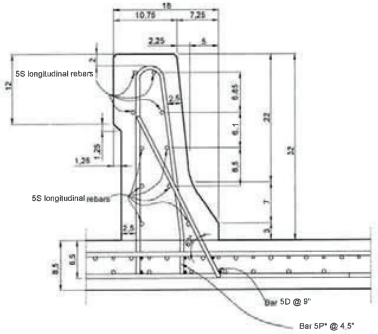

SECTION A-A
TYPICAL SECTION THRU TRAFFIC RAILING

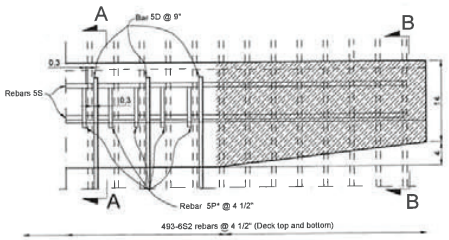

Plan - Railing End Transition
(Showing bars 5D, 5P*, and Deck rebars 493-6S2)

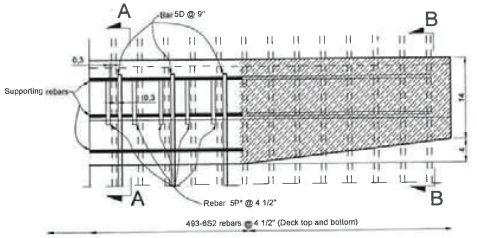

Plan - Railing End Transition
(Showing bars 5D, 5P*, supporting rebars and Deck rebars 493-6S2)

ANTONIO NANNI LICENSE
02/28/17

02/27/17	UNIVERSITY OF MIAMI	TRAFFIC RAILING North Side (5S option)	Sheet NO.
		(32" F SHAPE-GFRP REINFORCED) Section A-A	UM 2 - 1

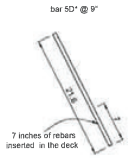

GFRP Rebars

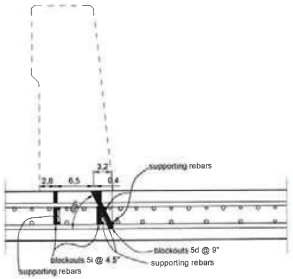

Construction: step 1

note:
- blockouts 5i and 5d could be GFRP or PVC pipes tied to specifically provided supporting rebars
- blockouts must be 1/4" clear of deck reinforcement
- blockouts 5i and 5d to be removed/drilled for step 2
- preferably use gfrp for better adherences when tied to supporting rebars since pvc present a not favorable smooth surface.

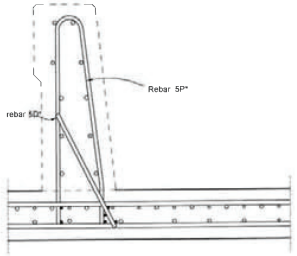

Construction: step 2

note:
- remove/drill blockouts 5i and 5d
- insert epoxiranchored 5P* and 5D*
- tie longitudinal rebars 5S to railings stirrups as per section A-A

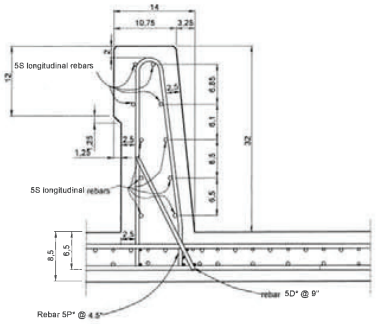

SECTION B-B
TYPICAL SECTION THRU TRAFFIC RAILING

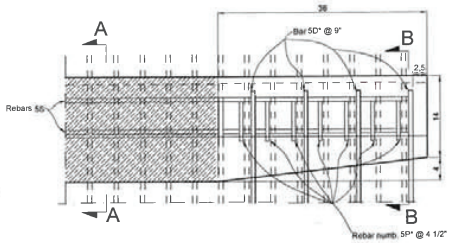

Plan - Railing End Transition
(Showing Bars 5D, 5P, and Deck rebars 493-6S2)

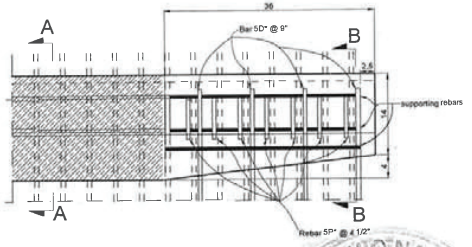

Plan - Railing End Transition
(Showing Bars 5D, 5P, supporting rebars and Deck rebars 493-6S2)

02/28/17

02/27/17	UNIVERSITY OF MIAMI	TRAFFIC RAILING North Side (5S option)	Sheet NO.
		(32" F SHAPE-GFRP REINFORCED) Section B-B	UM 2 - 2

Appendix E

CALCULATIONS TO SUPPORT GFRP-RC TRAFFIC RAILING DESIGN

Single Slope 36”

March 6th 2017

UNIVERSITY OF MIAMI
College of Civil Architectural & Environmental Engineering

Paolo Rocchetti
Guillermo Claure
Antonio Nanni

Input data in green cells as needed		
Geometry and concrete		
height of parapet	36	in
width of parapet - top	9	in
width of parapet - bottom	14.5	in
effective distance bent bar - bottom	10	in
	12	in
Clear cover	2	in
$f_{c'}$	5.5	ksi
ε_{cu}	0.003	
ϕlimerock	0.9	
Ec	3841	ksi

AASHTO LRFD 2009 for GFRP-RC Bridge Design Table 4.5.4-1
Designation of GFRP Round bars

Table 4.5.4-1—Designation of GFRP Round bars

Bar Size Designation	Nominal Diameter, in.	Nominal Area, in.^{2}
2	0.250	0.05
3	0.375	0.11
4	0.500	0.20
5	0.625	0.31
6	0.750	0.44
7	0.875	0.60
8	1.000	0.79
9	1.128	1.00
10	1.270	1.27

AASHTO LRFD 2009 for GFRP-RC Bridge Design Table 4.6.1-1

Bar Size Designation	Minimum Tensile Strength as Reported by Manufacturer, psi
2	110,000
3	110,000
4	100,000
5	95,000
6	90,000
7	85,000
8	80,000
9	75,000
10	70,000

Input data in green cells as needed						
Gfrp Reinforcement						
Name/numb	**diameter (in)**	**Area section (**	**f_{fu} (ksi)**	**f_{fd} (ksi)**	**ε_{fu}**	**ε_{fd}**
5 D bent	0.625	0.31	95	66.5	0.0146	0.010
5 C	0.625	0.31	95	66.5	0.0146	0.010
5 L longitudina	0.625	0.31	95	66.5	0.0146	0.010
5 L longitudina	0.625	0.31	95	66.5	0.0146	0.010
Ef	6500.0	ksi				
Ce	0.7	envi. Reduction				
ffv	26.00	ksi				

Rebars working in flexion: Mech. 1 (Simply supported with load distributed in a span of 3.5 ft.)						
type	number	total number	diameter (in)	Area section (in2)	D (in)	height of section (in)
5 L longitudina	5	10	0.625	0.307	6.69	9

Rebars working in flexion: Mechanism 2 (Cantilever section with load at impact location)						
type	number	Spacing (in)	diameter (in)	Area section (in2)	D (in)	height of section (in)
5 C	1.50	8.0	0.625	0.307	12.00	14.5
5 D bent	1.50	8.0	0.625	0.307	10.00	16.5

Rebars working for shear: Mechanism 1							
type	number of legs	number rebars	spacing (in)	diameter (in)	Area section (in2)	D (in)	Height of section (in)
5 C	1	1.50	8.0	0.625	0.307	8.50	11

rebars working for shear: Mechanis 2							
type	number of legs	number rebars	spacing (in)	diameter (in)	Area section (in2)	D (in)	height of section (in)
5 C	2	1.50	8.0	0.625	0.307	12.00	14.5
5 D bent	1	1.50	8.0	0.625	0.307	10.00	16.5

Results	Verified if Ratio<1

Development Length			Lreq/L
Lreq	19.51	in	
L provided	22.00	in	
VERIFIED			0.89

Flexural verification			
Limits for reinforcement			
VERIFIED			
Af/Afmin	1.13		
Flexural Strenght Mechanism 1			Mreq/Mr
VERIFIED			0.52
Flexural Strenght Mechanism 2			Mreq/Mr
VERIFIED			0.58

Shear verification	
Shear resistance only concrete	
VERIFIED	
Shear resistance with shear reinforcement	
Mechanism 1	Vfreq/Vf
VERIFIED	-0.847
Mechanism 2	Vfreq/Vf
VERIFIED without bent bar	0.80
Mechanism 2 including Bent bar	Vfreq/Vf
VERIFIED	0.53

Design Loads (TL - 4)		
AASHTO LRFD 2014 A13.7.2 (crash test)		
Mechanism 1		
Gv	27	in
Wv	4.5	kips
B	6.5	ft
Ftr	54	kips
He	23.75	in
Ltl	3.5	ft

Dimension		
Base	42	in
height	36	in
He inpact	23.75	in
div. slab	6	n°
vertical base	7	in
horiz base	6	in
tickness	12	in

Mechanism 1+ mechanism 2

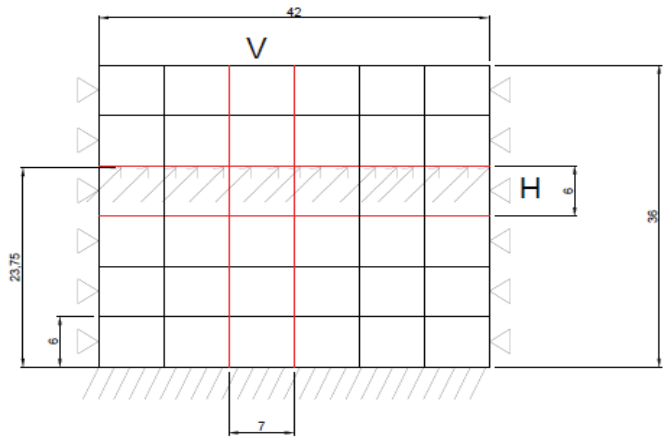

Beam H		
Inertia	864	in3
C1	46.9	in/E***

Beam V		
inertia	1008	in3
C2	31.01038	

V1=V2		
q1/q2	0.66	
qtot	1.66	*q2
qtot	15.43	kip/ft
q1	6.14	(kip/ft)
R1	10.75	kips
q2 (kip/ft	9.29	(kip/ft)
R2	32.51	kips

total reaction	54	kips
Ftr to beam V	32.5	

Mechanism 2 (Cantilever section with load at impact location)		
Vu	9.3	kips/ft
Mu	18.4	Kips*ft/ft

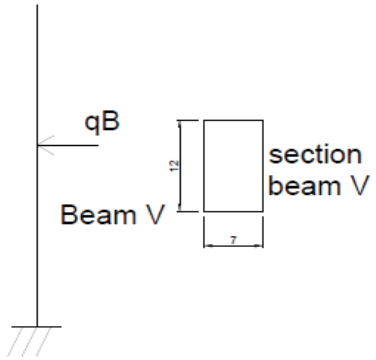

Ftr to beam H	21.5

Mechanism 1 (Simply supported with load distributed in a span of 3.5 ft.)		
Vu	10.7474645	kips
Mu	15.75	kip*ft

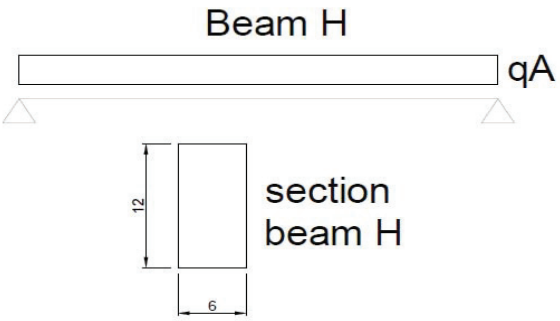

Geometry and concrete proprierty		
height parapet	36	in
Cc	2	in
$f_{c'super}$	5.5	ksi
ε_{cu}	0.003	
Ec	3841	ksi

AASHTO LRFD 2009 for GFRP-RC Bridge Design, 2009

$$\phi = \begin{cases} 0.55 & \text{for } \rho_f \le \rho_{fb} \\ 0.3 + 0.25\dfrac{\rho_f}{\rho_{fb}} & \text{for } \rho_{fb} < \rho_f < 1.4\rho_{fb} \\ 0.65 & \text{for } \rho_f \ge 1.4\rho_{fb} \end{cases} \qquad (2.7.4.2\text{-}1)$$

AASHTO LRFD 2009 for GFRP-RC Bridge Design, 2009

$$\ell_d = \frac{31.6\,\alpha\dfrac{f_f}{\sqrt{f'_c}} - 340}{13.6 + \dfrac{C}{d_b}} d_b \qquad (2.12.2.1\text{-}1)$$

Gfrp Reinforcement				
Name/numb	diameter (in)	Area section	f_{fu} (ksi)	f_{fd} (ksi)
5 D bent	0.625	0.307	95	66.5
5 C	0.625	0.307	95	66.5
5 L longitudinal back	0.625	0.307	95	66.5
5 L longitudinal front	0.625	0.31	95	95
ffv	26.00	ksi		

Safety factors		
Mechanism 1	ϕfl	0.56
Mechanism 2	ϕfl	0.55
Shear factor	ϕsh	0.75

Development Length		
AASHTO GFRP 2009 2.12.2.1		
β1	0.775	
$f_{c'super}$	5.5	ksi
Ef	6500.0	ksi
ε_{cu}	0.003	
f_{fd}	66.50	ksi
Ce	0.7	envi. Red
f_{fu}	95.0	ksi
ρ_{fb}	1.24	%
coefficient	1.4	
$1.4*\rho_{f\,b}$	1.73	%
α	1	
ff	65.3	ksi
C	2.3125	in
Ntot bars	10	
$\rho_{f\ \text{mechanism 1}}$	1.28	%
$\rho_{f\ \text{mechanism 2}}$	1.15	%
L	19.51	in

$$\rho_{fb} = 0.85\beta_1 \frac{f_c^{'}}{f_{fd}} \frac{E_f \varepsilon_{cu}}{E_f \varepsilon_{cu} + f_{fd}} \qquad (2.7.4.2\text{-}2)$$

$$f_f = \sqrt{\frac{\left(E_f \varepsilon_{cu}\right)^2}{4} + \frac{0.85\beta_1 f_c^{'}}{\rho_f} E_f \varepsilon_{cu}} - 0.5 E_f \varepsilon_{cu} \le f_{fd} \qquad (2.9.3.1\text{-}1)$$

$$A_{f,\min} \ge \max\left(0.16\sqrt{f_c^{'}}; 0.33\right) \frac{bd}{f_{fd}} \qquad (2.9.3.3\text{-}1)$$

$$M_n = A_f f_f \left(d - \frac{a}{2}\right) \qquad (2.9.3.2.2\text{-}1)$$

$$a = \frac{A_f f_f}{0.85 f_c^{'} b} \qquad (2.9.3.2.2\text{-}2)$$

$$M_n = A_f f_{fd} \left(d - \frac{\beta_1 c_b}{2}\right) \qquad (2.9.3.2.2\text{-}3)$$

$$c_b = \left(\frac{\varepsilon_{cu}}{\varepsilon_{cu} + \varepsilon_{fd}}\right) d \qquad (2.9.3.2.2\text{-}4)$$

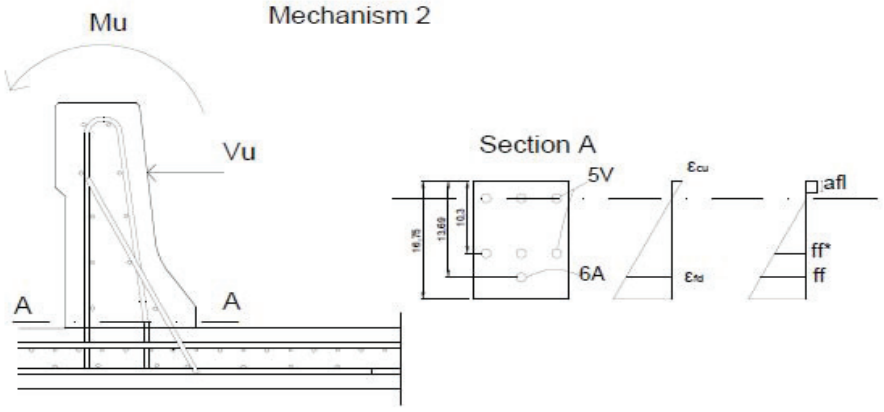

Flexural verification		
Limits for reinforcement		
D	6.69	in
B	36	In
f_{fd}	66.5	ksi
Af, min	1.4	in2
Af, provided	1.54	in2
VERIFIED		
Afmin/Af	1.13	

Flexural Strenght: mechanism 1		
D (in)	6.69	in
ff	66.5	ksi
If failure is governed by rupture of concrete		
afl	0.61	in
Mn	54	kips*ft
ϕfl	0.56	
Mr	30.3	kips*ft
Mu	15.75	kip*ft
If failure is governed by rupture of gfrp		
ε_{fd}	0.010	
ε_{cu}	0.003	
cb	1.52	
β1	0.775	
f_{fd}	66.50	ksi
Mn	51.89	kips*ft
ϕfl	0.56	
Mr	29.0	kips*ft
Mu	15.75	kip*ft
Mr in current case		
Mr	30.3	Kip*ft
Mu/Mr	0.52	
VERIFIED		

Flexural Strenght: mechanism 2			
	Vu	9.287163142	Kips/ft
	He	1.98	ft
	B	12	in
	Area	1.38	in2
	D	10.00	in
	ρf	1.15	

If failure is governed by rupture of concrete			
	ff	66.5	ksi
	ϕfl	0.55	
Contribute of 5A bent rebars	numb of bars	1.500	
	Af, provided	0.46	in2
	D	10.00	in
	afl	1.09	in
	Mn	24.13	
	Mr	13.46	
Contribute of stirrups 5V	ff*	79.8	ksi
	D	12.00	in
	numb of bars	1.500	
	Af, provided	0.46	in2
	Mn	35.08	Kips*ft/ft
	Mr	19.29	Kips*ft/ft
	Mr total	32.76	Kips*ft/ft
	Mu/Mr	0.56	
If failure is governed by rupture of gfrp			
	ϕfl	0.55	
Contribute of 5A bent rebars	D	10.00	in
	ρ_f	1.49	
	Af	0.461	in2
	cb	2.27	in
	β	0.775	
	f_{fd}	66.50	ksi
	Mn	23.3	Kips*ft/ft
	Mr	12.80	Kips*ft/ft
Contribute of close 5V	ff*	79.8	ksi
	D	12.00	in
	Af, provided	0.46	in2
	Mn	34.06	Kips*ft/ft
	Mr	18.73	Kips*ft/ft
	Mr total	31.53	Kips*ft/ft
	Mu / Mr tot	0.58	
	Mr in current case		
	Mr	31.5	Kip*ft
	Mu/Mr	0.58	
	VERIFIED		

AASHTO LRFD 2009 for GFRP-RC Bridge Design, 2009

$$k = \sqrt{2\rho_f n_f + (\rho_f n_f)^2} - \rho_f n_f \qquad (2.7.3\text{-}4)$$

$$A_{f,v} \geq 0.05 \frac{b_w s}{f_{fv}} \qquad (2.10.2.2.1\text{-}1)$$

$$V_c = 0.16\sqrt{f'_c} b_w c \qquad (2.10.3.2.1\text{-}1)$$

$$V_f = \frac{A_{fv} f_{fv} d}{s} \qquad (2.10.3.2.2\text{-}1)$$

$$f_{fv} = 0.004 E_f \leq f_{fb} \qquad (2.10.3.2.2\text{-}2)$$

Shear verification Mechanism 1		
B	36	in
ρf	0.0128	
ϕlimerock	0.9	
Ec	3841.5	ksi
Ef	6500.0	ksi
nf	1.69	
k	0.1873	
D	8.50	in
C	1.59	in
Vc	21.51	kips
ϕsh	0.75	
ϕsh*Vc	16.14	
Vu	10.74746	
VERIFIED		

5 C		
Vf requ.	-7.18	kips
Afv	0.55	in2
Shear resistance 5P and 5V		
B	36	in
Area section	0.307	in2
numb leg	1	
Af	0.307	in2
ffv	26.00	ksi
d	8.50	in
Spacing	8	in
Vf	8.48	kips
Vf tot	8.48	kips
VERIFIED		
Vfreq/Vf	-0.8466	

Shear verification Mechanism 2		
B	12	in
ρf	0.0128	
Vu	9.3	kips/ft
ϕlimerock	0.9	
Ec	3841.5	ksi
Ef	6500.0	ksi
nf	1.69	
k	0.1873	
D	12.00	in
C	2.25	in
Vc	6.82	kips
ϕsh	0.75	
ϕsh*Vc	5.1	kips

Vf requ.	1.59	kips/ft
S	8	in
N° 5V per foot	1.50	n per foot
numb of legs	2	
rebar per foot	3.0	
Area	0.307	in2
area tot	0.92	in2
ffv	26.00	ksi
Vf	2.00	kips/ft
VERIFIED without bent bar		
Vfreq/vf	0.80	

Shear resistance by bent bar		
S	8	in
bent bar	1.5	n per foot
Area	0.307	in2
area tot	0.46	in2
ffv	26.00	ksi
Vf	1.00	kips/ft
Vf tot	2.99	
VERIFIED		
Vfreq/vf	0.53	

Appendix F

FINAL DRAWINGS RC SS36" TRAFFIC RAILING

PENDULUM TEST SPECEMEN

MARCH 6th 2017

UNIVERSITY OF MIAMI
College of Civil Architectural & Environmental Engineering

Paolo Rocchetti
Guillermo Claure
Antonio Nanni

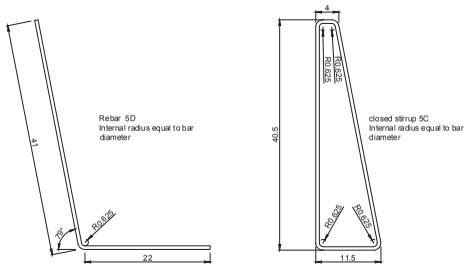

GFRP Rebars

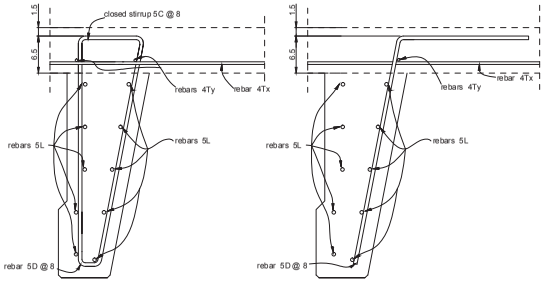

Construction: step 1

note:
- rebars 5D, 5C and longitudinal rebars 5L cast in form upside down
- rebars 5D, 5C sticking out with specified dimensions
- Add temporary rebars 4Tx and 4Ty tied to rebars 5C and 5D to give more rigidity to the case
- wood formwork to be remove and disposed off timely after the hardening of the concrete

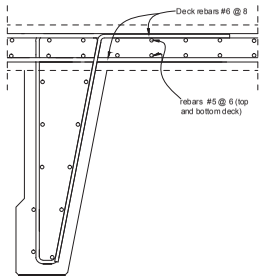

Construction: step 2

note:
- tie rebars 5C to deck reinforcement #6 and #5 with lenghts to be determined
- tie rebars 5D to deck reinforcement #5 with lenghts to be determined
- Cast the deck

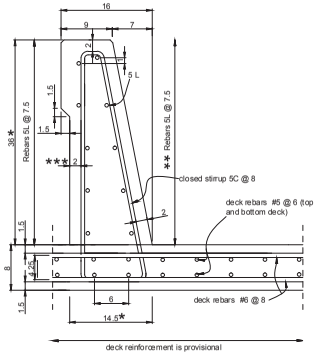

SECTION A - A
TYPICAL SECTION THRU TRAFFIC RAILING

*in comparison to F32" traffic railings, pendulum test specimen presents a thinner bottom section reducing from 18" to 14.5" and a taller section increasing from 32" to 36".
** to account for impact near an open joint, use same longitudinal/flexural (5L) reinforcement in both front and back sides of the railing.
*** proposed clear cover, 2 inches

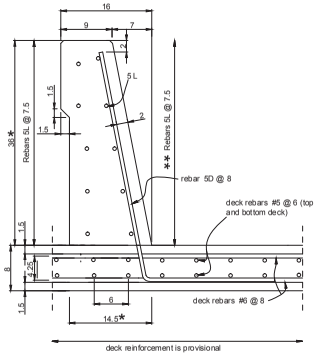

SECTION B - B
TYPICAL SECTION THRU TRAFFIC RAILING

*in comparison to F32" traffic railings, pendulum test specimen presents a thinner bottom section reducing from 18" to 14.5" and a taller section increasing from 32" to 36".
** to account for impact near an open joint, use same longitudinal/flexural (5L) reinforcement in both front and back sides of the railing.

Plan view of Traffic Railing
showing 1/4 length of test specimen

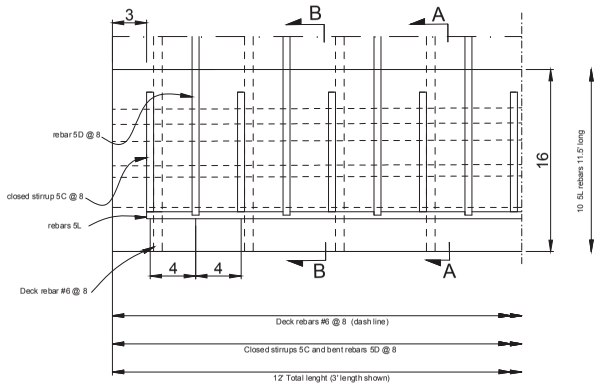

Note: All dimensions in inches, unless otherwise shown

03/09/17	UNIVERSITY OF MIAMI	TRAFFIC RAILING Pendulum Test Specimen	Sheet NO.
		(36" Single Slope-GFRP REINFORCED)	UMP 1